UNIVERSITY OF GENOA
DEPARTMENT OF EXPERIMENTAL MEDICINE

PhD COURSE IN EXPERIMENTAL MEDICINE

Curriculum: Pharmacology and Toxicology

Characterization of Mouse and Human Astrocytes in Amyotrophic Lateral Sclerosis: Effects of Oxidative Stress and Blockade of the Metabotropic Glutamate Receptor 5

Candidate

Mandeep Kumar

Tutor

Prof. Giambattista Bonanno

PhD Coordinator

Prof. Ernesto Fedele

Academic Year 2018-2021

XXXIV Cycle

TABLE OF CONTENTS

ABSTRACT

Amyotrophic lateral sclerosis (ALS) is a fatal neurodegenerative disorder due to upper and lower motor neuron (MNs) death. Recognized as a non-cell-autonomous disease, ALS is also characterized by damage and degeneration of glial cells, such as astrocytes, microglia, and oligodendrocytes. Astrocytes acquire a reactive and toxic phenotype defined by an abnormal proliferation and by the release of neurotoxic factors.

Recent studies reported that the uptake of [18F]-fluorodeoxyglucose (FDG) is increased in the spinal cord (SC) and decreased in the motor cortex (MC) of patients with ALS, suggesting that the disease might differently affect the two nervous districts with different time sequence or with different mechanisms. Here we show that MC and SC astrocytes harvested from newborn B6SJL-Tg (SOD1^{G93A}) 1Gur (SOD1^{G93A}) mice could play different roles in the pathogenesis of the disease. Spectrophotometric and cytofluorimetric analyses showed an increase in redox stress, a decrease in antioxidant capacity, and a relative mitochondria respiratory uncoupling in MC SOD1^{G93A} astrocytes. By contrast, SC mutated cells showed a higher endurance against oxidative damage, through the increase in antioxidant defense and a preserved respiratory function. Thus, SOD1^{G93A} mutation differently impaired MC and SC astrocyte biology in a very early stage of life.

One major cause for MN degeneration in ALS is represented by glutamate-mediated excitotoxicity, due to the alteration of glutamate transmission mechanisms, including glutamate receptor function. In this context, the Group I metabotropic glutamate receptor 5 (mGluR5) has been proposed to play an important role in ALS, since it is largely overexpressed during disease progression and is involved in the altered neuronal and glial cellular processes. My research group previously demonstrated that mGluR5 produces abnormal glutamate release in the spinal cord of the SOD1^{G93A} mouse model of ALS and that halving its expression has a positive impact on in-vivo disease progression, including motor neuron survival, astrogliosis, and microgliosis. They also investigated the consequences of reducing the mGluR5 expression in SOD1^{G93A} mice on the reactive phenotype of spinal cord astrocytes cultured from late symptomatic (120 days old) SOD1^{G93A} mice. Also in this model, reducing the mGluR5 expression ameliorated the astrocyte phenotype.

Here, I translated this study to human astrocytes derived from healthy donors and ALS patients. We investigated the in-vitro pharmacological treatment effect of chloro-4-((2,5-dimethyl-1-(4-(trifluoromethoxy)phenyl)-1H-imidazol-4-yl)ethynyl)pyridine (CTEP), a negative allosteric modulator of mGluR5 on i-astrocytes differentiated from the inducible neural progenitor cells (iNPCs) obtained from the skin fibroblast (i-astrocytes) of two ALS patients and two healthy donors. The overexpression of anti-glial fibrillary acid protein (GFAP), S100 calcium-binding protein β (S100β), and Complement component 3 (C3), three markers of astrogliosis, was reduced in CTEP-treated i-astrocytes. The same positive effect was obtained in the case of NLR family pyrin domain containing 3 (NLRP3) and nuclear factor erythroid 2-related factor 2 (NRF2), markers strictly related to inflammation and oxidative stress respectively, which are upregulated in ALS astrocytes. In-vitro pharmacological treatment with CTEP also reduced the expression of mGluR5 in mutated i-astrocytes. In addition, the CTEP treatment caused a decrement in antioxidant enzymatic activity such as malondialdehyde (MDA), glucose-6-phosphate dehydrogenase (G6PD), Glutathione reductase (GR), Glutathione peroxidase (GP), and catalase compared to the untreated samples, suggesting that the drug could cause a reduction of oxidative stress.

Altogether, these results indicate that reduction of mGluR5 activation has a positive impact on i-astrocytes in ALS patients supporting the idea that the in-vivo amelioration of the disease progression, registered after mGluR5 genetical or pharmacological silencing, involve an astrocyte phenotype improvement also in humans. As a whole, mGluR5 may represent a potential therapeutic target to preserve MNs from death, also by modulating the reactive astroglial phenotype in ALS.

1. INTRODUCTION

Amyotrophic lateral sclerosis (ALS) is defined as a multisystem neurodegenerative disorder, with disease heterogeneity at the clinical, genetic, and neuropathological level (Hardiman *et al.,* 2017; Brown *et al.,* 2017). The clinical features of ALS consist of adult-onset focal muscle weakness and wasting. The weakness most commonly arises in the limb muscles, then spreads in proximal muscles. Dysarthria, dysphagia, and dysphonia is present in about 25%–30% of cases. There is a high degree of variability in the age at onset, site, and disease progression of ALS. In most patients, the median survival rate after the onset of symptoms is 3 years, where death is mostly attributed to respiratory failure. About 50% of cases are suffer from extra-motor manifestations and 10%–15% of cases may also suffer from an additional diagnosis of frontotemporal dementia (FTD) (Phukan *et al.,* 2007).

At the genetic level, ALS is known to be associated with more than 20 genes. The five most common genetic causes are hexanucleotide expansions in chromosome 9 open reading frame 72 (C9orf72), mutations in superoxide dismutase 1 (SOD1), TAR DNA-binding protein 43 (TARDBP), fused in sarcoma (FUS), and TANK-binding kinase 1 (TBK1) (Brown *et al.,* 2017). The most common neuropathological mutation of ALS is TDP-43, which is reported to be found in more than 95% of ALS cases. In basal conditions TDP-43 is mainly localized to the nucleus, but in ALS it is mis-localize to the cytoplasm to form aggregates and become phosphorylated. Other proteins, such as SOD1, FUS, and their mutations have been described (Neumann *et al.,* 2006).

The diagnosis of ALS depends on the presence of both upper motor neuron (UMN) and lower motor neuron (LMN) signs. Most of the clinicians do not rely on the available revised El Escorial criteria (Brooks *et al.,* 2000) or the Awaji algorithm (de Carvalho *et al.,* 2008), because of lack of sensitivity (Schrooten *et al.,* 2011). Furthermore, these criteria are only for research purposes to select patients for clinical trials. Therefore, to reduce the delay in diagnosis, there is a high need for new clinical diagnostic criteria for ALS. Recently, Shefner *et al.,* demonstrated new simplified diagnostic criteria for ALS that helps to reduce the diagnostic delay, requiring only combined UMN and LMN dysfunction in one body region, or LMN dysfunction in at least two regions (Shefner *et al.,* 2020).

The first drug used to treat ALS is riluzole, which is approved by the European Medicines Agency. Riluzole is an aspecific glutamate release inhibitor, which has a small but significant effect on survival in ALS (Bensimon *et al.,* 1994). Despite the vast knowledge

about the disease, more than 40 randomized clinical trials have been negative (Mitsumoto *et al.,* 2014).

1.1 Epidemiology and Etiology

ALS has an estimated global incidence of 1.75–3 per 100000 persons per year and a prevalence of 10–12 per 100000 persons in Europe (Logroscino *et al.,* 2010, Marin *et al.,* 2017). The highest risk of developing ALS is in the age group between 45-75 years. The mean age for the onset of symptoms is 58–63 years for sporadic ALS (sALS) and 40–60 years for familial ALS (fALS) (Logroscino *et al.,* 2010). It is also reported that men have a higher risk of developing ALS than women (Manjaly *et al.,* 2010). The estimated ratio for developing ALS is 1:350 in men and 1:400 in women (Johnston *et al.,* 2006, Ryan *et al.,* 2019).

Related to other neurodegenerative conditions, ALS is caused by several factors such as genetic, environmental, and aging-related factors. As reported before, more than 30 genes have been linked with ALS and it is expected that more genetic factors exist. The genetic structure of ALS is complex, where monogenetic mutations with high effect size explain about 15% of patients, but other common and rare genetic variants with low and moderate effect size appear to contribute to ALS as well (Al-Chalabi *et al.,* 2010).

1.2 Causes and Risk Factors of ALS

SOD1 was the first ALS-related gene discovered in 1993, which is known to be responsible for 20% of fALS and 1%–2% of sALS (Rosen *et al.,* 1993). Mutations in the SOD1 gene do not cause ALS but rather contribute to the protein aggregation, disturbing multiple critical cellular functions. In 2008 and 2009, the genes encoding the RNA-binding proteins TDP-43 and FUS were discovered. These mutations are responsible for 3%–5% of fALS and more than 1% of sALS (Sreedharan *et al.,* 2008, Kabashi *et al.,* 2008, Kwiatkowski *et al.,* 2009, Vance *et al.,* 2009). Mutations of C9orf72 were discovered in 2011 and are responsible for 30%–50% of fALS and for 7%–10% of sALS (DeJesus-Hernandez *et al.,* 2011, Renton *et al.,* 2011). Mutations in TBK1 are the fifth most common cause of ALS, responsible for about 1% of patients (Cirulli *et al.,* 2015, Freischmidt *et al.,* 2015) but up to 10% of patients with ALS-FTD (Le Ber *et al.,* 2015). Out of these five, SOD1 mutations have high penetrance, as compared to other mutations. Rarely patients were reported with mutations

in more than one of these genes, suggesting that ALS can be oligogenic in origin (van Blitterswijk *et al.,* 2012).

A very few genetic risk factors are known to be associated with ALS. An at-risk genotype is UNC13A (van *et al.,* 2009) and intermediate repeat expansions in ATXN2 increase the chance of developing ALS (Elden *et al.,* 2010). Aside from genetic factors, many studies revealed environmental risk factors such as smoking, body mass index, physical exercise, occupational and environmental exposures to metals or pesticides, head injury, and viral infections (Pupillo *et al.,* 2018, Ingre *et al.,* 2015).

1.3 Mutated proteins in fALS

The familiar form of ALS is mostly inherited in an autosomal dominant manner. Until now, more than 30 genes are identified, and researchers are continuing to better search for ALS-associated genes (Renton *et al.,* 2014; Cirulli *et al.,* 2015), and four of them are responsible for more than 70% of cases (Chiò *et al.,* 2014).

As depicted above, the SOD1 was the first mutated gene identified (Rosen *et al.,* 1993), mutated in 25% of fALS (Saccon *et al.,* 2013; Kiernan *et al.,* 2011). Consequently, other recent mutations were discovered, such as TARDBP (Arai *et al.,* 2006; Mackenzie *et al.,* 2007), FUS (Vance *et al.,* 2009), and C9orf72 (DeJesus-Hernandez *et al.,* 2011; O'Rourke *et al.,* 2015).

1.3.1 Superoxide Dismutase 1 (SOD1)

SOD1 mutations are composed of approximately 2% of all ALS cases and 20-25% of fALS cases (Al-Chalabi and Leigh, 2000). It is reported that more than 180 SOD1 polymorphisms are associated with ALS (Wright *et al.,* 2019). Most of them are missense mutations and D90A (aspartate at codon 90 changed to alanine) is the most common variant represented in North America. The other two most studied mutations are A4V (alanine at codon 4 changed to valine) and G93A variant (glycine at codon 93 changed to alanine) are reported in 50% and 25% of fALS cases in the U.S.A. population, respectively (Gurney *et al.,* 1994). These mutations showed similar symptoms to human disease and caused MNs degeneration (Pansarasa *et al.,* 2018; Andersen, 2006). These different mutations have significant variability as to phenotype, disease progression, and severity (Mejzini *et al.,* 2019). Patients with A4V, G93A, H43R (histidine at codon 43 changed to arginine), L84V (leucine at codon

84 changed to valine), G85R (glycine at codon 85 changed to arginine) or N86S (asparagine at codon 86 changed to serine) variants showed rapid disease progression and shorter survival, while patients carrying D90A, G93C (glycine at codon 93 changed to cysteine) or H46R (histidine at codon 46 changed to arginine) mutations generally have longer life expectancies (Yamashita and Ando, 2015). In addition, ALS patients with different mutations showed distinct clinical features; for example, AV4 mutation relates to the limb-onset form of ALS (Juneja *et al.,* 1997) and patients with the D90A variant show a slowly progressive paresis, starting in the legs and gradually spreading upstream, together with atypical features such as bladder disturbance (Andersen *et al.,* 1996). SOD1 gene mutations in fALS cause a loss of function of the protein leading to an altered free oxygen radical species (ROS) scavenging (Deng *et al.,* 1993) and the subsequent motor neuron death.

A study also revealed that mutant SOD1 inhibits the protein transport between the endoplasmic reticulum (ER) and Golgi in neuronal cells, a crucial mechanism for cell survival (Soo *et al.,* 2015). This inhibition is also associated with mutations in TDP-43 and FUS. Even if these mutations act through different processes, each mechanism is dependent on the Ras-related protein (Rab1) function. Rab1 is mainly involved in regulating all the intracellular vesicle trafficking events, and this is not functional in sALS (Soo *et al.,* 2015). SOD1 mutation was also reported in the pathogenesis of sALS by the detection of modified 32 kDa SOD1 polypeptide together with the well-known 16 kDa SOD1 in the spinal cord extracts of fALS and sALS patients (Gruzman *et al.,* 2007). The other studies revealed that the 32 kDa protein can acquire toxic properties typical of mutant SOD1, thus determining the development of aggregates, in the nuclei of astrocytes of spinal cords of ALS patients (Ezzi *et al.,* 2007; Forsberg *et al.,* 2011). The SOD1 level was strongly reduced inside the nuclei of MNs and leukocytes of sALS patients and this led to increased DNA damage and, consequently, to a more severe disease progression (Cereda *et al.,* 2013; Sau *et al.,* 2007).

1.3.2 TAR-DNA-binding protein 43 (TDP-43)

TDP-43 is mainly involved in more than 95% of ALS patients (Neumann *et al.,* 2006). TDP-43 is an RNA and DNA-binding protein localized in the nuclear and involved in multiple processes such as transcription, splicing, micro-RNA maturation, RNA transport, and stress granule formation (Mackenzie *et al.,* 2010). The literature report that most ALS cases are caused by the aggregation of ubiquitinated or misfolded proteins, which is also one of the

main pathological mechanisms involved in other neurodegenerative disorders such as Alzheimer's (AD) and Parkinson's diseases (PD) (Leigh *et al.,* 1991). TDP-43 was reported as a component of these protein aggregates both in fALS and sALS patients (Arai *et al.,* 2006; Neumann *et al.,* 2006, Mejzini *et al.,* 2019). Therefore, the cytoplasmic neuronal inclusions of TDP-43 in the brain and spinal cord are now considered a pathological hallmark of ALS.

TDP-43 is a DNA/RNA binding protein composed of 414 amino acids whose gene is localized in chromosome 1. TDP-43 is predominantly a nuclear protein but in the case of neurodegeneration it can be also present in the cytoplasm, next to post-transcriptional modifications (Ayala *et al.,* 2008). It is also reported that in patients with ALS or FTD, TDP-43 is phosphorylated and excised at C-terminals in the brain cortex and becomes non-functional (Neumann *et al.,* 2006). TDP-43 is known to regulate gene expression and is involved in the regulation of mRNA and non-coding RNA stability, and in the mRNA transport and translation (Buratti and Baralle, 2010; Tollervey *et al.,* 2011; Ratti and Buratti, 2016). The number of TDP-43 animal models such as Caenorhabditis elegans, Zebrafish, Drosophila, mice, and rats demonstrated the importance of mutated TDP-43in ALS studies (Picher-Martel *et al.,* 2016).

1.3.3. *Fused in Sarcoma/Translocated in liposarcoma (FUS/TLS)*

Another RNA/DNA binding protein, called FUS/TLS, was found to be mutated soon after the discovery of TDP-34. This mutation is present in 4% of fALS and some rare sALS cases (Kwiatkowski *et al.,* 2009; Vance *et al.,* 2009). FUS/TLS is a 526 amino acids protein localized in the nucleus, and mutation is caused mainly at the C-terminal region, which is responsible for protein-protein interactions, alternative splicing, and nuclear localization (Lagier-Tourenne *et al.,* 2010). A study found that the cytoplasmic inclusion of FUS/TLS in neurons and glial cells in the brain and spinal cord of patients. The authors reported that FUS/TLS binds several microRNAs, some of which are shared with TDP-43, both in mice and in humans (Lagier-Tourenne *et al.,* 2010).

1.3.4   Chromosome 9 open reading frame 72 (C9orf72)

In 2011, another ALS mutation was discovered in a non-coding region of C9orf72 (DeJesus-Hernandez *et al.,* 2011, Renton *et al.,* 2011). This mutation resulted in the expansion of the GGGGCC repeat hexanucleotide. C9orf72 codes for a protein with unknown domains and functions but highly conserved across species (Bigio, 2011). It is also expressed in normal and neoplastic cell (DENN) proteins which are regulators of cytoplasmic and membrane protein traffic (Levine *et al.,* 2013). C9orf72, represents 20-40% of fALS and 5% of sALS cases, and 10-30% familial and 2-10% of sporadic forms of FTD (DeJesus-Hernandez *et al.,* 2011; Renton *et al.,* 2011). ALS and FTD patients show hundreds or even thousands of hexanucleotide repetitions as compared to healthy individuals that ranged from 2-23 hexanucleotide units (DeJesus-Hernandez *et al.,* 2011; Renton *et al.,* 2011). Two main mechanisms are involved in the pathology of ALS/FTD: loss of function of the protein, caused by a decreased expression level of C9orf72, and gain of function of the protein due to an accumulation of RNA foci in the brains and spinal cord (Taylor *et al.,* 2016).

The loss of function mechanism was confirmed in cell culture studies, in which the depletion of C9orf72 increased the toxicity of aggregation-prone proteins such as polyglutamine-expanded ataxin 2 (Sellier *et al.,* 2016). The complete removal of C9orf72 in mice did not cause motor impairment but showed abnormal macrophages and microglia activation as well as neuroinflammation (Taylor *et al.,* 2016). These observations raise the possibility of a non-cell-autonomous contribution to ALS, even if the loss of function of C9orf72 cannot be the sole driver of the disease (Taylor *et al.,* 2016).

The second hypothesis involves the accumulation of RNA-binding protein that results in the toxic gain of function (La Spada and Taylor, 2010). In addition, repeat-associated non-AUG (RAN) translation produced toxicity of dipeptide repeat proteins (DPRs: poly-GA, -GP, -GR, -PA, -PR) (Zu *et al.,* 2011). These dipeptides are known to accumulate in the cytoplasm and nucleus of the brain and spinal cord and result in the inclusion of proteins that are negative for TDP-43 (Zu *et al.,* 2013; Mackenzie *et al.,* 2013; Ash *et al.,* 2013; Mori *et al.,* 2013). The total amount of inclusions depends on the DPR protein involved. DPRs are mainly in the form of poly-GA (Glycine-Alanine) and, to a lesser extent, in other forms such as poly-GP (Glycine-Proline), poly-GR (Glycine-Arginine), poly-PR (Proline-Arginine), poly-PA (Proline-Alanine). However, only a slight pathological correlation of poly-GA, but

not other DPRs, has been reported in C9orf72-associated ALS. The contribution of other DPRs to pathogenesis is still unclear (Zongbing *et al.,* 2020).

1.4 Pathogenesis of ALS

The neuropathological signs of ALS are defined by loss of the neuromuscular junctions, axonal retraction, and subsequent cell death of upper and lower motor neurons. It is reported that several molecular pathways are implicated in the pathogenesis of ALS, such as failure of proteostasis, excitotoxicity, neuroinflammation, mitochondrial dysfunction, oxidative stress, oligodendrocyte dysfunction, cytoskeletal disturbances, axonal transport defects, disturbed RNA metabolism, nucleocytoplasmic transport deficits, and impaired DNA repair (Taylor *et al.,* 2016).

1.4.1. Oxidative Stress

Oxidative stress (OS) is linked to the pathogenesis of many neurodegenerative diseases. OS is the result of increased production of ROS and frequent decrease in the antioxidant defenses (Sies., 2015). During the normal cell life cycle, various molecules are produced such as hydrogen peroxide (H_2O_2), superoxide anion (O_2^-), hydroxyl radical (HO), and reactive nitrogen species (RNS). Many cell functions require oxygen as a substrate such as signal transduction, gene transcription, oxidative phosphorylation, and ATP production (Halliwell, 2006; Uday *et al.,* 1990). In the case of OS, oxygen molecules can damage the cell structure by causing the oxidation of various molecules such as lipids, protein, and DNA/RNA (Yu *et al.,* 2009).

Lipid peroxidation results in an increase in membrane fluidity and permeability, which can increase the entrance of ions into the cell (Brown and Murphy., 2009). Lipid peroxidation also modifies the structural and functional properties of the cell that results in increased protein aggregation and proteolysis (Halliwell and Gutteridge., 1984). Mitochondria give rise to RNS/ROS because of the presence of redox enzymes (Halliwell., 2007). Mitochondria dysfunctions lead to the apoptosis of cells, neurons and reduce the protective action of reactive species (Wang *et al.,* 2013; Redza-Dutordoir and Averill-Bates., 2016).

Apart from the SOD1 mutation, OS also been found in C9orf72, TDP-43, and FUS familial forms of ALS, suggesting a correlation between RNA dysmetabolism and OS. A study demonstrated that OS causes TDP-43 delocalization from the nucleus to the cytoplasm and

increases its tendency to aggregate (Cohen *et al.,* 2015). On the other hand, TDP-43, FUS, and C9orf72 can co-localize with mitochondria and cause OS. ALS patients show decreased antioxidant response and increased production of free radicals and ROS. For instance, the nuclear factor erythroid 2-related factor 2 (Nrf2) was decreased in ALS patients (Sarlette *et al.,* 2008). Nrf2 elevates the synthesis of pro- and anti-inflammatory enzymes, such as cyclooxygenase-2 (COX-2), iNOS, and heme oxygenase-1 (HO-1) (Petri *et al.,* 2012). Therefore, many studies focused on Nrf2 activators such as analogs of 2-cyano-3, 12-dioxooleana-1,9-dien-28-oic acid (CDDO), tert-butylhydroquinone, DL-sulphoraphane, lipoic acid, fumaric acid, and curcumin in the $SOD1^{G93A}$ mouse model of ALS to slow down the disease progression (Neymotin *et al.,* 2011; Petri *et al.,* 2012).

Glial and infiltrated immune cells are the primary producers of ROS and RNS in the CNS (D'Ambrosi *et al.,* 2018). In ALS, OS also contributes to the degeneration of the neuromuscular junction. A study on ALS mice showed a decrease in the neuromuscular junction number due to increased sensitivity of the nerve terminal to ROS. Besides, overstimulation of MNs result in the abnormal secretion of acetylcholinesterase and decreased acetylcholine level in the synaptic cleft (Pollari *et al.,* 2014). Some studies revealed that the level of glutathione (GSH), an antioxidant in mammalian cells, is lower in the motor cortex of ALS patients as compared to healthy volunteers (Weiduschat *et al.,* 2014; Cohen *et al.,* 2012). In addition, TDP-43 mutation also induced OS and mitochondrial damage due to the nuclear accumulation of Nrf2 (Duan *et al.,* 2010; Shodai *et al.,* 2013). A study on post-mortem tissue of ALS patients showed a decrease in Nrf2 mRNA and protein levels (Petri *et al.,* 2012), and increasing the level of Nrf2 in astrocytes showed a significant beneficial effect in ALS mice (Vargas *et al.,* 2006).

1.4.2. *Mitochondria Dysfunction*

Mitochondria play an important role in cell survival and metabolism. Mitochondria produce ATP through oxidative phosphorylation and have a major role in phospholipid biogenesis, calcium homeostasis, and apoptosis. Mitochondria also play a vital role in neurons; despite only 2% body mass, brain neurons require 20% of body ATP production (Nicholls *et al.,* 2000; Engl *et al.,* 2015). Furthermore, mitochondria also modulate neurotransmitter release by modulating calcium dynamics (Rizzuto *et al.,* 2012). Neurons are long-lived cells and more susceptible to the accumulating damage from mitochondrial dysfunction (Payne *et al.,*

2015). Therefore, mitochondrial dysfunction has been linked to many neurodegenerative disorders including ALS. There are several factors linked to ALS-associated mitochondria dysfunction such as defective oxidative phosphorylation, production of ROS, impaired calcium buffering capacity, and defective mitochondrial dynamics.

In ALS patients, structural mitochondria changes are characterized by a swollen and vacuolated appearance (Atsumi., 1981). Some sporadic ALS patients also display axonal swellings, neurofilament accumulations, swollen mitochondria, and secondary lysosomes (Okamoto *et al.,* 1990). Similar features are also present in animal and cell models of ALS (Hong *et al.,* 2012; Wang *et al.,* 2013). In addition, the SOD1[G93A] transgenic mice showed abnormal clusters along the axon (Magrane *et al.,* 2014). Overexpression of ALS mutant FUS R521G (arginine at codon 521 changed to glycine) or R521H (arginine at codon 521 changed to histidine) in cultured motor neurons resulted in mitochondrial shortening which was exacerbated by the presence of FUS in the cytosol (Tradewell *et al.,* 2012). Subtle fragmentation of the mitochondrial network has also been identified in fibroblasts of ALS patients with C9orf72 repeat expansions (Onesto *et al.,* 2016), and swollen mitochondria were reported in an iPSC model of C9orf72-associated ALS (Dafinca *et al.,* 2016).

1.4.2.1 ALS-associated proteins interacting with mitochondria

Several proteins that have been linked to familial and sporadic ALS interact with mitochondria (Deng *et al.,* 2015; Higgins *et al.,* 2002; Wang *et al.,* 2016; Mattiazzi *et al.,* 2002). The interaction of these ALS-associated proteins with mitochondria leads to mitochondrial damage. Mutant SOD1 localizes to the intermembrane space, where it aggregates, and reduces the activity of the electron transport chain complexes (Ferri *et al.,* 2006; Vijayvergiya *et al.,* 2005). Furthermore, SOD1 aggregates have been proposed to interfere with the activity of voltage-dependent anion channel 1 (VDAC1) which is responsible for the exchange of ATP, ADP, and other respiratory substrates across the outer mitochondrial membrane. Direct interaction of ALS mutant SOD1 with VDAC1 inhibits channel conductance and reduces its permeability to ADP in pre-symptomatic and symptomatic disease stages in the spinal cord of SOD1[G93A] rats (Israelson *et al.,* 2010).

The accumulation of TDP-43 in mitochondria appears mediated by internal mitochondrial targeting sequences in TDP-43 (Wang *et al.,* 2016). Mitochondrial localization of FUS correlated with augmented ROS levels (Deng *et al.,* 2015), and overexpression of FUS

reduces mitochondrial ATP production (Stoica *et al.,* 2016). Several mitochondrial proteins have been identified as possible C9orf72-interacting proteins, such as the members of the inner mitochondrial membrane (IMM) solute carrier family, VDAC3, and translocase of the IMM. Furthermore, C9orf72 was detected in mitochondria-enriched fractions (Blokhuis *et al.,* 2016).

1.4.3. Glutamate Excitotoxicity

In physiological conditions, glutamate is released from the presynaptic neuron to activate the postsynaptic glutamate receptors, which results in an influx of Na^+ and Ca^{2+} ions into the cell generating the action potential. In 1978, Olney coined the concept of excitotoxicity that is caused by over-stimulation of the glutamate receptors (Olney 1978). This overstimulation can damage neurons and leads to several neurodegenerative disorders including ALS (Coyle 1993, Lipton *et al.,* 1994). Classical and slow excitotoxicity exists (Doble 1999). Classical excitotoxicity causes neuronal degeneration with increased extracellular glutamate concentration up to 2–5 μM, while slow excitotoxicity is the death of a weak postsynaptic neuron in the presence of normal synaptic glutamate levels (Novelli 1998). Glutamatergic neurotransmission plays an important role in both types of excitotoxicity. Glutamate released from the presynaptic glutamate release activates both ionotropic and metabotropic glutamate receptors. The ionotropic receptors are divided into AMPA (α-amino-3-hydroxy-5-methyl-4-isoxazole propionic acid), NMDA (N-methyl-D-aspartate), and KA (kainate) receptors (Collingridge 1989). Originally, the NMDA receptor was responsible for excitotoxicity (Choi 1988). More recently, it became clear that the activation of AMPA receptors is also important (Prehn *et al.,* 1995). Ca^{2+} influx through NMDA receptors, Ca^{2+} permeable AMPA receptors, or voltage gated Ca^{2+} channels are the predominant mediator of neuronal injury (Carriedo *et al.,* 1996, Van Den Bosch *et al.,* 2000). The influx of Ca^{2+} ions can result in the activation of several enzymes, such as protein kinase C, phospholipases, lipases, endonucleases, proteases, protein phosphatases, xanthine oxidase, and NO synthase. In addition, mitochondrial dysfunction due to increased Ca^{2+} uptake in mitochondria and subsequent formation of ROS contributes to excitotoxic cell death (Dykens 1994., Carriedo *et al.,* 2000).

Several studies linked glutamate excitotoxicity and the pathophysiology of ALS. A study on postmortem tissue from ALS patients showed reduced functional transport of glutamate and

EAAT2 immunoreactivity (Rothstein *et al.,* 1995). The same study showed that the depletion of EAAT2 in SOD1^{G93A} mice leads to neuronal death (Rothstein *et al.,* 1996). Studies on the same mouse model of ALS showed that the loss of EAAT2 contributes to disease progression. Rats carrying the SOD1^{G93A} mutation show reduced synaptosomal glutamate uptake and increased extracellular levels of glutamate (Rothstein *et al.,* 2005, Guo *et al.,* 2003, Howland *et al.,* 2002). The expression of EAAT2 is reduced at pre-symptomatic stages and abolished at the end stage in some transgenic models (Howland *et al.,* 2002). Overexpression of EAAT2 in SOD1^{G93A} mice may be neuroprotective, delaying the onset of motor deficits and reducing activation of caspase 3, a potent promoter of apoptotic cell death pathways (Guo *et al.,* 2003).

My research group reported that abnormal synaptic glutamate levels could also be sustained by excessive glutamate release. Utilizing the SOD1^{G93A} mouse, they demonstrated that neuronal glutamate release induced by stimuli leading to exocytosis, such as high KCl, ionomycin, or hypertonic sucrose, is elevated in pre-symptomatic and symptomatic G93A mutant mouse spinal cord (Milanese *et al.* 2011; Bonifacino *et al.* 2019). Increased cytosolic calcium concentration, the associated over-activation of Ca^{2+}/calmodulin-dependent protein kinase II (CaMK-II), which has been already shown in sporadic ALS patients (Hu *et al.,* 2003) and, in turn, the phosphorylation of Synapsin I (Syn-I), an event that contributes to fill up the readily releasable pool of vesicles and to boost vesicles fusion, support the stimulus-evoked excessive glutamate release. Moreover, increased phosphorylation of glycogen synthase kinase-3 at the inhibitory sites, an event favouring SNARE protein assembly, and the consequently detected higher number of SNARE protein complexes at the nerve terminal membrane further boost this event (Milanese *et al.* 2011; Bonifacino *et al.* 2016)

Exocytotic glutamate release was also excessive by activating presynaptic Group I metabotropic glutamate receptors (mGluR1 and mGluR5) in the spinal cord of SOD1^{G93A} mice (Giribaldi *et al.,* 2013). The authors report that both mGlu1 and mGlu5 were overexpressed at the nerve terminal level and that receptor activation stimulated the release of the excitatory amino acid at much lower concentrations of agonists than in control mice. Glutamate release, as well as mGluR1 and mGluR5 expression, were also enhanced in early symptomatic SOD1^{G93A} mouse spinal cord (Bonifacino *et al.,* 2019),

The literature also indicates that both MNs are particularly vulnerable to AMPA receptor-mediated excitotoxicity. Administration of AMPA receptor agonists induced motor neuron degeneration in animals which could be reversed by the antagonist of AMPA receptors, while NMDA failed to damage spinal motor neurons (Corona *et al.,* 2004). Studies showed that MNs cultured on astrocytes showed Ca^{2+} influx through Ca^{2+}-permeable AMPA receptors, which was crucial for inducing motor neuron death. Other neurons were resistant to AMPA receptor over-stimulation (Carriedo *et al.,* 2000). Little or no effects of agonists of NMDA receptors was evidenced in these cultured MNs (Van Den Bosch *et al.,* 2006).

1.4.4 *Failure of proteostasis*

The aggregation of proteins disturbs the normal protein homeostasis and induces cellular stress. The overload of misfolded proteins leads to their degradation after ubiquitination via the ubiquitin-proteasome system. Alternatively, protein aggregates can also undergo lysosomal degradation by the autophagy pathway after binding to p62 (Höhn *et al.,* 2020; Corti *et al.,* 2020).

Multiple ALS-related genes hold an important role in protein aggregation and impaired degradation. Indeed, ubiquilin-2 (UBQLN2) has a role in the delivery of ubiquitinated proteins to the proteasome (Deng *et al.,* 2011). Several mutations are also present in genes involved in the autophagy pathway, such as SQSTM1 (encoding the protein p62, which targets ubiquitinated proteins to the phagophore) (Fecto *et al.,* 2011), optineurin (OPTN, functioning as a receptor for autophagy) (Maruyama *et al.,* 2010), TBK1 (activating OPTN by phosphorylation) (Freischmidt *et al.,* 2015), valosin-containing protein (Johnson *et al.,* 2010) and the C9orf72 (Webster *et al.,* 2016).

1.4.5. *Disturbed RNA metabolism*

Several RNA-binding proteins are involved in the pathogenesis of ALS. Mutations in the genes of two RNA-binding proteins, TDP-43 and FUS, have introduced to the mechanism of dysregulation of RNA metabolism to ALS (Buratti *et al.,* 2010). Further mutations in other RNA-binding proteins were reported in ALS, such as angiogenin, syntaxin, matrin-3, heterogeneous nuclear ribonucleoproteins A1) and A2B1, and ataxin-2 (Boeynaems *et al.,* 2016). In ALS, these proteins are mis-localized to the cytoplasm with aggregation resulting in toxicity.

1.4.6   Cytoskeletal disturbances and axonal transport defects

Various protein factors in ALS are involved in the maintenance of cytoskeletal integrity and axonal transport, such as profilin-1 and tubulin alpha-4A (De Vos *et al.,* 2017). Mutations in these proteins destabilize the tubulin network and cause axonal transport deficits. Another complex, the dynactin complex, stabilizes the binding of cargoes and modulates motor function. Point mutations in the gene encoding the dynactin1 subunit of the dynactin complex may cause ALS or FTD (Bercier *et al.,* 2019; Munch *et al.,* 2004).

1.5 Clinical Features

The main clinical features of ALS are progressive muscle weakness, followed by muscle atrophy and slowness of movements with muscle stiffness. This muscle weakness typically spreads to adjacent body regions and results in developing the disease pathology within the motor system (Ravits *et al.,* 2009).

ALS is usually demonstrated unilaterally at distal muscles in upper or lower limb muscles (Turner *et al.,* 2011), with thenar muscles being more affected than hypothenar muscles (Simon *et al.,* 2014). At the onset of the disease, the first interosseous muscle and finger extensors are more affected than finger flexors (Margaret *et al.,* 2016). In the lower limb, the anterior tibial muscle and hamstrings are affected earlier than the gastrocnemius muscle and quadriceps muscles, respectively (Jenkins *et al.,* 2020).

ALS most commonly present dysarthria or dysphagia, less commonly dysphonia, or reduced mouth closure or chewing problems. It is also associated with axial muscle weakness and difficulties with posture in the late stages of the disease (Parvizi *et al.,* 2001). A neurological examination showed the presence of both upper MNs and lower MNs in patients with classic ALS. ALS is a complex clinical syndrome with different motor and extra-motor manifestations that result in distinct phenotypic presentations of the disease with varying trajectories of the disease (Al-Chalabi *et al.,* 2016).

1.6 Phenotypes of ALS

ALS is known to have multiple phenotypes based on the involvement and regional distribution of both UMN and LMN (van Es *et al.,* 2017; Al-Chalabi *et al.,* 2016). Due to

the different life expectancy, degree of cognitive and behavioral impairment, it is important to recognize the different motor phenotypes (Chiò *et al.,* 2011).

1.6.1. Phenotypes of ALS based on the involvement of upper MN versus lower LMN

The classic ALS showed the symptoms of both upper MN and lower MN loss in one or more body regions. On the other hand, primary lateral sclerosis (PLS) is described by progressive spasticity and slowing of movements with isolated UMN (Pringle *et al.,* 1992). The symptoms should begin in the lower limbs but can start in the bulbar region as well. PLS represents 3%–5% of all motor neuron diseases and it can involve into ALS after 3 to 4 years of disease onset. The median survival of PLS patients is more than 20 years but the patients with UMN predominant ALS have a shorter survival compared to PLS. UMN predominant ALS has a slower disease progression compared to classic ALS. LMN predominant ALS patients have very few UMN signs.

Progressive muscular atrophy is identified by progressive isolated LMN signs without involvement of UMN dysfunction, although up to 30% of progressive muscular atrophy patients will develop UMN signs during disease progression.

1.6.2. Phenotypes of ALS based on the CNS region involved

Bulbar ALS is a destructive type of ALS occurring in about 30% of patients and is characterized by a fast decline in patient survival and reduction of disease onset. Bulbar upper MN dysfunction results in spastic dysarthria, which is identified by slow, labored, and distorted speech. Bulbar lower MN dysfunction is characterized by tongue wasting and fasciculation, followed by flaccid dysarthria and dysphagia.

Pseudobulbar palsy is described by the absence of facial expressions, spastic dysarthria, difficulty in chewing, dysphagia, and tongue protrusion (Finegan *et al.,* 2019). The jaw jerk is exaggerated or clonic due to the involvement of the upper MN. Pseudobulbar palsy can be differentiated from progressive bulbar palsy, affecting the lower MNs.

Mill's syndrome (hemiplegic variant) defines a hemiplegic or asymmetrical pattern. The symptoms are gradually progressive, and the progression is usually more ascending than descending. It can also involve the facial muscles.

About 3% of patients have respiratory ALS, characterized by diaphragm weakness as the initial problem. These patients have a poor prognosis. In axial variant ALS, the disease starts in paravertebral muscles, with stooped posture as a presenting symptom.

Flail arm ALS is also known as brachial amyotrophic diplegia, man-in-the-barrel syndrome, or Vulpian–Bernhardt syndrome and identifies progressive weakness in the upper limbs. About 77% of patients develop bulbar symptoms and males are more preponderant than females (male to female ratio 3:1) (Wijesekera *et al.,* 2009).

Flail leg ALS is characterized by progressive weakness of lower limbs, symmetrical as predominantly charaterizedby a lower MN pattern of weakness. There is no significant weakness in the upper limbs and bulbar region up to 12 months from the disease onset, and progression is slightly slower than classic ALS.

1.6.3 Phenotypes of ALS based on additional frontotemporal involvement

FTD is the most common cause of dementia after Alzheimer's disease in patients aged 65 years or more. About 50% of ALS patients show degeneration of frontal and anterior temporal lobes, resulting in language impairments or behavioral changes. This can be identified by using the Edinburgh cognitive and behavioral ALS (Niven *et al.,* 2015). ALS without cognitive or behavioral impairment is associated with memory dysfunctions or reduced visuospatial function (Strong *et al.,* 2017).

1.7 Genetics classification of ALS

Many studies showed that 90% of ALS are sporadic cases with no clear genetic linkage. However, 10% of cases show a familial heritage (Maruyama *et al.,* 2010, Turner *et al.,* 2013). In the last few years, there is a rapid increase in the genetic causes of ALS. Moreover, the correlation between the genetic subtypes and the pathological subtypes has become clearer. In addition to SOD1, TARDBP, FUS, UBQLN2, and C9orf72, several other genes are also associated with ALS.

1.7.1 Genetics of fALS

Among those all-genetic causes, 30-50% cases are associated with C9orf72, 20-25% are caused due to the mutation in the SOD1 gene, 4-5% cases of fALS are the result of a mutation in TARDBP and FUS genes and the rest are due to other mutations such as alsin,

senataxin (SETX), spatacsin, vesicle-associated membrane protein-associated protein B (VAPB). angiogenin (ANG), factor-induced gene 4, optineurin (OPTN).

1.7.1.1 *Superoxide Dismutase 1 (SOD1) /ALS1*

The first mutation identified in fALS was SOD1, which maps to chromosome 21q22. Patients with SOD1 mutation present with limb onset, starting in the lower limb rather than the upper limb. Literature reveals that more than 180 mutations are affecting the functional domains of SOD1 predominantly in missense mutations. Mutations in SOD1 have been reported in ~20% of fALS and ~1-4% of sALS (Pasinelli *et al.,* 2006). SOD1 mutant ALS patients show variation in some factors such as the age of onset, severity, rate of disease progression, and duration, indicating that the phenotype is modified by genetic and environmental factors (Maruyama *et al.,* 2010). The $SOD1^{D90A}$ mutation which is inactive in a Scandinavian population is linked to autosomal dominant ALS in other genetic groups (Pasinelli *et al.,* 2006). Patients with $SOD1^{A4V}$ mutations have more death rate and more penetrance power (Pasinelli *et al.,* 2006). The $SOD1^{A89V}$ mutation has less penetrance, variable age at onset, and sensory neuropathy (Rezania, *et al.,* 2003). The $SOD1^{I113T}$ mutation is highly diverse in the age of onset, clinical manifestations, disease progression, and penetrance (Lopate *et al.,* 2010, Mackenzie *et al.,* 2007).

1.7.1.2 *Alsin/ALS2*

ALS2 is a rare disease with a mean age of onset of 65 years, characterized by limb and facial spasticity, spastic dysarthria, uncontrolled laughter, lower motor neuron signs, and bladder dysfunction (Pasinelli *et al.,* 2006, Hadano *et al.,* 2006). Alsin is a Rab5 and Rac1 guanine nucleotide exchange factor that promotes neurite outgrowth in cell cultures (Hadano *et al.,* 2006). Alsin plays a neuroprotective role by protecting cell cultures from mutant SOD1 toxicity (Kanekura *et al.,* 2004). Alsin overexpression inhibits $SOD1^{G93A}$-induced endosomal Rac1 activation and reactive oxygen species production. The alsin mutations disrupt the endolysosomal system and result in the aggregation of immature vesicles and misfolded proteins in neurons (Li *et al.,* 2011, Otomo *et al.,* 2008). Studies showed that alsin knock-out mice could result in motor neuron damage, with no specific features consistent with ALS or other MN diseases. These mice showed increased vulnerability to oxidative

stress, indicating that alsin mutation might be a risk factor rather than a direct cause of MN degeneration (Cai *et al.,* 2008, Gros-Louis *et al.,* 2008).

1.7.1.3   Senataxin (SETX)/ALS4

ALS4 is a rare, autosomal dominant ALS form characterized by distal limb weakness and muscle atrophy. It has slow disease progression consistent with a normal life span (Chance *et al.,* 2017). ALS4 has linked to chromosome 9q34 and shows three distinct mutations in the SETX gene in 3 families with ALS (Chen *et al.,* 2004). SETX gene encodes a ubiquitously expressed DNA/RNA helicase protein involved in DNA repair, replication, recombination, transcription, RNA processing, transcript stability, and translation initiation (Moreira *et al.,* 2004, Grohmann *et al.,* 2001). Mutation in the SETX gene caused MN degeneration that may result from the aberrant RNA processing (Skourti-Stathaki *et al.,* 2011).

1.7.1.4   Spatacsin (SPG)/ALS5

ALS5 is the most common form of recessive fALS with a mean onset age of 25 years. It has a prolonged progressive rate, and patients can survive more than three decades. ALS 5 is linked to chromosome 15q15-21 and mutations in the SPG11 gene (Hentati *et al.,* 1998, Stevanin *et al.,* 2007). SPG11 gene mutation causes clinical, pathological, and genetic features of ALS (Orlacchio *et al.,* 2010). SPG11 is a protein with four transmembrane domains, a leucine zipper, and a coil domain. This protein was identified in the CNS, especially in the cortical and spinal MNs and in the retina (Murmu *et al.,* 2011).

1.7.1.5 Fused in sarcoma (FUS)/ALS6

ALS6 is characterized by a wide range of disease onset, from 26–80 years, with a mean duration of 33 months (Pasinelli *et al.,* 2006). Most patients show lower MN predominance, with no cognition and bulbar region involvement. The locus for ALS6 has been mapped to chromosome 16p11.2 encoding the FUS gene (Sapp *et al.,* 2003). Mutations in the FUS gene are identified in a large Cape Verde family with autosomal recessive ALS (Lanson *et al.,* 2012). They can also be found in patients with frontotemporal dementia (FTD) and juvenile ALS with basophilic inclusions (Bäumer *et al.,* 2010). Besides, FUS is also involved in Huntington's disease (HD) (Doi *et al.,* 2010). The N-terminus of the FUS gene plays an

important role in the transcriptional activation of the gene. Mutation at the C-terminus interrupts the transport of FUS into the nucleus, which results in the cytoplasmic localization of FUS and the formation of stress granules (Dormann *et al.,* 2010, Bosco *et al.,* 2010). A study in the transgenic Drosophila model observed age-dependent progressive motor neuron damage when WT R524S (arginine at codon 524 changes to serine) or P525L (proline at codon 525 changed to leucine) mutant FUS is over-expressed in photoreceptors (Chen *et al.,* 2011).

1.7.1.6 Vesicle associated membrane protein B (VAPB)/ALS8

ALS8 was identified in a large Brazilian family, in which 28 males and females were affected across four generations. The onset develops between 31-45 years and symptoms are characterized by postural tremor, fasciculations, slow progressive upper and lower limb weakness. ALS8 is Linked with a novel locus at chromosome 20q13.3, and the mutation analysis in the VAPB protein showed the presence of a proline instead of serine in position 56 (Nishimura *et al.,* 2004). VAPB is an integral endoplasmic reticulum (ER) membrane protein involved in various functions like intracellular vesicle trafficking, lipid transport, and the unfolded protein response. Mutations in the VAPB domain led to VAPB aggregation into ER clusters, resulting in a decreased ER anchoring of lipid-binding proteins and motor neuron degeneration (Nishimura *et al.,* 2004, Chen *et al.,* 2010). The reduced expression of VAPB in human and mouse models of ALS suggests the involvement of VAPB in ALS (Teuling *et al.,* 2007, Tudor *et al.,* 2010). However, a study demonstrated that overexpression of VAPB^{P56S} in mouse spinal cord could produce VAPB aggregates, but it is not linked with MN degeneration, meaning that the mutant VAPB aggregates may cause MN degeneration by loss of function rather than gain-of-toxicity (Qiu *et al.,* 2013).

1.7.1.7 Angiogenin (ANG)/ALS9

ALS9 is an autosomal dominant adult-onset disease exhibiting the classic signs of ALS. Few patients also display the symptoms of Parkinson's and FTD. Angiogenin is positioned at chromosome 14q11.2 and was first identified in patients from Ireland and Scotland (Greenway *et al.,* 2004). Few fALS cases bear both ANG and FUS mutations or SOD1 mutations. ANG is a pancreatic ribonuclease that plays an important role in inhibiting the translation of proteins and helps in rRNA biogenesis and cellular proliferation (Millecamps

et al., 2010, Luigetti *et al.,* 1924). ANG mediates neovascularization and promotes neurite outgrowth during early embryonic development. Mutations in the ANG gene results in the loss of ribonucleolytic activity and nuclear translocation activity (Padhi *et al.,* 2012).

1.7.1.8 TAR DNA binding protein (TARDBP)/ALS10

ALS10 was first reported in fALS cases in 2008. Previous studies showed more than TARDBP 40 mutations in different groups with an incidence of ~4-5% in fALS and up to 2% in sALS. TARDBP-related ALS patients present with predominant limb onset and a wide variation in the duration and age of onset (30–77 years). TARDBP mutations have been recognized in both ALS-FTD and FTD cases. TARDBP is one of the major components of cytoplasmic inclusions in ALS and FTD (Sreedharan *et al.,* 2008) and it can be also found in other neurodegenerative disorders such as HD, AD, and PD (Da Cruz *et al.,* 2011). TDP-43 is a DNA/RNA binding protein, known to be involved in various functions including gene transcription, RNA splicing, microRNA processing, and stabilization and transport of mRNA. TDP-43 has many binding targets, such as FUS, vasolin containing protein (VCP), progranulin, and other transcripts encoding neurodegenerative disease-associated proteins as well as many other RNA processing genes (Buratti *et al.,* 2012).

1.7.1.9   FIG 4/ALS11

ALS 11 is an adult-onset ALS with a rapidly progressive course, characterized by early bulbar involvement and slight cognitive impairment. The causative gene for ALS11 is a Sac1 domain-containing protein 3 located on chromosome 6q21 (Pasinelli *et al.,* 2006). FIG 4 is a phosphoinositide 5-phosphatase involved in trafficking endosomal vesicles back to the trans-Golgi network (Michell *et al.,* 2009). Mutations in FIG 4 result in neurodegeneration in sensory and autonomic ganglia, motor cortex, and striatum (Chow *et al.,* 2007, Zhang *et al.,* 2007). Moreover, mutant mice without Vac14, the gene coding for a FIG 4 interactor, show neurodegeneration. Mutations in FIG 4 and Vac14 lead to cytoplasmic inclusion formation containing p62, LC3-II, and LAMP-2, suggesting that autophagy may play a role in the gene mutation-induced neurodegeneration (Zhang *et al.,* 2007).

1.7.1.10   Optineurin (OPTN)/ALS12

ALS12 has slow disease progression characterized by lower limb onset and upper MN involvement. A genetic study showed homozygous deletion of exon 5 and another homozygous nonsense (Q398X) mutation in chromosome 10p13 (Pasinelli *et al.,* 2006). A cohort study on fALS and sALS patients revealed two homozygous mutations and one heterozygous missense mutation (E478G). OPTN is known to co-localize with FUS, TDP43, and SOD1 in inclusion bodies of sALS and fALS patients. This protein is involved in protein trafficking, maintenance of the Golgi complex, and exocytosis (Maruyama *et al.,* 2010). Mutations in the OPTN protein induces neurotoxicity through loss of function (Sakaguchi *et al.,* 2011, Wild *et al.,* 2011). OPTN mutation uninterrupted NF-κB neurotoxicity (Maruyama *et al.,* 2010). Literature demonstrated the role of OPTN in autophagy through phosphorylation by TBK1 (Wild *et al.,* 2011) and clearance of protein aggregation via a ubiquitin-independent way (Korac *et al.,* 2013)

1.7.1.11 Valosin containing protein (VCP)/ALS14

ALS 14 is characterized by limb-onset motor neuron symptoms with an average onset of the disease of 49 years (Pasinelli *et al.,* 2006). A single heterozygous missense mutation was reported in an Italian family in the gene coding for VCP, located in chromosome 9p13.3. Further analysis of 210 fALS patients showed three more VCP mutations in four patients. VCP mutations are a rare cause of fALS, and clinical features could include FTD, Paget's disease, inclusion body myopathy, and parkinsonism (Johnson *et al.,* 2010).

VCP is involved in various cellular functions, such as protein homeostasis through endoplasmic reticulum-associated degradation (ERAD), Golgi biogenesis, assembly of peroxisomes, vesicle transport and fusion, and autophagy. VCP can induce ER stress by activating the unfolded protein response that leads to the aggregation of misfolded proteins and results in apoptotic cell death (Pasinelli *et al.,* 2006, Johnson *et al.,* 2010). A study on control and ALS patients showed that the amount of VCP in the skin of ALS patients is higher than in controls (Ishikawa *et al.,* 2013).

1.7.1.12   Ubiquilin 2 (UBQLN2)/ALS15

ALS15 is an X-linked dominantly inherited disease with upper MN and lower MN involvement (Pasinelli *et al.,* 2006). Some of the patients also reported dementia. UBQLN2

gene maps to chromosome Xp11. A genetic study reported a point mutation in the coding region of the UBQLN2 gene, which substituted proline with histidine (Kaye *et al.,* 2000). Furthermore, four more missense mutations were identified in four families, all substituting proline with some other amino acid (Deng *et al.,* 2011). UBQLN2 is a ubiquitin-protein, which controls protein degradation by delivering ubiquitinated proteins to the proteasome. Mutations in UBQLN2 disturb the protein degradation pathway, which results in the aggregation of protein and neurodegeneration. UBQLN2 mutations are also present in other ALS patients, such as Ubiquitin, p62, TDP-43, FUS, and OPTN, but negative for SOD1 (Deng *et al.,* 2011, Daoud *et al.,* 2011)

1.7.1.13 SIGMAR1/ALS16

ALS 16 is characterized by initial signs of spasticity and hyperreflexia of upper MN, which can also proceed to lower MN and paralysis. Homozygosity mapping found a linkage on chromosome 9p13.2-21.3 with the mutation in SIGMA non-opioid intracellular receptor1 (SIGMAR1) gene (Al-Saif *et al.,* 2011). The linkage studies were done in one Dutch and one Scandinavian family to identify the connection between familial ALS with FTD and the chromosome 9p13.2-21.3 (Morita *et al.,* 2006). It was found that in the Scandinavian family, ALS and FTD occur separately; however, in the Dutch family, all the members showed both ALS and FTD symptoms ((Morita *et al.,* 2006, Luty *et al.,* 2010). A genetic study identified a nucleotide substitution in the SIGMAR1 gene in a patient with ALS and FTD. The mutation disrupted the stability of the transcript and dysregulated the channel activity (Luty *et al.,* 2010).

1.7.1.14 ALS-FTD1 and ALS-FTD2

ALS-FTD1 and ALS-FTD2 are adult-onset disorders that present with the symptoms of both fALS and FTD. ALS-FTD1 is known to be linked to chromosome 9q21-q22, mapped in 16 ALS-FTD families (Hosler *et al.,* 2000). ALS-FTD2 has been linked to chromosome 9p21. A hexanucleotide GGGGCC repeat expansions in the C9orf72 gene has recently been identified as the genetic defect of ALS-FTD2 (DeJesus-Hernandez *et al.,* 2011). Currently, C9orf72 mutation is the most common genetic cause of fALS and FTD, accounting for approximately 34.2 and 25.9% of the cases, respectively (van Blitterswijk *et al.,* 2012).

Along with the FTD and ALS, C9orf72 mutation also shows other features, such as memory loss, psychosis, akinetic-rigid and cerebellar signs (Rademakers *et al.,* 2012).

1.7.1.15 Dynactin 1 (DCTN1)

DCTN1 mutations determine a slow and progressive autosomal dominant form of ALS characterized by hereditary motor neuronopathy. The genetic studies first identified the mutation in the p150 subunit of the DCTN1 gene, mapped on chromosome 2p13. After that, three more mutations have been found in the DCTN1 gene in sALS, fALS, and ALS-FTD families (Münch *et al.,* 2004). The dynactin binds with the microtubule motor protein dynein during the axonal transport of vesicles and organelles (Holzbaur *et al.,* 1996). The mutation in the DCTN1 gene leads to impaired axonal transport in motor neurons and results in neurodegeneration. Several studies identified the role of dynactin in the pathogenesis of ALS (Laird *et al.,* 2008, Puls *et al.,* 2003). G59S (glycine at codon 59 changed to serine) is a major component of the dynein/dynactin complex, and the mutation in the G59S can cause motor neurodegeneration. A study demonstrated that G59S p150glued knock-in mice showed loss of spinal motor neurons, increase of reactive astrogliosis, and excessive accumulation of cytoskeleton and synaptic vesicle proteins at the neuromuscular junctions (Lai *et al.,* 2007). Valérie Bercier and colleagues showed that a decrease of DCTN1 mRNA and protein can lead to sALS (Bercier *et al.,* 2019).

1.7.1.16   Other rare mutations in fALS

A genome analysis used the microsatellite markers on a set of families with ALS cases and identified a mutation in the D-amino acid oxidase (DAO) gene located on chromosome 12q22-23 in a single three-generation family. This mutation is characterized by the classical ALS signs, with early bulbar involvement and a limited decline in cognitive skills (Mitchell *et al.,* 2010). Mutations in the R199W (arginine at codon 199 changed to tryptophan) position of the DAO gene decrease the cell viability, increase the formation of ubiquitinated aggregates, and result in the apoptosis of MN cultures (Barker *et al.,* 1977). A co-culture of MNs and astrocytes with R199W mutation showed motor neuron death (Mitchell *et al.,* 2010). This neurodegenerative effect could generate either from the accumulation of aberrant proteins or from impaired enzyme activity. Impaired enzyme activity leads to the

accumulation of D-serine, which increases glutamate transmission and causes motor neuron death (Sasabe *et al.,* 2012).

A large European family was identified with ALS3 mapped to chromosome 18q21, which codes for 50 genes but the exact gene causing the disease is yet to be identified. In one fALS family, designated as ALS7, ALS patients show signs of adult-onset fALS with rapid disease progression (Pasinelli *et al.,* 2006).

1.7.2 Genetics of sALS

The major clinical difference between sALS and fALS is the age of onset. sALS is mainly recognized in older patients. All other clinical features, including extrapyramidal and cerebellar signs or cognitive involvement, are the same as fALS (Czaplinski *et al.,* 2006). The proportion of sALS is higher in men than in women (Pasinelli *et al.,* 2006). The exact cause of sALS in most cases is not known. Some fALS genes such as C9orf72, TDP-43, FUS, and SOD1 have also been reported in a small proportion of sALS cases (Turner *et al.,* 2013). The crosslink between genetic and environmental factors may contribute to the pathogenesis of sALS (Maruyama *et al.,* 2010).

1.7.2.1   Apurinic endonuclease (APEX1)

Mutation analysis in 117 Scottish sALS patients showed an SNP association ending in a D148E amino-acid change in APEX1 and confirms that APEX1 mutations may cause sALS in a particular geographic population (Hayward *et al.,* 1999). APEX1 is known to decrease oxidative stress by participating in the process of DNA repair and DNA binding of transcription factors. Mutated APEX1 lost the redox activity and failed to stimulate cell proliferation. APEX1 redox activity also protects neurons from ionizing radiations that produce reactive oxygen species and oxidative DNA damage (Vasko *et al.,* 2011).

1.7.2.2   Charged multivesicular body protein 2B (CHMP2B)

The CHMP2B mutation was first revealed in a Danish family characterized by a predominant lower MN phenotype, and one patient also showed signs of FTD. Later, three missense mutations in the CHMP2B gene were found in 433 ALS patients (Skibinski *et al.,* 2005). CHMP2B belongs to the CHMP family and is involved in the degradation of surface receptor proteins and trafficking of proteins between plasma membrane, trans-Golgi

network, and lysosomes (Skibinski *et al.,* 2005, Cox *et al.,* 2010). Mutation in the CHMP2B can result in disrupted endosomal structure, dendritic retraction, and autophagosomal aggregation (Belly *et al.,* 2010, Ghazi-Noori *et al.,* 2012).

1.7.2.3   *Neurofilaments*

Neurofilaments are neuronal cytoplasmic filaments present in the cytoskeleton of myelinated axons. Neurofilaments are formed by different molecular mass subunits encoded as neurofilaments light (NEFL), medium (NEFM), and heavy (NEFH). The over-accumulation of neurofilaments, mainly NEFH, causes ALS in a small proportion of patients (Al-Chalabi *et al.,* 1999). One study demonstrated that the overexpression of NEFH and NEFL can cause paralytic symptoms in mice associated with axonal atrophy and motor dysfunction. NEFL plays a role in neurofilament assembly. One study in NEFL-null mice showed a reduction in axons (Couillard-Després *et al.,* 1998). Apart from ALS, NEFL mutations also cause   the Charcot-Marie-Tooth disease, a hereditary sensory and motor neuropathy (Mersiyanova *et al.,* 2000).

1.7.2.4   *Paraoxonase (PON)*

PONs is consisted of 3 units named PON1, PON2, and PON3 located on the 80-kb block of chromosome 7q21.3. PON1 and PON3 are mainly expressed in the liver, enter the blood, and show protective action against atherosclerosis, whereas PON2 is expressed in many tissues (Giordano *et al.,* 2011). One study quantified the expression of PON1 and PON2 in the mouse brain (Giordano *et al.,* 2011, Horner *et al.,* 2003). PON proteins participate in lactone hydrolysis and detoxification of organophosphate pesticides, neurotoxins, and aromatic esters, which are associated with sALS (Saeed *et al.,* 2006, Valdmanis *et al.,* 2008). Recently, a genetic study in fALS and sALS patients identified seven mutations in the PON genes (Ticozzi *et al.,* 2010). Moreover, PON2 knockout mice induced neurotoxicity caused by oxidative stress as compared to wild-type mice taking advantage of the neuroprotective role of PON2 (Giordano *et al.,* 2011).

1.7.2.5   *Peripherin (PRPH)*

PRPH is a type III intermediate filament present in neurons in the peripheral nervous system. In neuronal injury, the expression of PRPH increases in the spinal, MNs indicating a role in

axonal regeneration (Mizuno *et al.,* 1999). A study showed MN degeneration in overexpressing PRPH mice (Beaulieu *et al.,* 1999). One study conducted on 122 Italian ALS patients revealed two missense PRPH mutations, named p.R133P (arginine at codon 133 changed to proline) and p.D141Y (aspartic acid at codon 141 changed to tyrosine), that have a deleterious effect on protein structure and function (Corrado *et al.,* 2011). Some mouse models show PRPH splice variants, which may contribute to ALS pathogenesis. A pathogenic isoform of PRPH, named Per61, was found in MNs of both mutant SOD1 and TDP-43 mice but not in wild-type c mice (Robertson *et al.,* 2003, Schwab *et al.,* 2012). One recent study reported the overexpression of another PRPH splice variant (Per28) in ALS patients (Xiao *et al.,* 2008).

1.7.2.6   *Survival motor neuron (SMN) 1 and 2*

SMN, also known as 'GEMS' (Gemini of the coiled bodies, plays an important role in mRNA metabolism. SMN forms a complex with several spliceosomal small nuclear ribo-nucleoproteins) (Lefebvre *et al.,* 1997, Veldink *et al.,* 2005). The SMN genes map to chromosome 5q13 and are present in humans in two copies, the telomeric copy named SMN1 and the centromeric copy named SMN2 (Lefebvre *et al.,* 1995).

The damage in the assembly and function of the spliceosome could cause motor neuron degeneration. Mutation in the SMN1 gene (was first identified in SMA, which is the second most frequent autosomal recessive disorder found in childhood. After this discovery, most research has focused on the role of these genes in ALS (Corcia *et al.,* 2002). Later, four studies have described quantitative PCR results of SMN1 or SMN2 genes in sporadic ALS (Veldink *et al.,* 2001, Corcia *et al.,* 2002, Veldink *et al.,* 2005, Corcia *et al.,* 2006). They compared the SMN1 copy number of 890 ALS patients with controls. Three out of four studies stated that the SMN1 copy number increased in the ALS population. A study conducted on 110 ALS patients and 100 controls detected an increase in the frequency of SMN2 deletions in sALS patients (Veldink *et al.,* 2005).

1.7.2.7   *Vascular endothelial growth factor (VEGF)*

VEGF acts as a hypoxia-responsive element and is known to play an important role in angiogenesis. VEGF is also involved in some other processes, such as inflammation and tumor progression (Dvorak *et al.,* 1995). In addition to hypoxia, other stimuli regulate the

expression of the VEGF gene, such as nitric oxide, estrogen, and a large variety of growth factors, like insulin-like growth factor (IGF-1), tumor necrosis factor-alpha (TNF-α), epidermal growth factor (EGF), transforming growth factor-beta (TGFβ), interleukin- (IL-) 6, and IL1-β. Six different VEGF factors exist, named VEGF-A, placental growth factor (PlGF), VEGF-B, VEGF-C, VEGF-D, and VEGF-E. Recent studies showed that VEGF-A, VEGF-B, and VEGF-C directly affect neural cells (Raab *et al.,* 2007). There are mainly two classes of VEGF receptors, tyrosine kinase, and the non-tyrosine kinase receptors.

In 2001, the first study was published demonstrating the role of VEGF in ALS (Oosthuyse *et al.,* 2001). Mutation in the VEGF gene in mice resulted in a new and unexpected role for VEGF in MN degeneration. The authors produced mice with a homozygous deletion in the hypoxia response element (HRE) site in the VEGF promoter region. About 60% of mice died before or around birth due to vascular abnormalities in the lung, and 40% of survived mice showed symptoms of MN degeneration after five months. After 17 months, these mice reported losing almost 30% of MNs in the ventral horns of the spinal cord. A study revealed that deletion in mice of HRE from the VEGF promoter could cause MN degeneration as in ALS (Oosthuyse *et al.,* 2001). Research conducted in mutant SOD1 rats showed that intramuscular and intra-cerebroventricular administration of VEGF prolonged survival (Storkebaum *et al.,* 2005). Literature demonstrated a significant decrease in the expression of VEGF and its receptors in the spinal cords of ALS patients (Brockington *et al.,* 2006). A broad study was conducted on ALS patients and controls from Sweden, Belgium, and England to identify the specific mutations. The results showed that specific SNPs in the VEGF gene are associated with a lower level of VEGF expression and a higher risk of ALS (Lambrechts *et al.,* 2009).

1.7.2.8   *Progranulin (PGRN)*

Progranulin is a highly conserved glycoprotein expressed in multiple cell types, both in the CNS and in peripheral tissues. It is a precursor of granulins and is involved in functions like cell growth, survival, repair, and inflammation. PGRN also regulates the lysosomal function and microglia responses in the CNS (Townley *et al.,* 2018). Previous studies showed the association of PGRN and activated microglia in several neurodegenerative diseases (Baker *et al.,* 2006). Mutation in the PGRN gene leads to protein haploinsufficiency, which can cause neuropathologic frontotemporal lobar degeneration (FTLD) associated with the

accumulation of TDP-43 inclusions. PGRN mutations also cause neuronal ceroid lipofuscinosis. A study conducted by Schymick and colleagues showed that PGRN nonsense and deletion mutations cause ubiquitin-positive, tau negative FTD (Schymick *et al.,* 2007).

1.7.2.9 Ataxin-2 (ATXN2)

Ataxin-2 is a cytoplasmic protein encoded by the ATXN2 gene containing a polyglutamine (poly Q) tract with normally 22–23 repeats present in the N-terminal part of the protein (Ross *et al.,* 2011, Sequeiros *et al.,* 2010). In healthy individuals, CAG repeats in ATXN2 are interspersed with CAA codons to form the most common repeat length of 22 repeats [(CAG)8- CAA(CAG)4CAA(CAG)8] (Imbert *et al.,* 1996). Spinal cerebellar ataxia type 2 (SCA2) was the first disease associated with polyQ repeat expansions in ATXN2 (Gispert *et al.,* 1993). Sequencing showed that SCA2 consists of 37 uninterrupted CAG repeats (Pulst *et al.,* 1996, Sanpei *et al.,* 1996). In rare late-onset diseases, long lengths (32–33) CAG repeats were found, and intermediate-length polyQ repeats (23–34) were found in ALS patients (Pasinelli *et al.,* 2006)

ATXN2 is known to interact with two common ALS proteins, FUS and TDP-43, and modifies their cellular toxicity. ATXN2 and TDP-43 form an RNA-dependent complex, and long polyQ repeats stabilize ATXN2 and increase its interaction with TDP-43. This leads to enhanced dislocation of TDP-43 into the cytoplasm in the spinal cord MNs of ALS patients (van den Heuvel *et al.,* 2014, Elden *et al.,* 2010).

1.8 Metabotropic Glutamate Receptors

As described above, ionotropic glutamate receptors are ligand-gated ion channels and mediate fast excitatory synaptic signalling and have a key role in synaptic plasticity (Wollmuth, 2018). Metabotropic glutamate receptors (mGluRs) are G protein-coupled receptors (GPCRs) that modulate synaptic transmission and neuronal excitability. They are mainly divided into three groups based on their sequence homology, pharmacology, and transduction mechanism (Kim *et al.,* 2020).

- Excitatory Group I receptors (mGluR1 and mGluR5)
- Inhibitory Group II receptors (mGluR2 and mGluR3)
- Inhibitory Group III receptors (mGluR4, mGluR6, mGluR7, mGluR8)

The structure of GPCRs shares a common domain composed of 7 transmembrane helices, an extracellular N-terminal domain, and an intracellular C-terminal domain. This structure allowed the identification of several families of GPCRs (Pin *et al.,* 2003). mGluRs were marked as a new family of GPCRs, which were discovered when the mGluRs were cloned (Houamed *et al.,* 1991; Masu *et al.,* 1991). The structure of mGluRs consists of a large N-terminal extracellular signal sequence, a hydrophilic extracellular agonist-binding domain that contains nineteen cysteine residues, the seven transmembrane domains (7TM), and a cytoplasmic C-terminal domain variable in length (Conn and Pin, 1997). The cysteine-rich extracellular domain and the extracellular loops are maintained among all the members of the mGluR family. Another characteristic shared by these receptor family is the N-terminal binding site, composed of two globular domains with a hinge region that can deeply modify its conformation depending on the ligand interaction (Conn and Pin, 1997).

1.8.1 *Group I Metabotropic Glutamate Receptors*

Group-I type of mGluRs includes mGluR1 and mGluR5 and is mainly distributed in the CNS, specifically at synaptic and extrasynaptic sites in both neurons and glia. Depending on the different C-terminal domains, they can be classified into various variants such as mGluR1a, 1b, 1c, 1d, and mGluR5a, 5b. Apart from the postsynaptic location, several studies demonstrated the expression of group I mGluRs also in presynaptic terminals by immunocytochemical and biochemical analyses (Pin *et al.,* 2003; Raiteri, 2008; Schoepp, 2001; Muly *et al.,* 2003; Musante *et al.,* 2008). Various studies reported the functional interaction between heterodimers of mGluR1 and mGluR5 (Fazal *et al.,* 2003; Musante *et al.,* 2008). The composition of the heterodimer also plays a role in the case of knocking down mGluR1 or mGluR5 (Milanese *et al.,* 2014; Bonifacino *et al.,* 2017).

Both mGluR1 and mGluR5 can exert different functions based on their localization in the brain (Moroni *et al.,* 1998; Reid *et al.,* 1999; Fazal *et al.,* 2003). The literature showed that mGluR1 is highly involved in the regulation of sensory and motor functions while mGluR5 is mainly involved in synaptic plasticity, learning and memory.

mGluR1 and mGluR5 expressed in microglia participate in cell migration (Liu *et al.,* 2009) and modulate the inflammatory phenotype (Pinteaux-Jones *et al.,* 2008). Similarly, the expression of mGluR5 in astrocytes participates in enhancing cell repair after injury, either

through the actions of neurotrophins and growth factors or through the production of cytokines and inflammatory mediators (Planas-Fontanez, 2020).

Group I mGluRs are activatory by coupling with Gq/11 protein that results in the stimulation of various downstream pathways (Nicoletti *et al.,* 2011). Moreover, Group I mGluRs can modulate additional downstream of Gq/11 protein, as well as signalling pathways regulated by Gi/o, Gs, and by other molecules independent from G proteins (Hermans and Challis 2001). Accordingly, the PLC and PKC activation and the increase of intracellular Ca^{2+} levels are not the unique consequences of Group I mGluR activation. An example is represented by a study carried in-vitro in rat cerebral cortical astrocytes expressing a high level of mGlu5 receptors. The mGluR1 and mGluR5 agonist, 3,5-dihydroxyphenylglycine (3,5-DHPG), caused an accumulation of cyclic AMP (cAMP) in these cells. Even though the direct link between mGluR5 and Gs protein has not been demonstrated, the mechanism is independent of PKC, PLC, and intracellular Ca^{2+} level (Balazs *et al.,* 1998).

The G proteins coupling is mainly controlled by the intracellular loops 2 and 3, and by the C-terminal domain (De Blasi *et al.,* 2001). A study revealed that the long C-terminal domain of mGluR1a enhances the coupling efficiency by exerting a small agonist-independent activity (Prezeau *et al.,* 1996). In addition, this domain also interacts with scaffolding proteins such as Homer-1, which can interact with mGluR5 and mGluR1a and regulate the insertion and the clustering in the cellular membrane or other cellular compartments (Pin *et al.,* 2003). Homer-1 is known to interact with phosphatidylinositide 3-kinase enhancer L and activates the phosphatidylinositide 3-kinase (PI3K) (Ahn and Ye, 2005). This interaction is linked with the activation of a PI3K-dependent anti-apoptotic signaling pathway that supports neuronal survival and sheds light on the relationship between NMDA and mGluR1a. Accordingly, Ca^{2+} rise by NMDAR activation results in calpain-mediated truncation of the C-terminal domain of mGluR1a. The truncated mGluR1a maintains its ability to increase cytosolic Ca^{2+} and no longer activates the neuroprotective PIK3-dependent signalling pathway (Caraci *et al.,* 2012; Xu *et al.,* 2006).

Another pathway that connects Group I mGluRs and NMDARs is tyrosine-protein kinase Src. The activation of mGluR5 induces phosphorylation of NR2A and NR2B domains of the NMDAR, increasing Ca^{2+} currents. Dysregulation of this pathway leads to increased excitotoxicity and results in neuronal death (Takagi N *et al.,* 2012). The extracellular signal-

regulated kinases (ERK) cascade pathway is also linked with Group I mGluRs, which regulate gene expression, cell proliferation, differentiation, and survival (Thandi *et al.,* 2002). Group I mGluRs have been shown to activate ERK in cortical glia (Peavy RD and Conn PJ, 1998) and primary astrocytes (Schinkmann *et al.,* 2000). The ERK pathway is activated via Gi/o protein (Thandi *et al.,* 2002). These data suggest that mGluR1 and mGluR5 not only exhibit different anatomical and cellular distributions in the CNS (Hubert *et al.,* 2001; Valenti *et al.,* 2002), but they also differ in the downstream signalling partners and the resulting activated pathways (Thandi *et al.,* 2002).

1.8.2 Group I Metabotropic Glutamate Receptors: Activation and Pharmacology

Recent evidence supports the heterodimerization of GPCRs, making it possible to interact via different sequence elements to target the protein-protein interaction interfaces (Milligan, 2006; Milligan and Smith, 2007). The same emerged for mGluRs (Doumazane *et al.,* 2011). Various studies looking at protein shared sequences of the extracellular N-terminal domains of the mGluRs allowed elucidating the structure and function of these metabotropic receptors.

Briefly, the extracellular N-terminal domain of mGluRs revealed a bilobate structure. The lobes (LBs) are separated by a cleft where glutamate binds. These LBs are usually in an open state in the absence of ligand, and they close in its presence (Pin *et al.,* 2003). Whereas quivering was observed between the open and closed states even without ligand, stabilizing in the closed state. Because of these structural characteristics, such a protein domain was called the Venus Flytrap domain (VFD). This constant equilibrium between the two states is crucial for the ligand affinity to the receptor (Pin *et al.,* 2003). A very first study on mGluR1 showed that in the open form glutamate exclusively binds lobe 1 (LB1), whereas, in the closed state, it makes additional contacts with residues of lobe 2 (LB2), stabilizing the closed condition of mGluR1 (Pin *et al* 2003). VFD can also change from an active to a resting state. Accordingly, in the absence of the ligand, the two VFDs likely will be in an open state, and this orientation corresponds to the resting state. Upon binding the agonist to at least one VFD, this closes to the other, allowing the correct association between the two LBs, stabilizing the active orientation of the dimer. The active orientation is further stabilized upon binding the agonist in the second VFD and after the association with a cation (like Ca^{2+}) at the interface between the two LBs (Pin *et al.,* 2003). Open and closed

conformations depend on the distance between the LB1 and LB2 to form a unique VFD domain; thus, the active and resting states are linked to the distance between the two LBs. A number of Group I mGluRs agonists have been identified such as 3-hydroxyphenylglycine (3-HPG) and (S)-3,5-dihydroxyphenylglycine (3,5-DHPG). They selectively activate Group I mGluRs, but not Group II and III s. Moreover, mGluR5 can be specifically activated by (R,S)-2-Amino-2-(2-chloro-5-hydroxyphenyl)acetic acid (CHPG) (Doherty *et al.,* 1997; Conn and Pin, 1997).

Moreover, several antagonists and allosteric modulators can bind Group I mGluRs mainly in the heptahelical domains of mGluRs and alter the conformational state of the receptors (Stansley and Conn, 2019). CPCCOEt was the first negative allosteric modulator of mGluR1 identified (Annoura *et al.,* 1996). This compound inhibits the mGluR1 signaling without affecting glutamate binding (Litschig, *et al.,* 1999). Another compound, 2-chloro-4-((2,5-dimethyl-1-(4-((trifluoromethoxy)phenyl)-1H-imidazol-4-yl(ethynyl)pyridine (CTEP), an oral bioavailable mGluR5 negative allosteric modulator optimized for chronic *in-vivo* treatments in rodents (Lindemann *et al.,* 2011) and already tested in mouse models of Huntington's and Parkinson's diseases (Abd-Elrahman *et al.,* 2017; Farmer *et al.,* 2020). Also, some other very potent and selective mGluR1 antagonists were identified such as LY367385 (Clark *et al.,* 1997), SIB-1757, SIB-1893 (Varney *et al.,* 1999), and fenobam (Porter *et al.,* 2005). More recently, MPEP showed an in-vitro protective effect against excitotoxicity induced by AMPA and NMDA (D'Antoni *et al.,* 2011; Takagi *et al.,* 2012). Several PAMs active at Group I mGluRs have also been developed, including the selective mGluR5 PAMs, such as DFB, CPPHA, CDDPB (VU29, and ADX47273, and PAMs specific for mGluR1, such as Ro 67-7476Ro 67-4853VU71 (Niswender and Conn, 2010).

1.8.3 Group I Metabotropic Glutamate Receptors: Regulation and Desensitisation

Group I mGluRs undergo homologous or heterologous changes after their activation, similarly to the other GPCR families (De Blasi *et al.,* 20 01). Multiple mechanisms are responsible for these changes, however, the PKC activation-induced phosphorylation of the intracellular residues of threonine and serine of mGluR1 and mGluR5 plays a major role. This mechanism has been verified in several systems, including primary neuronal cultures, hippocampal slices, astrocytes, and synaptosomes (De Blasi *et al.,* 2001).

Nevertheless, PKC activation is not the sole mechanism since G-protein-coupled receptor kinases (GRKs) are also involved in this phenomenon. These proteins (GRK1-GRK6) are targeted to the membrane protein and phosphorylate some residues of the C-terminal domain of the receptor. Phosphorylation allows β-arrestin to bind at the newly generated binding site to uncouple the receptor from the G protein, and induce its internalization (De Blasi *et al.,* 2001). Other proteins involved are CaMKII, huntingtin-binding protein optineurin, and second messenger-dependent protein kinases (Dhami and Ferguson, 2006).

1.8.4 *Group I Metabotropic Glutamate Receptors: Pathological Aspects*

Group, I mGluRs are mainly involved in the dysregulation of glutamate neurotransmission in several neurodegenerative diseases such as ALS, epilepsy, AD, PD, HD, ischemia and stroke, Fragile x mental disorder, stress disorders, and anxiety (Recanses *et al.,* 2007; Ribeiro *et al.,* 2017). Overexpression of mGluR5 has been reported in reactive astrocytes surroundings Aβ plaques, spinal cord lesions, multiple sclerosis (MS) lesions, hippocampal astrocytes from Down syndrome patients, and in ALS (Spampinato *et al.,* 2018).

Group I mGluRs play an important role in ALS. Studies demonstrated that in healthy humans, mGluR1 is mainly expressed in the spinal cord ventral horn neurons and mGluR5 in the dorsal horn neurons (Tomiyama *et al.,* 2001; Aronica *et al*, 2001), while astrocytes express low levels of These receptors. In ALS patients, reactive glial cells show a high expression of mGluR1 and mGluR5 in the gray and white matter (Aronica *et al.,* 2001). An in-vitro study confirmed this finding by adding cerebrospinal fluid (CSF) from ALS patients to rodent astrocyte cultures, which resulted in significant increases in astrocyte proliferation (Anneser *et al.,* 2004). Another study showed that the activation of Group I mGluRs with the non-selective agonist 3,5-DHPG negatively altered the phenotype of astrocytes and microglia that surround motor neurons, whereas the treatment with receptors antagonists inhibited the gliosis (Anneser *et al.,* 2004). A study evidenced the overexpression of Group I mGluRs in the striatum, hippocampus, and frontal cortex of SOD1^{G93A} mice during the progression of the disease (Brownell *et al.,* 2015). The involvement of astrocytes and the link with mGluR5 expression during ALS progression were also confirmed by Rossi and colleagues, who showed that SOD1^{G93A} astrocytes are very vulnerable to glutamate and undergo cell death mediated by mGluR5 (Rossi *et al.,* 2008).

Several studies proposed the selective blockade of Group I mGluRs as a therapeutic strategy in ALS. Rossi and colleagues showed that the non-competitive mGluR5 antagonist MPEP slows down astrocyte degeneration, delays the onset of the disease, and prolongs the SOD1^{G93A} mice survival (Rossi *et al.,* 2008). This activity was also confirmed in neurons by the reduction of AMPA-mediated toxicity (D'Antoni *et al.,* 2011).

SOD1^{G93A} mice showed an increase in glutamate release in response to Group I mGluRs activation (Giribaldi *et al.,* 2013). mGluRs regulate the glutamate synaptic transmission through several transduction pathways and influence the expression of glutamate transporters GLT-1 and GLAST expressed by astrocytes (Aronica *et al.,* 2003). A study provides in-vitro evidence for a crosstalk between mGluR5 and GLT-1 in SOD1^{G93A} rat astrocytes, advancing the hypothesis that mGluR5 acts as a sensor of synaptic glutamate concentration, which modulates the uptake activity in glial cells (Vermeiren *et al.,* 2005).

1.8.5   *Effects of the Downregulation of Group I mGluRs in the SOD1^{G93A} Mouse Model of ALS*

Based on previous results published by my research group, which showed the abnormal exocytotic release of glutamate in pre-symptomatic and late symptomatic SOD1^{G93A} mice (Milanese *et al.,* 2011; Bonifacino *et al.,* 2016) and which is associated with the increase in the activity and overexpression of Group I mGluRs (Giribaldi *et al.,* 2013; Bonifacino *et al.,* 2019b). They also evaluated the impact of mGluR1 in ALS by downregulating mGluR1 in the SOD1^{G93A} genetic background. Halving mGluR1 significantly decreased the disease onset and progression, increased the life span, reduced astrogliosis and microgliosis, and increased the number of motor neurons in spinal cord. They also identified that glutamate release induced by 30μm 3,5-DHPG in SOD1^{G93A} and WT mice lacking mGluR1 was lower than in controls, suggesting that the mGluR1 reduction abolishes the excessive glutamate release (Milanese *et al.,* 2014). Similar results were obtained in SOD1^{G93A} mice (Bonifacino *et al.,* 2017; 2019a). The authors bred SOD1^{G93A} mice with mGluR5 knock-down mice to halve the receptor expression. They bred the F1 generation again with mGluR5 knock-down mice to obtain a SOD1^{G93A} mouse knock out for mGluR5. These animals showed the encouraging results seen in the case of mGluR1 knock down mice. They were more evident with the complete ablation of the receptor (Bonifacino *et al.,* 2017; 2019a).

This genetically based evidence underly the importance of verifying whether the pharmacological blockade of mGluR1 and/or mGluR5 can represent a valid approach for ALS treatment. In a recent study, we orally treated SOD1^{G93A} mice with the mGluR5 negative allosteric modulator CTEP starting at an early symptomatic stage of the disease (90 days of life) until the late stage. Treated mice exhibited a more favourable clinical course in motor performance and life span, being female mice more responsive to the drug treatment. These results were accompanied by enhanced motor neuron preservation and decreased astrogliosis and microgliosis (Milanese *et al.,* 2021)

1.9 Non-Cell Autonomous Aspects of ALS

ALS is a neurodegenerative and multifactorial disease that involves different cell types such as astrocytes, neurons, microglia, and oligodendrocytes (Ilieva *et al.,* 2009, Lee *et al.,* 2012). Mutated genes are expressed in multiple cell types. Thus, ALS can arise from a combination of damaged MNs and their glial partners rather than only from the neuronal lineage. Several studies supported this statement. Using a mouse model of ALS with genetic mutation restricted to neurons, the authors showed that ALS progression slowed down (Pramatarova *et al.,* 2001, Lino *et al.,* 2002). Also, the literature showed slow ALS progression when the mSOD1 was conditionally deleted in individual glial populations (microglia, astrocytes, or oligodendrocytes) but not in MNs (Boillée *et al.,* 2006, Kang *et al.,* 2013). These results indicated that glial cells play an essential role in the disease onset and progression and highlighted a solid non-neuronal signature in ALS.

1.9.1 Astrocytes in ALS

Astrocytes are the most abundant non-neuronal cells in the CNS known to play numerous functions in the brain. Astrocytes provide metabolic support to the neurons and maintain the neurotransmitter homeostasis and blood brain barrier (BBB) integrity. Therefore, there is increasing evidence that astrocytes strongly contribute to neurodegeneration, and our understanding of the processes, which occur in the damaged CNS, is crucial for potential therapy development.

1.9.1.1 Downregulation of Glutamate Transporters in Astrocytes

Glutamate buffering is one of the significant functions of astrocytes. Glutamate clearance from the excitatory synapses is essential in normal synaptic transmission, and its impairment leads to neuron damage (Armada-Moreira *et al.,* 2020). Multiple amino acid transporters (EAATs) mediate glutamate uptake in healthy tissue. EAAT1 and EAAT2 are mainly expressed in astrocytic membranes, and they take up most of the synaptic glutamate (Mahmoud *et al.,* 2019). During ALS progression, astrocytes may lose the majority of EAAT2 in the spinal cord of the SOD1^{G93A} murine models, and astrocyte transplantation restores the function (Lepore *et al.,* 2008, Qian *et al.,* 2017). Caspase-3 plays a role in glutamate transport and disease by producing two fragments from EAAT2 protein (Boston-Howes *et al.,* 2006). These fragments are accumulated in the astrocyte nuclei in the spinal cord and lead to disease progression (Gibb *et al.,* 2007). This accumulation causes morphological changes in astrocytes, and the aggregation of EAAT2 dysregulates astrocytic gene expression. These genes are related to mitochondrial functions and cellular respiration (Foran *et al.,* 2011). The reduction of EAAT2 expression results in the imbalance of glutamate transport into the astrocytes. Therefore, excessive glutamate accumulates in the synaptic cleft and causes pathological neuronal stimulation, disrupting ionic homeostasis in neurons. This process may result in MNs damage and death in ALS (Gibb *et al.,* 2007, Foran *et al.,* 2011, Rosenblum *et al.,* 2017).

1.9.1.2 Reactive Astrogliosis

Studies have shown that astrocytes change their morphology during ALS, and become reactive in response to various stimuli, such as soluble factors secreted by microglia. This process leads to the secretion from astrocytes of various pro- and anti-inflammatory cytokines, chemokines, interferons, and growth factors, along with components of the extracellular matrix (Zamanian *et al.,* 2012). Reactive astrocytes reduce neuronal degeneration by preventing the spread of lesions and restricting ongoing inflammation by preventing infiltration of activated immune cells (Faulkner *et al.,* 2004). Besides, the modifications of the extracellular matrix, which are an essential part of reactive astrogliosis and glial scar formation, contribute to the inhibition of axonal regeneration and growth.

However, activated astrocytes in ALS have slightly different properties (Qian *et al.,* 2017, Haidet-Phillips *et al.,* 2011). Astrocytes obtained from SOD1^{G93A} mice have higher proliferative potential in vitro than wild-type astrocytes (Díaz-Amarilla *et al.,* 2011) and are larger in situ than healthy tissue, with more hypertrophied processes (Qian *et al.,* 2017). They showed high expression of typical markers for astrogliosis, such as non-filamentous GFAP (Lepore *et al.,* 2008). This elevation becomes substantial during disease progression (Díaz-Amarilla *et al.,* 2011, Almad *et al.,* 2016). In addition, SOD1^{G93A} astrocytes overexpress the Na$^+$/K$^+$ ATPase (Gallardo G *et al.,* 2014) and reduce EAAT2 levels.

1.9.1.3 Non-cell Autonomous Effect

Activated astrocytes are known to decrease the survival and recovery of MNs (Liddelow *et al.,* 2017, Tyzack *et al.,* 2017). This non-cell-autonomous damaging effect has been established in several studies using astrocyte-conditioned media for MN culture (Nagai *et al.,* 2007, Meyer *et al.,* 2014, Tripathi *et al.,* 2017). This effect is mediated by astrocyte-specific soluble factors such as cytokines or growth factors (IL-6, CXCL1, 10 and 12, tumor necrosis factor-alpha (TNF-α) or transforming growth factor-beta (TGF-β). In ALS astrocytes, these molecules are highly expressed and secreted to the surrounding tissue and cause morphological changes in MN, specifically smaller cellular bodies and shorter axons (Tripathi *et al.,* 2017). Apart from the morphological changes, secreted substances can cause axonal swelling and accumulation of mutated SOD1 and ubiquitin-positive aggregates in MN axons. Aggregates continue to rise during ALS (Gomes *et al.,* 2019), which corresponds with the progress of reactive astrogliosis. The accumulation of mutated SOD1 protein leads to MN degeneration through the impairment of mitochondrial functions (Shi *et al.,* 2010), together with increasing nitrosative stress (Rojas *et al.,* 2014, Madill *et al.,* 2017). Defective mitochondria release various pro-cell death factors and result in MN necroptosis (Re *et al.,* 2014). Like SOD1astrocytes, astrocytes obtained from humans and mice with C9orf72 or TDP-43 mutation also damaged MNs (Hautbergue *et al.,* 2017, Gupta *et al.,* 2017). Studies demonstrate that astrocytes obtained from C9orf72 patients showed reduced metabolic and proteasome functions (Gupta *et al.,* 2017, Mordes *et al.,* 2018). A recent study on human astrocytes conducted by Allen and colleagues found a reduced ability of the astrocytes to metabolize glycogen and thus utilize cellular energy sources (Allen *et al.,* 2019). Besides, astrocytes from both mSOD1 and C9orf72 decrease the glutamate transporters, which results

in the accumulation of glutamate in the synaptic cleft and excitotoxicity to MNs (Fomin V *et al.,* 2018). Aside from soluble molecules, C9orf72 astrocytes known to release extracellular vesicles containing specific microRNAs, which can cause axonal retraction and worsen overall MN survival (Varcianna *et al.,* 2019). On the other hand, TDP-43 astrocytes showed to form intracellular cytoplasmic inclusions, called stress granules (Ishii *et al.,* 2017, Khalfallah *et al.,* 2018). These stress granules consist of insoluble phosphorylated TDP-43 protein together with ubiquitin and alpha-synuclein (Koga *et al.,* 2018, Mackenzie *et al.,* 2017). Like the other ALS models, the TDP-43M337V astrocytes become reactive and show increased oxidative damage (Moujalled *et al.,* 2017, Ke *et al.,* 2015). The reactive astrocytes then upregulate small HSPs (Gorter *et al.,* 2019), which usually respond to cellular damage as a protective and stress response (Webster *et al.,* 2019).

1.9.2 Microglia in ALS

Microglia are one of the primary immune-competent cells of the brain and spinal cord and play an important role in supporting normal CNS function. Microglia exist in two states, resting and activated (Cherry *et al.,* 2014). A two-photon imaging study demonstrated that the healthy adult brain has a dynamic number of ''resting'' microglia (Nimmerjahn *et al.,* 2005), which play an essential role in maintaining homeostasis (Luo and Chen, 2012). On the other hand, ''surveillant'' microglia participate in many physiological functions, such as synaptic pruning, adult neurogenesis, and modulation of neuronal networks (Kettenmann *et al.,* 2013). Microglia activation is a major factor in the pathogenesis of ALS. However, literature demonstrated that microglial activation could play neuronal protection and injury. During the activation stage, microglia exhibit changes in cell number, morphology, surface receptor expression, and production of growth factors and cytokines. These changes altered the activation state of microglia. Macrophages induced the activation of M1 phenotype, whereas IL-10 induces activation of M2 polarization. M1 microglia promote neuronal injury by triggering the release of proinflammatory cytokines such as TNF-α and IL-1β and increasing oxidative stress by reducing the expression and release of trophic factors In contrast, M2 microglia promote tissue repair by blocking the release of proinflammatory cytokines and supporting Th2 functions that enhance neuronal survival (Benoit *et al.,* 2008, Geissmann *et al.,* 2008, Martinez *et al.,* 2008).

Several studies demonstrated that M1 microglia show hyper-reactivity to inflammation in ALS (Kreft *et al.,* 2007; Spector *et al.,* 2007; Nicolini *et al.,* 2018). A study conducted on TDP-43 ALS patients showed activation of microglia that resulted in the upregulation of pro-inflammatory NOX2, TNF- α, and IL-1β (Zhao *et al.,* 2015). Similarly, in the $SOD1^{G93A}$ model, morphological and functional activation of microglia upregulates the ROS and cytokine release (Zhao *et al.,* 2010). In addition, $SOD1^{G93A}$ microglia are involved in the toxic pathway by significantly increasing the expression of ER stress pathways (Vickers *et al.,* 2017). Therefore, modulating the microglia phenotype or inhibiting the M1 toxicity may represent a therapeutic approach to ALS. Several findings also showed the coexistence of the two opposite phenotypes, more than the transition from M2 to M1 during ALS progression. For example, beneficial components of inflammation, such as insulin growth factor-1 (IGF-1), whose release is suppressed in a proinflammatory (M1) environment but encouraged in an M2 protective one (Suh *et al.,* 2013), are overexpressed by $SOD1^{G93A}$ microglia not only in the pre-symptomatic stage but also in the end-stage (Kreft *et al.,* 2007).

1.9.2.1 T Cell Regulation of Microglial Activation

The presence of T cells plays an important role in the disease progression in animal models of fALS. In association with M2 microglia, T cells, infiltrate the CNS in the early disease stage and stabilize the disease progression (Beers *et al*. 2008; Chiu *et al*. 2008). T cells are not present at the late stage of the disease, which rapidly affects survival. Studies found increased proinflammatory cytokines and reduced mRNA of trophic factors, suggesting that functional CD^{4+} T cells are required to induce M2 microglia during the slow phase of the disease (Beers *et al.,* 2008). Transplantation of CD^{4+}T cells significantly improved survival and restored the M2 microglia phenotype (Beers *et al.,* 2008). A recent study confirmed that passively transferred CD^{4+} and CD^{25+} cells delayed motoneuron loss, improved neurological function, and increased life expectancy of SOD1 mice (Banerjee *et al.,* 2008). These results demonstrated that CD^{4+}T cells promote the M2 microglia phenotype and extend disease duration by prolonging the disease slow phase, thus supporting the concept of a well-orchestrated and complex dialog among microglia, T cells, and neurons.

1.9.2.2 Neuroprotective Microglia

Microglia release trophic and anti-inflammatory factors that prompt neuroprotective effects and survival in WT and mutated SOD1 mice (Beers *et al.* 2006; Boillée *et al.* 2006b). Previous studies showed that WT microglia release neurotrophic factors such as IGF-1 and attenuated free radicals and proinflammatory cytokines (Xiao *et al.* 2007; Beers *et al.* 2006; Weydt *et al.* 2004). Moreover, microglial treated with IL-4 suppressed the M1 microglia phenotype, reduced ROS release, enhanced IGF-1 secretion, and improved motoneuron survival (Zhao *et al.* 2006). Furthermore, a study regulated microglia neurotoxicity using CX3CR1, which modulates the neuron-to-microglia signalling (Cardona *et al.* 2006). These reports suggest that WT microglia treated with IL-4 or CX3CL1 show more M2 phenotype characteristics which may promote neuroprotection in ALS mice.

1.9.2.3 Neurotoxic Microglia

Apart from the neuroprotective activity, microglia can also exert neurotoxic actions by releasing ROS and inflammatory factors. In the case of ALS, microglia appear to switch from the M2 phenotype to the M1 phenotype, with increased expression of NADPH oxidase 2 and proinflammatory cytokines, including TNF-α and IL-1β (Beers *et al.* 2008; Henkel *et al.* 2006; Hensley *et al.,* 2002; Alexianu *et al.,* 2001). M1 activation known to be enhanced after repeated injection of LPS, resulting in reduced survival (Nguyen *et al.* 2004). LPS increases microglial activation and motoneuron toxicity by blocking NOX activity (Li *et al.,* 2008; He *et al.,* 2002). Therefore, microglia can play neuroprotective and neurotoxic roles depending on the different phenotypic activation states.

1.9.3 Oligodendrocytes in ALS

Oligodendrocytes play an essential role in CNS with the primary functions to form myelin sheath and provide neurons with metabolic support (Lee *et al.,* 2012; Morrison *et al.,* 2013). Myelin sheath helps maintain the long-term axonal integrity using metabolic and trophic support and is essential for rapid electrical nerve conduction Abnormalities in these functions can cause several neurodegenerative diseases (Nave *et al.,* 2010; Nave *et al.,* 2010). Injury to oligodendrocytes leads to damaged myelin structure and demyelination. After injury, remyelination can start where activated oligodendrocytes migrate and differentiate to replace cells lost during pathological conditions (Franklin *et al.,* 2017).

However, the efficacy of this repair process is generally low, which results in permanent deficits and functional impairments (Gruchot *et al.,* 2019). Oligodendrocytes provide neurons with energy support by transporting various energy substrates, including lactate, pyruvate, and ketone bodies, across the membranes by monocarboxylate transporters (MCTs). These transporters are mainly expressed by oligodendrocytes (Pierre *et al.,* 2005; Rinholm *et al.,* 2011). Downregulation or inhibition of these transporters results in axon degeneration (Morrison *et al.,* 2013).

The involvement of oligodendrocytes has been studied in ALS. Studies showed pathological inclusions in oligodendrocytes in the post-mortem tissue of ALS patients. These aggregates were mainly found in the cytoplasm of both sALS and fALS patients (Murray *et al.,* 2011, Seilhean *et al.,* 2009). Moreover, oligodendrocytes degenerate also in the gray matter of the ventral spinal cord of ALS patients. In addition to oligodendrocytes, NG^{2+} oligodendroglia precursor cells show reactive changes. A study reported the increase in NG2 immunoreactivity and thick hypertrophic NG^{2+} in ALS patients as compared to control (Kang *et al.,* 2013).

1.9.3.1 Mechanisms Contributing to Oligodendrocyte Pathology And Dysfunction in ALS

     - ALS-causing mutant genes

The overexpression of mutant ALS-associated genes, such as SOD1, is harmful to oligodendrocytes, can induce demyelination, and promote MN degeneration (Kim *et al.,* 2020). Two mechanisms can cause MN degeneration by oligodendrocyte. The first is associated with poor lactate release due to MCT1 downregulation, and the second involves cell-cell interaction between axons and enwrapping oligodendrocytes (Ferraiuolo *et al.,* 2016). Furthermore, other ALS mutations such as TDP-43 and FUS also triggered oligodendrocyte degeneration and increased the tendency to form toxic aggregates (Mackenzie *et al.,* 2011; Brettschneider *et al.,* 2014).

Moreover, mutations of the polyubiquitin-binding protein OPTN, reported in familial and sporadic ALS forms (Maruyama *et al.,* 2010), were involved in various pathways, such as neuroinflammation, necroptosis, and autophagy, these are dysregulated in ALS patients (Markovinovic *et al.,* 2017). A study showed that the genetic ablation of OPTN in oligodendrocytes or microglia, but not in MNs and astrocytes, induces progressive axonal

pathology and myelin abnormalities in the mouse spinal cord. Another study showed that OPTN deficiency activated RIPK-1, which increased oligodendrocyte vulnerability to necroptosis (Ito *et al.,* 2016).

- *Impaired mRNA processing*

A recently developing aspect of oligodendrocyte dysfunction in ALS includes alterations in mRNA metabolism (Barton *et al.,* 2019; Hoch-Kraft *et al.,* 2020). Most of the genes mutated in ALS are involved in RNA trafficking, including TDP-43, FUS, and C9orf72 (Barton *et al.,* 2019). Therefore, impaired transport of mRNAs and translation into functional myelin proteins can cause myelin defects in ALS patients (Hoch-Kraft *et al.,* 2020). Interestingly, TDP-43 aggregates have been detected in spinal cord OLs from ALS patients and found to be associated with impaired MBP mRNA translation and myelin abnormalities in ALS patients (Brettschneider *et al.,* 2014). Myelin damage has also been described in mature oligodendrocytes bearing mutant FUS aggregates (Mackenzie *et al.,* 2011). Furthermore, mice with the FUS form of ALS exhibit a toxic gain-of-function and cytoplasmic mislocalization of this protein, both MNs and oligodendrocytes, and showed the downregulation of myelin-related genes (Scekic-Zahirovic *et al.,* 2017). These results suggest that, in the presence of FUS mutations, oligodendrocyte dysfunction develops independently of MN damage and primarily contributes to functional deficits.

- *Neuroinflammation*

Glial cell activation plays an important role in neuroinflammation during the pathogenesis of ALS (Liu *et al.,* 2017). After activation, these cells induce a detrimental phenotype and lead to the death of MNs (Boillée *et al.,* 2006; Yamanaka *et al.,* 2008). The association between oligodendrocytes and CNS-resident neuroinflammatory cells is necessary for to maintain myelin (Nutma *et al.,* 2020; Lloyd *et al.,* 2019). Microglia and astrocytes broadly interact with oligodendrocytes to control myelin homeostasis during development and adulthood by providing lipids and other nutrients necessary for myelination (Camargo *et al.,* 2017). Therefore, the pro-inflammatory activation of microglia and astrocytes may contribute to myelin damage and promote oligodendrocyte and MN degeneration (Beers *et al.,* 2011; Guttenplan *et al.,* 2020).

- *Oxidative Stress*

The detrimental activation of glial cells and the impairment of mitochondrial metabolism leads to increased oxidative damage in oligodendrocytes (Pegoretti *et al.,* 2020). This increased oxidative stress represents one of the main pathological mechanisms involved in ALS patients and animal models (Carrera-Juliá *et al.,* 2020). The oligodendrocyte integrity is negatively affected by oxidative stress due to the reduction in antioxidant enzymes and the reserve pool of progenitors needed for myelin repair (Back *et al.,* 1998). Oxidative stress is the consequence of exposure to ROS and other free radicals (French *et al.,* 2009). On this basis, radical scavengers can be an appropriate therapeutic approach. For example, edaravone, a ROS scavenger drug, has already been approved for ALS treatment in Japan and USA (Carrera-Juliá *et al.,* 2020).

1.10   ALS Treatment

The molecular mechanisms of neuronal death in ALS are still largely unknown. Scientists showed several hypotheses that can causes neuronal death, such as oxidative stress, a deficit in trophic factors, chronic inflammation, and possibly glutamate-induced excitotoxicity (Jackson *et al.,* 2002; McGeer *et al.,* 2005). Various factors are also responsible for the survival MNs, such as their targets, skeletal muscle, and myelinated Schwann cells surrounding the peripheral axons (Grieshammer *et al.,* 1998; Riedel *et al.,* 1996). At present, there are no effective drugs for the treatment of ALS. Riluzole is the only approved drug in Europe and inhibits glutamate release (Rowland *et al.,* 2001). The antioxidant edaravone has been approved in Japan and USA. The European Medicine Agency asked for further evidence to approve the drug. In this chapter, I will discuss the potential compounds, the use of stem cells, and immunotherapy for ALS treatment.

1.10.1 Drug Therapy

Riluzole was the first drug approved by the Food and Drug Administration in 1995 to treat ALS. This drug was approved mainly for its anti-excitotoxic properties (Miller *et al.,* 2012). It exerts its neuroprotective action by blocking the Na^+ channels and reducing glutamate release (Schwartz *et al*, 2002). Moreover, it also works as an anti-glutamatergic agent, mainly reducing the NMDA receptor activity and increasing glutamate uptake by activating

glutamate transporters (Wang *et al.,* 2004). However, it can prolong survival in patients only from three to six months, with no improvement in muscle strength and only a small positive effect on patients' quality of life (Miller *et al.,* 2012).

Edaravone is the second drug approved in Japan in 2015, USA in 2017 and Canada in 2019. Edaravone is a ROS scavenger and inhibits peroxyl radical-induced peroxidation. It protects cells from oxidative stress by scavenging the H_2O_2, upregulating the peroxiredoxin-2, downregulating the protein disulfide isomerase A3, and inhibiting apoptosis (Jaiswal, 2019). Apart from the therapeutic effect, edaravone has some limitations, such as it requires repeated intravenous administration and is effective when administered in the early phase of the disease only. Due to very little data, it is challenging for clinicians to prescribe this drug for long-term therapy (Hardiman and van den Berg, 2017).

Researchers are continuously studying various new therapeutic approaches. Several drugs in the pipelines focus on different targets. In the past, many preclinical studies fostered the activation of clinical trials by using drugs reducing, for instance, excitotoxicity by various mechanisms (Ben-Ami *et al.,* 2009; Pascuzzi *et al.,* 2010; Berry *et al.,* 2013), the inflammatory components of ALS (Pasinetti 2006; Nowicka *et al.,* 2019), oxidative stress (Ikeda *et al.,* 2005; 2011), or protein aggregation (Cudkowicz *et al.,* 2008). Unfortunately, all attempts failed till now. At present, about 50 therapeutic clinical trials are recruiting patients (https://clinicaltrials.gov/ct2/results?cond=ALS+%28Amyotrophic+Lateral+ Sclerosis%29&Search=Apply&recrs=a&age_v=&gndr=&type=&rslt=)

1.10.2   *Stem Cell Therapy*

Stem cell therapy is a new and promising approach to treat ALS because of its ability to slow the progression of MN disease or even replace motor neurons (Harper *et al.,* 2004). It is known that mouse embryonic stem cells can be converted into specific neuronal subtypes such as MNs (Wichterle *et al.,* 2002). Stem cells can be obtained from multiple sources. Embryonic stem cells can be converted into pluripotent cells, which can differentiate into different cell types (Pandya *et al.,* 2012). A study converted embryonic neural cells into neural stem cells, to differentiate them to astrocytes (Kriegstein *et al.,* 2009). Another study showed the beneficial effect of the human fetal neural stem cells transplanted into the spinal cords of SOD1 mutant mice. They provide a neuroprotective effect by forming synapses and increasing MNs (Hefferan *et al.,* 2012). In addition, neural progenitor cells have the property

to secrete glial cell line-derived neurotrophic factor (GDNF) and brain-derived neurotrophic factor (BDNF) (Klein *et al.,* 2005).

Stem cell-derived mesenchymal stem cells (MSCs) are known to release trophic factors, anti-inflammatory cytokines, and immunomodulatory chemokines to delay disease progression (Mazzini *et al.,* 2012). A clinical trial revealed the safety and immunomodulatory activity of MSCs in ALS patients (Karussis *et al.,* 2010). Another study reported the therapeutic use of human skeletal muscle-derived stem cells in ALS mice. They significantly delayed ALS symptoms and improved motor activity (Canzi *et al.,* 2012). The systemic injection of MSC in SOD1^{G93A} mice led to a high MN number and, consequently, delayed symptoms and bettered motor performance (Uccelli *et al.,* 2012). A patent proposed using stem cell-derived from the placenta for ALS treatment. This therapy promoted stem cell differentiation into adipocyte, chondrocyte, and osteocyte lineages. (Hariri *et al.,* 2013). Finally, induced pluripotent stem cells (iPSC) are somatic cells and can be obtained by converting adult fibroblasts into pluripotent stem cells (O'Connor *et al.,* 2012). The iPSC-derived cells can be used to model the disease and to test potential compounds in vitro. Moreover, a study stated that human iPSC-differentiated into mature neurons showed beneficial results in the SOD1^{G93A} mouse model (Popescu *et al.,* 2013). Another study confirmed that iPSCs obtained from fibroblasts of a senior ALS patient differentiated into MNs (Dimos *et al.,* 2008).

1.10.3 Immunotherapy

Mutation in the SOD1 enzyme induces oxidative stress or accumulation of free radicals that contribute to the progression of ALS. This cytotoxic activity is associated with protein misfolding/aggregation, leading to a focus on immunotherapy in ALS (Watanabe *et al.,* 2001). Mouse monoclonal antibodies against SOD1 were produced to determine effectiveness as a passive immunization for ALS. A study showed that administration of the D3H5 antibody for 42 days significantly decreased toxic SOD1 in the spinal cord, reduced the weight loss, and extended the lifespan of SOD1^{G93A} mice (Gros-Louis *et al.,* 2010). Another study used the recombinant WT-apo SOD1 vaccine to induce protective immunity. The treatment significantly increased lifespan and delayed the onset of the disease in transgenic mice models (Takeuchi *et al.,* 2010).

2. AIMS AND OBJECTIVES

This project consists of two parts:

1) Evaluation of the role of endoplasmic reticulum in the differential endurance against redox stress in cortical and spinal astrocytes from new-born SOD1^{G93A} mice.
2) Evaluation of the effect of CTEP in pharmacological modulation of mGluR5 receptors on the activation state and metabolic functions of astrocytes obtained from human ALS patients.

As to the first aim, many studies demonstrated the degeneration of upper and lower MNs in (ALS, which represents a non-cell-autonomous disease modulated by astrocytes (Dewil *et al.,* 2007; Ferraiuolo *et al.,* 2016). Indeed, the increase of ROS (Bowling *et al.,* 1995; Singh *et al.,* 2019) in these glial cells results in neuronal damage in ALS patients and precedes the motor impairment in experimental disease models (Mizielinska *et al.,* 2013; Forsberg *et al.,* 2011; Bruijn *et al.,* 1997). The absence of non-invasive methods to evaluate redox stress in the central nervous system did not permit the estimation of the role of astrocyte dysfunction in the progression of ALS in patients. Nevertheless, recent evidence indicates a direct relationship between [18F]-fluorodeoxyglucose (FDG) uptake and oxidative stress, reporting a link between tracer retention and the activation of a specific pentose phosphate pathway (PPP) dedicated to the reduction of NADP to NADPH (Thurfjell *et al.,* 2014).

This pathway is triggered by the enzyme hexose-6P dehydrogenase (H6PD) (Nishimura *et al.,* 2011; Csala *et al.,* 2006; Marini *et al.,* 2016), which can process FDG and FDG6P, as well as many phosphorylated and free hexoses within the endoplasmic reticulum (ER). Moreover, the association of ER-PPP has been found to play an important role in FDG uptake in cancer cells (Cossu *et al.,* 2020; Cossu *et al.,* 2020b), skeletal muscles (Bauckneht *et al.,* 2020; Marini *et al.,* 2020), cardiomyocytes (Bauckneht *et al.,* 2020), and, more importantly, neurons and astrocytes (Cossu *et al.,* 2019). Accordingly, the high FDG uptake in the SC, recently documented in symptomatic ALS patients (Marini *et al.,* 2016), can cause enhanced redox stress in the environment surrounding the lower motor neurons. Interestingly, this same observation was found in the motor cortex (MC) (Marini *et al.,* 2018), suggesting that the different FDG uptake in MC and SC might indicate the presence of different metabolic patterns in the environments of upper and lower motor neurons.

Thus, to evaluate the mechanisms underlying the different metabolic patterns of the MC and SC, the present study evaluated the redox balance, mitochondrial function, ultrastructure, and FDG uptake of astrocytes harvested from the MC and SC of new-born SOD1^{G93A} mice.

The second aim focussed on the critical role of human astrocytes (in ALS). At the beginning of my Ph.D., I was supposed to spend a period at the Sheffield Institute for Translational Neuroscience, the University of Sheffield, in the laboratory of Prof. Laura Ferraiuolo to learn how to obtain the inducible neural pluripotent cell(iNPC)-derived human astrocytes (i-astrocytes). Unfortunately, due to the COVID-19 pandemic, this was impossible. Thanks to the collaboration with the Sheffield team, we managed to set up the protocol to differentiate iNPSc into i-astrocytes at the University of Genova. However, we had to skip obtaining iNPSc from human skin fibroblast by using different retroviral vectors (Meyer *et al.,* 2014). As we explained in the introduction, astrocytes have several physiological functions in the CNS. Astrocytes help to remove toxin metabolites, control ions levels and neurotransmitters in the extracellular space, release trophic factors and nutrients, favour synapse maturation, enhance pre-and postsynaptic function (Barres, 2008). They also participate in the formation of blood vessels and the blood-brain barrier (Volterra and Meldolesi, 2005; Sykova and Chavatal, 1993), sustain the neuronal energy demands (Magistretti, 2006; Tsacopoulus and Magistretti, 1996), and regulate the immune response (Philips *et al.,* 2014).

During neurodegeneration, astrocytes get into a reactive state, called astrogliosis, and change their morphology and gene expression profile (Liddelow and Barres, 2015; Liddelow *et al.,* 2017). Accordingly, several changes in astrocytic phenotype have been found in ALS models (Rossi *et al.,* 2008; Diaz-Amarilla *et al.,* 2011; Papadeas *et al.,* 2011; Lepore *et al.,* 2008; Yamanaka and Komine, 2018; Guttenplan *et al.,* 2020) and ALS patients' tissues (Hamby and Sofroniew, 2010; Rossi and Volterra, 2009).

An interesting link between these cells and glutamate excitotoxicity is represented by the overexpression of Group I metabotropic receptors in activated astrocytes (Aronica *et al*, 2001). Interestingly, a treatment with receptor antagonists reduces astrogliosis, slows down astrocytic degeneration, and prolongs SOD1^{G93A} mouse survival (Anneser *et al.,* 2004; Rossi *et al.,* 2008). Based on these data and focussing on our encouraging results, indicating that in vivo knocking down and knocking out of mGluR5 as well as by a pharmacological

negative allosteric modulation of mGluR5 in SOD1G93A mice, reduced astrogliosis (Bonifacino *et al.,* 2017; Bonifacino *et al.,* 2019a; Milanese *et al.,* 2021), we planned to investigate the impact of mGluR5 blockade in human astrocytes. For this purpose, we characterize the phenotype of human astrocytes obtained from iNPSc of human patients with SOD1 and C9orf72 mutations after reducing mGluR5 activity by treating in-vitro i-astrocytes with the negative allosteric modulator of mGluR5, CTEP.

The literature also reports alterations in the energy metabolism in ALS animal models and ALS patients (Dupuis *et al.,* 2011; Browne *et al.,* 2006). Mitochondria show altered morphology in skeletal muscle, liver, spinal cord, and motor cortex neurons (Sasaki *et al.,* 1999; Martin., 2011; Marini *et al.,* 2020) and defects in Ca^{2+} buffering (Mattiazzi *et al.,* 2002; Kawamata *et al.,* 2010). These findings support the assumption that alterations of energy metabolism play a pivotal role in ALS onset but at present, these events have not been characterized in ALS i-astrocytes. Here, we focused on the mitochondrial metabolism of i-astrocytes obtained from iNPSc.

3. MATERIAL AND METHODS

3.1 Animals

B6SJL-Tg (SOD1*[G93A])1Gur mice expressing a high copy number of mutant human SOD1 with a Gly93Ala substitution (SOD1[G93A] mice) were originally obtained from Jackson Laboratories (Bar Harbor, ME, USA) and maintained by crossing SOD1[G93A] male mice with background-matched B6SJL wildtype (WT) females (Gurney *et al*., 1994). SOD1[G93A] mice represent the most widely used animal model for ALS preclinical studies since it recapitulates several pathological hallmarks of ALS in human patients (Kim *et al*., 2016). Mice carrying the SOD1[G93A] mutation were identified by analyzing the tissue extracts from tail tips (Bonifacino *et al*., 2017). Briefly, tissue was homogenized and freeze-thawed twice. SOD1 was evaluated by staining for its enzymatic activity on 10% non-denaturing polyacrylamide gel electrophoresis by incubation for 15 min under shaking with 4-nitro blue tetrazolium chloride (NTB; Merck, Darmstadt, Germany) and then with riboflavin (Merck, Darmstadt, Germany), supplemented with tetramethyl ethylenediamine (Carl Roth GmbH Karlsruhe, Germany). Gels were illuminated with a white-light box for 10–15 min: under light exposure, riboflavin is reduced, leading to the production of O^{2-}, which reduces NBT to form formazan, a dark blue colour precipitate.

Experiments were conducted in accordance with the European Communities Council Directive (EU Directive 114 2010/63/EU for animal experiments) and with the Italian D.L. No. 26/2014 and were approved by the local ethical committee and by the Italian Ministry of Health (project authorization No. 482/2017-PR). All efforts were made in minimizing animal suffering and using the minimal number of animals necessary to produce statistically reliable results

3.2 Human Tissue Samples

Human skin fibroblast samples were obtained from Laura Ferraiuolo, Professor at University of Sheffield. Informed consent forms were obtained from all subjects before sample collection.

3.3 Mouse Astrocytes Preparation

Astrocytes were isolated from the MC and SC of 2 days old SOD1[G93A] or WT mice according to Paluzzi and colleagues with some modifications (Paluzzi *et al*., 2007). Two days after birth, pups (P1-2) were anesthetized and sacrificed by cervical dislocation to

remove MC and SC under binocular dissection (Nikon SMZ-2T, Japan) in HBSS at 4 °C. Each dissected SC was gently homogenized in 1 mL Dulbecco's modified Eagle medium (DMEM; Euroclone, Cat# ECM0728L) containing 10% fetal bovine serum (Euroclone, Cat# ECS0180L), 1% glutamine (Euroclone, Cat# ECB3004D) and 1% penicillin/streptomycin (Euroclone, Cat# ECB3001D). Then, tissue suspension was seeded in a 35 mm Petri dish (Euroclone, Cat# ET2035), precoated with poly-L-ornithine hydrochloride (1.5 μg/mL; Sigma, Cat# P2533) and laminin (3 μg/mL; Sigma, Cat# L2020). MC was isolated from the brain under binocular dissection (Nikon SMZ-2T, Japan, CAT# 2049) and homogenized in 8 mL of complete DMEM as above. Tissue suspension was seeded in two 25 cm^2 flasks (Euroclone, Cat# ET7026). Samples were placed at 37 °C in humidified 5% CO_2 incubator, and the medium containing tissue fragments was replaced with fresh complete DMEM after 24 h and then every 48 h. After 7 days in vitro (DIV), astrocytes were shaken for 15 min to remove microglia cells, detached by Trypsin-EDTA (Euroclone, Cat# ECB3052B), replated and cultured to confluence. After 15 DIV, cell cultures were again shaken for 15 min, and astrocytes were collected for the experiments. For immunofluorescence (IF) studies, astrocytes were detached after 7 DIV, as described above, and replated onto 12 mm diameter poly-L-ornithine and laminin precoated glass coverslips placed at the bottom of 24-well plates. After 15 DIV, astrocytes were processes for IF staining.

3.4 Human iNPCs Maintenance Protocol

We received the iNPCs samples from the University of Sheffield. Sample were frozen in liquid nitrogen for future experiment.

3.4.1 *Split iNPCs into Human iNPCs Proliferation Media*

For iNPCs proliferation, the human iNPCs proliferation medium, consisting of DMEM/F-12, 1% N2, 1% B27, 20 ng/mL FGF2, 4 mg/mL and 1x accutase (Gibco, catalog number: 11599686) was used. Tissue culture plates (10 cm) coated with human fibronectin (1mg/ml in PBS; Sigma-Aldrich, catalog number: FC010-10MG) at room temperature. After 5 minutes, the coating solution was removed, and iNPCs were cultured in 12 ml of human iNPCs proliferation media for 5 days by changing the medium every 48 hours.

After 5 days of culture, iNPCs were split. The proliferation medium was removed, and cells were washed in 5 ml room temperature PBS. Then, 1ml accutase was added to the iNPCs, and cells were incubated at 37°C for 4 min. iNPCs were detached by gently shaking the plates, added with 5 ml room temperature PBS and transferred to 15 ml Falcon tubes (Greiner-Bio, catalog number: 188271). iNPCs were centrifuged at 200 x g for 4 min at room temperature and resuspended in human iNPCs proliferation medium. iNPCs were plated in fibronectin-coated 10 cm tissue culture plates. iNPCs were incubated at 37°C in a 5% CO_2 atmosphere for 2-4 days, or until the iNPCs reached 80-90% confluency, and then split again as described above (Figure 1).
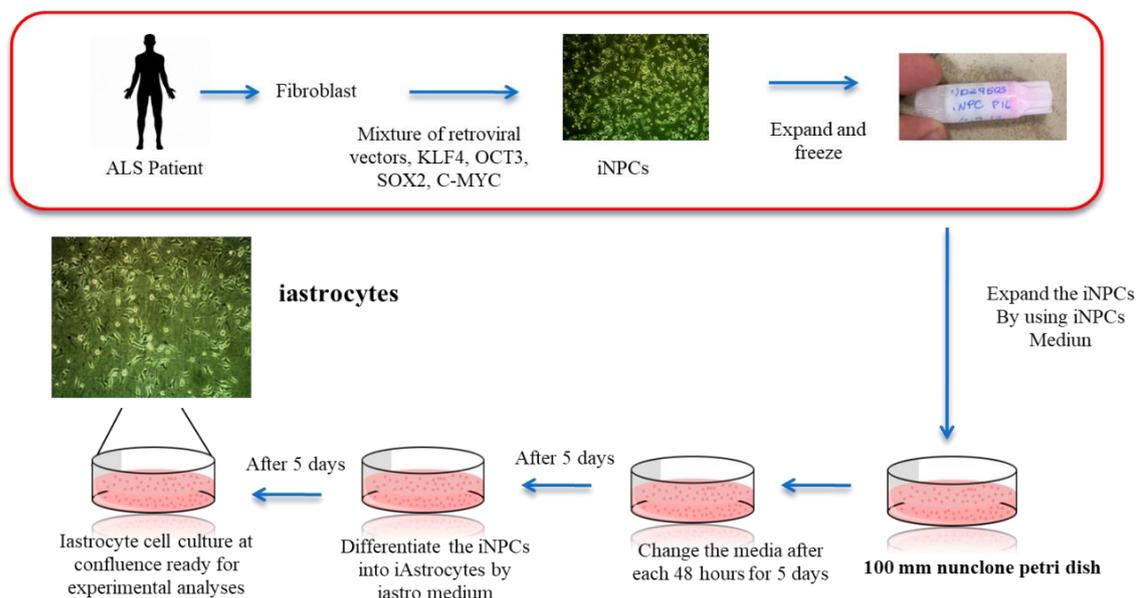
Figure 1: Experimental Protocol for iNPCs to i-astrocytes

3.5 Differentiation of iNPCs into i-astrocytes

For differentiation of iNPCs into i-astrocytes, human fibronectin-coated (1 mg/ml) in PBS 1:400; 5 min) tissue culture plates were prepared. Human iNPCs proliferation medium was removed from iNPCs cultures, and cells were washed with 5 ml room temperature PBS. After removing PBS, cells added with 1 ml accutase. iNPCs were incubated with accutase at 37°C for 4 min. iNPCs were detached by gently shaking the plates, added with 5 ml room temperature PBS, and transferred to 15 ml Falcon tubes. iNPCs were centrifuged at 200 x g for 4 min at room temperature and resuspended in human iNPCs proliferation medium. At this point, 12 ml warm human i-astrocyte differentiation medium consisting of DMEM/F12,

0.5% N2, 10% FBS, 1% Pen Strep was added to the 10 cm tissue culture plates coated with fibronectin. Resuspended iNPCs were then introduced in the tissue culture plates. The i-Astrocyte differentiating cells were incubated at 37 °C in a 5% CO_2 atmosphere for 5 days or until the i-astrocytes reach 80-90% confluency, and then split the i-astrocytes on different plates according to the experiment (figure 2).
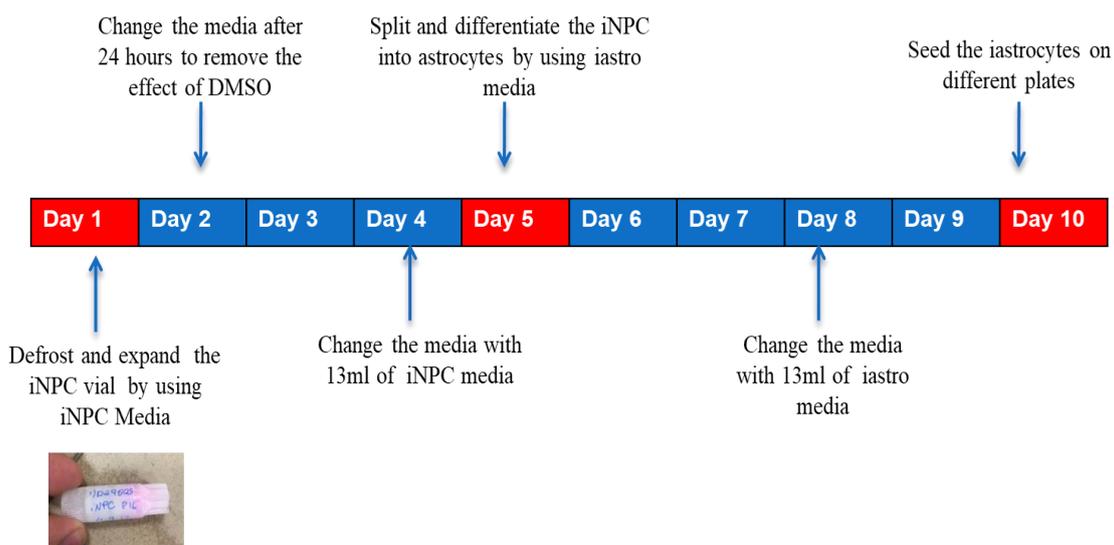

Figure 2: Differentiation of iNPCs to i-astrocytes

3.6. Pharmacological treatment with CTEP

Control, SOD1^{A4V}, and C9orf72 i-astrocytes were seeded at a density of 2-3 x 10^4 cells/well in 24-well plates containing 12 mm diameter pre-coated glass coverslips. The pharmacological treatment with CTEP, synthesized, purified, and kindly provided by Prof. Silvana Alfei [Organic Chemistry Unit of the Department of Pharmacy, University of Genoa (Alfei and Baig, 2017)], was performed as follows: i-astrocytes were treated for three days either with 0.1 μM CTEP dissolved in 140 μM DMSO or with the vehicle. CTEP/DMSO and DMSO were diluted in complete DMEM to the correct final concentration and replaced every 48 h. On day 5 cells were washed twice with PBS 1X and complete i-astrocytes media was added for a further 24 h. Then, i-astrocytes were fixed with 4% PFA and immunofluorescence analysis was performed, as previously described, to investigate astrogliosis (figure 3).
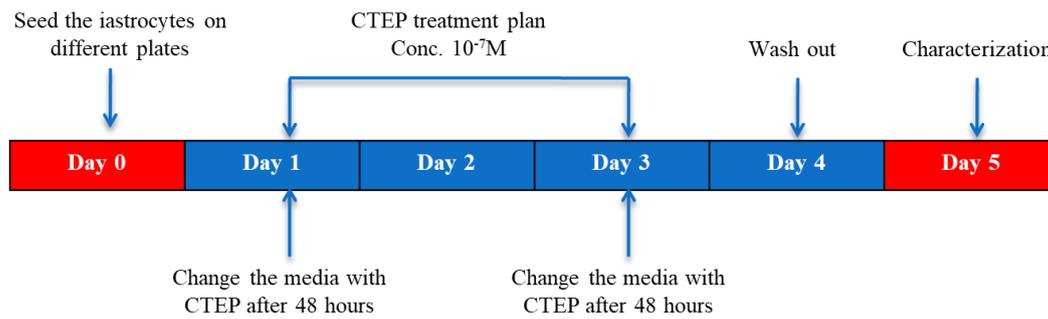
Figure 3: Pharmacological treatment plan of i-astrocytes with CTEP

3.7 Flow Cytometry

MC and SC neonatal astrocytes from WT or SOD1^{G93A} pups were detached by trypsin-EDTA and centrifuged for 5 min at 500×g. About 5×10^5 cells were resuspended and saturated for unspecific bonds by incubating with 0.5% bovine serum albumin (BSA) in phosphate-buffered saline (PBS, pH 7.4) for 15 min at RT. Aliquots of the suspension were stained (1h at RT) with the following fluorochrome-conjugated antibodies for flow cytometry: mouse monoclonal anti-GFAP antibody conjugated with Alexa Fluor A488 (Thermo Fisher Scientific, Cat# 53-9892-82), rat monoclonal anti-ACSA2 antibody conjugated with phycoerythrin (PE) (Miltenyi Biotec, Cat# 130-102-365) and rat monoclonal anti-TMEM119 antibody conjugated with Alexa Fluor A488 (Abcam, Cat# ab225497). For GFAP staining, cell suspensions were previously fixed and permeabilized, 20min at 4°C, by using the Cytofix/Cytoperm Fixation/Permeabilization Kit (BD Bioscience, Cat# 554714). After staining, cells were centrifuged (5min at 500×g) and pellets were resuspended in PBS for flow cytometry analyses. Cell debris and dead cells were excluded from analysis by 7-aminoactinomycin D (7-AAD) labelling. Data were acquired on a Guava easyCyte 6 flow cytometer (Merck Millipore, Burlington, MA, USA) and processed using the GuavaSoft 3.1.1 software (Merck Millipore).

3.8 Confocal Microscopy Immunofluorescence

3.8.1 Mouse astrocytes

SC and MC neonatal astrocytes from WT or SOD1^{G93A} pups were cultured onto 12 mm glass coverslips. Cells were washed three times with PBS and postfixed with 4%

paraformaldehyde (Sigma-Aldrich, Cat#47608) in PBS for 15min at RT. Cells were permeabilized with methanol for 5 min at −20°C, washed three times with PBS and saturated with 0.5% BSA in PBS for 15 min at RT. Samples were incubated with mouse monoclonal anti-glial fibrillary acid protein (GFAP, 1:500; Sigma Aldrich, Cat#G3893) and rat monoclonal anti-integrin alpha-M/beta-2 (CD11b, 1:500; Abcam, Cat#ab8878) primary antibodies overnight at 4°C. Astrocytes were then washed three times with 0.5% BSA in PBS and incubated with donkey anti-mouse Alexa Fluor A488-conjugated (1:3000; Thermo Fisher Scientific, Cat# R37118) and goat anti-rat Alexa Fluor A647-conjugated (1:3000; Thermo Fisher Scientific, Cat# A-21247) secondary antibodies for 1 h at RT. Cells were washed three times with PBS, and coverslips were assembled on microscopy glass slides by using ProLong Gold antifade mountant (Thermo Fisher Scientific, Cat# P10144). Fluorescence image ($512 \times 512 \times 8$ bit) acquisition was performed by a three-channel Leica TCS SP5 laser-scanning confocal microscope, equipped with 458, 476, 488, 514, 543 and 633 nm excitation lines, through a plan apochromatic oil immersion objective 63x (1.4 NA). Light collection configuration was optimized according to the combination of chosen fluorochromes, and sequential channel acquisition was performed to avoid crosstalk. Leica "LAS AF" software package was used for image acquisition.

3.8.2 Human i-astrocytes

WT, SOD1^{A4V}, and C9orf72 i-astrocytes, seeded on coated 12 mm diameter glass coverslips were washed three times with PBS 1X and fixed with 4% paraformaldehyde (PFA, Sigma-Aldrich, Cat# 47608) for 15 min at RT, in the dark. After fixing, cells were permeabilized with methanol for 5 min at -20 °C, washed three times with PBS 1X (3 x 5 min), and treated with a solution of 0.5% bovine serum albumin (BSA) in PBS 1X (0.5% PBS/BSA) for 15 min at RT. Primary antibodies were properly diluted in 3% PBS/BSA and incubation was performed overnight at 4 °C. The list of antibodies and their final dilutions are reported in Table 1. The day after, astrocytes were washed three times with 0.5% PBS/BSA (3 x 5 min) and labeled with secondary antibodies diluted 1:3000 in 3% PBS/BSA for 1 h at RT (Table 1). Cells were washed three times with PBS 1X, and the coverslips were assembled on a microscopy glass slide by using Fluoroshield TM containing DAPI (Sigma-Aldrich, Cat# F6057), to label nuclei. Fluorescence image (512 x 512 x 8 bit) acquisition was performed by a three-channel TCS SP5 laser-scanning confocal microscope (Leica, Wetzlar, Germany)

equipped with 458, 476, 488, 514, and 633 nm excitation lines, through a plan-apochromatic oil immersion objective 63x/1.4. The light collection was optimized according to the combination of the chosen fluorochromes, and sequential channel acquisition was performed to avoid crosstalk. The Leica "LAS AF" software package was used for image acquisition. The quantitative analyses of co-localization and the relative protein expression level were obtained by calculating co-localization coefficients (Manders *et al*., 1992) and normalizing the results with the expression of glyceraldehyde 3-phosphate dehydrogenase (GAPDH), the housekeeping marker.

Primary Antibody	Working Dilution	Manufacturer and Catalogue number
Mouse monoclonal anti-glial fibrillary acid protein (GFAP) antibody	1:1000	Sigma Aldrich, Cat# G3893
Mouse monoclonal anti-S100β antibody	1:500	Merck Millipore, Cat# MAB079
Rabbit polyclonal ant-mGluR5 antibody	1:500	Abcam, Cat# ab53090
Rabbit polyclonal anti- nuclear factor erythroid 2–related factor 2 (Nrf-2) antibody	1:500	Abcam, Cat#ab31163
Rabbit monoclonal anti- NLR family pyrin domain containing 3 (NLRP-3) antibody	1:500	Cell Signalling, Cat#15101
Rabbit monoclonal anti-complement C3 antibody	1:1000	Prodotti Gianni, Cat#EPR19394
Mouse monoclonal anti-glyceraldehyde 3-phosphate dehydrogenase (GAPDH) antibody	1:1000	Sigma Aldrich, Cat# G8795
Rabbit polyclonal anti-glyceraldehyde 3-phosphate dehydrogenase (GAPDH) antibody	1:1000	Sigma Aldrich, Cat# G9545
Secondary Antibody	Working Dilution	Manufacturer and Catalogue number
Donkey anti-rabbit Alexa Fluor A488-conjugated	1:3000	Thermo fisher Scientific, Cat# R37118
Donkey anti-mouse Alexa Fluor A488-conjugated	1:3000	Thermo fisher Scientific, Cat# A21202
Donkey anti-mouse Alexa Fluor A647-conjugated	1:3000	Thermo fisher Scientific, Cat# A31571
Donkey anti-rabbit Alexa Fluor A647-conjugated	1:3000	Thermo fisher Scientific, Cat# A31573

Table 1: List of primary and secondary antibodies with the respective working dilution, the supplier company, and the catalogue number.

3.9 Enzymatic Assays

Cultured cells were centrifuged at 1000×g for 2 min to remove the growth medium. The pellet was suspended in PBS supplemented by protease inhibitors. Obtained homogenates were thus sonicated twice for 10s in ice, with a break of 30s. The activity of H6PD and glucose-6-phosphate dehydrogenase (G6PD) was assayed using a double-beam spectrophotometer (UNICAM UV2, Analytical S.n.c., Italy) to follow the reduction of NADP at 340 nm (Csala *et al*., 2006; Marini *et al*., 2016). H6PD enzymatic function was tested in the presence of Tris-HCl Ph 7.4 100 mM, 2-deoxyglucose-6P (2DG6P) 10 mM and NADP 0.5 mM. By contrast, G6PD activity was assayed in the presence of Tris-HCl pH 7.4 100 mM, G6P 10 mM and NADP 0.5 mM. Complex I activity was assayed following the reduction of ferrocyanide (FeCN), at 420 nm, using the following solution: TRIS7.4, NADH 0.6 mM, antimycin 50 µM and FeCN 0.8 mM. Antioxidant capacity was evaluated following the instructions of the manufacturer of a dedicated kit (Abcam; Cat #ab65329) that provides a complete description of the total cell antioxidant power associated with the endogenous scavengers, expressed as Trolox equivalent antioxidant capacity content (Cossu *et al*., 2020; Marini *et al*., 2020). Similarly, NADP/NADPH ratio was tested using a dedicated Assay Kit (Abcam; Cat#ab65349), following the manufacturer's instructions. Finally, malondialdehyde (MDA) levels were evaluated by the thiobarbituric acid reactive substances assay (Marini *et al*., 2020; Miceli *et al*., 2020). In all cases, enzymatic activity was normalized for total protein concentrations tested using Bradford analysis (Kruger., 2009).

3.10 Seahorse Analysis

Astrocyte oxygen consumption rate (OCR) and extracellular acidification rate (ECAR) were determined using a Seahorse XFp Extracellular Flux Analyzer (Agilent Technologies). Twenty-four hours prior to the assay, 10,000 astrocytes/well were seeded in XF plates. OCR and ECAR were monitored according to the manufacturer's instructions. Briefly, the day of the experiment, the medium was replaced with Agilent Seahorse DMEM, pH 7.4, enriched

with glucose (11 mM), glutamine (2 mM) and pyruvate (1 mM). Three measurements of OCR and ECAR were taken for the baseline and after sequential injection of the ATP-synthase inhibitor oligomycin A (1 μM) and the ATP synthesis uncoupler carbonyl cyanide-4-trifluoromethoxyphenylhydrazone (FCCP) (0.8 μM).

3.11 In Vitro FDG Extraction

In vitro FDG uptake of astrocytes was evaluated using the LigandTracer White instrument (Ridgeview, Uppsala, SE) according to our previously validated procedure (Cossu *et al*., 2020; Bauckneht *et al*., 2020; Scussolini *et al*., 2019). Briefly, the device consists of a beta-emission detector and a rotating platform harboring a standard Petri dish. The rotation axis is inclined at 30° from the vertical so that the organ alternates its position from the nadir (for incubation) to the zenith (for counting) every minute. For each group, 600,000 astrocytes were seeded the day before the experiments under standard conditions. Soon before the experiment, culture medium was replaced with DMEM containing glucose at 5.5 mM and enriched with 1.8 to 2.2 MBq/mL FDG. Tracer kinetic uptake was measured over 120 min of experiments. All experiments were performed in triplicate, and data were normalized for cell number.

3.12 Western Blot Analysis

3.12.1 Mouse Astrocytes

Whole-cell lysates of SC and MC neonatal astrocytes from WT or SOD1^{G93A} pups were prepared using EB Lysis Buffer (HEPES pH 7.4 20 mM, NaCl 150 mM, glycerol 10% and Triton X-100 1%) with protease inhibitor cocktail and phosphatase inhibitors (PhosStop) (Roche, Basel, Switzerland) and sodium orthovanadate. Petri dishes were scraped to collect the whole lysates and incubated on ice for 15 min. Lysates were finally centrifuged for 5 min at 13,200 rpm at 4 °C to remove cellular debris. Protein cell extracts and SDS polyacrylamide gel electrophoresis (NW04120box, BOLT Bis-Tris plus 4–12%, Invitrogen) were performed using standard protocols. Proteins were detected with ECL Detection Reagent (BioRad, Hercules, CA, USA). Protein quantification was performed using Bradford protein assay (BioRad, Hercules, CA, USA). Antivinculin (Sigma, V9131) was

used as loading control. We tested the following antibodies: anti-cytochrome c (Santa Cruz Biotechnology, inc., H-104, Cat# sc-7159) and anti-mitofusin 2 (Mfn2, Thermo Fisher, Cat# PA5-72811). Secondary antibodies were horseradish peroxidase-conjugated anti-mouse (Cat#G21040) and anti-rabbit (Cat# G21234) (Molecular Probes, Thermo Fisher Scientific, Waltham, MA, USA), and the detection of proteins was performed with ECL Detection Reagent (BioRad, Hercules, CA, USA).

3.12.2 Human i-astrocytes

Control, SOD1^{A4V} and C9orf72 i-astrocytes were detached with accutase 1X, diluted in 3 volumes complete i-astrocytes media to block the enzymatic activity and centrifuged at 700 x g for 5 min at RT. Pellet was washed in PBS 1X and centrifuged at 17,000 x g for 5 min at 4°C. PBS was removed and cell pellet stored at -80°C. Western blot analyses were conducted using standard procedures. Cell pellets were lysed using lysis Buffer (150 mM NaCl, 20 mM TRIS-HCl pH 7.4, 2 mM EDTA and 1 % NP40) containing a protease inhibitor cocktail for mammalian cells (Sigma Aldrich, Cat# P8340) and total protein was measured by Bradford assay (Bradford MM, 1976). Samples were incubated with a denaturing solution containing: 8% w/v SDS, 125 mM Tris-HCl (pH 6.8), and 1.25% v/v DTT. After 10 min of incubation at 37 °C, the sample was boiled for 5 min and 40% w/v sucrose, and 0.008% bromophenol blue were added.

Electrophoresis was carried out using a Mini Protean III (Bio-Rad Laboratories, Hercules, CA, USA) apparatus, in which both faces of the gel sandwich were immersed in the buffer. To a better resolution of both middle and low-molecular weight proteins, 4-20% precast gradient gels (Bio-Rad, Cat# 4568094) were used. The electrophoretic run was performed at 4 °C, setting constant current at 70 mA, with denaturing running buffer. Proteins separated by SDS-PAGE were transferred onto nitrocellulose membrane (NC, Bio-Rad Laboratories) by electroblotting at 400 mA for 2 h in Tris-glycine buffer (50 mM Tris, 380 mM glycine) plus 20% methanol. The membrane was blocked with PBS/0.1% Tween 20 (PBSt) containing 5% non-fat dry milk for 1 h and incubated over night at 4 °C with primary antibodies (Table 2), The list of antibodies and their final dilutions are reported in Table 2. After 3 washes with PBS, NC was incubated for 1 h at RT with specific secondary antibodies conjugated with horse radish peroxidase (HRP) (Bio-Rad Laboratories) and developed with Clarity Western ECL Substrate (Bio-Rad Laboratories). Bands were detected and analyzed

for density using the Alliance 6.7 WL 20 M enhanced chemiluminescence system and UV1D software (UVITEC, Cambridge, UK). Each band was converted by into a densitometric trace allowing calculations of intensity; signals were normalized to the signal of GAPDH, and results expressed as Relative Optical Density (R.O.D.).

Primary Antibody	Working Dilution	Manufacturer and Catalogue number
Mouse monoclonal anti-glial fibrillary acid protein (GFAP) antibody	1:1000	Sigma Aldrich, Cat# G3893
Mouse monoclonal anti-S100β antibody	1:500	Merck Millipore, Cat# MAB079
Rabbit polyclonal ant-mGluR5 antibody	1:500	Abcam, Cat# ab53090
Rabbit polyclonal anti- nuclear factor erythroid 2–related factor 2 (Nrf-2) antibody	1:500	Abcam, Cat#ab31163
Rabbit monoclonal anti- NLR family pyrin domain containing 3 (NLRP-3) antibody	1:500	Cell Signalling, Cat#15101
Rabbit monoclonal anti-complement C3 antibody	1:1000	Prodotti Gianni, Cat#EPR19394
Mouse monoclonal anti-glyceraldehyde 3-phosphate dehydrogenase (GAPDH) antibody	1:1000	Sigma Aldrich, Cat# G8795
Rabbit polyclonal anti-glyceraldehyde 3-phosphate dehydrogenase (GAPDH) antibody	1:1000	Sigma Aldrich, Cat# G9545
Secondary Antibody	**Working Dilution**	**Manufacturer and Catalogue number**
goat polyclonal anti-mouse IgG (HRP) antibody	1:3000	Bio-Rad, Cat# 0300-0108P
goat polyclonal anti-rabbit IgG (HRP) antibody	1:3000	Bio-Rad, Cat# STAR124P

Table 2: List of primary and secondary antibodies used to perform western blot analysis, reporting the working dilution, the supplier company, and the catalogue number.

3.13 Evaluation of Malondialdehyde

To assess lipid peroxidation, malondialdehyde (MDA) concentration was evaluated using the thiobarbituric acid reactive substances (TBARS) assay. This test is based on the reaction of MDA, a breakdown product of lipid peroxides, with thiobarbituric acid (TBA). The

TBARS solution contained 15% trichloroacetic acid (TCA) in 0.25 N HCl and 26 mM thiobarbituric acid. To evaluate the basal concentration of MDA, 600 μL of TBARS solution were added to 50 μg of total protein dissolved in 300 μL of Milli-Q water. The mix was incubated for 60 min at 95°C. Afterward, the sample was centrifuged at 14,000 rpm for 2 min and the supernatant was spectrophotometrically analyzed at 532 nm (Cappelli *et al*., 2020).

3.14 Enzymatic Antioxidant Defences Assay

All assays were performed on 50 μg of total protein and data were normalized on the sample protein content. Glucose 6-phosphate dehydrogenase (G6PD) activity was evaluated as a marker of antioxidant defences, following the NADP reduction, at 340 nm. The assay mixture contained: 100 mM Tris HCl pH 7.5, 5 mM MgCl2, 10 mM glucose-6-phosphate, and 0.5 mM NADP (Ravera *et al*., 2021).

Glutathione reductase (GR) activity was spectrophotometrically assayed, following the oxidation of NADPH at 340 nm. The assay mix contained 100 mM Tris HCl, pH 7.4, 1 mM EDTA, 5 mM GSSH, and 0.2 mM NADPH (Marini *et al*., 2020).

Glutathione peroxidase (GP) activity was spectrophotometrically assayed, following the decomposition of H_2O_2 at 240 nm. The assay mix contained 100 mM Tris HCl, pH 7.4, 5 mM H_2O_2, 5 mM GSH (Marini *et al*., 2020).

Catalase activity was spectrophotometrically assayed, following the decomposition of H_2O_2 at 240 nm. The assay mix contained 50 mM phosphate buffer, pH 7.0, and 5 mM H_2O_2 (Villa *et al*., 2021).

3.15 Statistical Analysis

All experimental groups were studied in triplicate. Data are presented as mean ± standard deviation (SD). Differences among the experimental conditions were tested using t-test, two-way analysis of variance (ANOVA), and the Bonferroni test was used to test the statistical hypothesis. Significance was considered for *p* values <0.05. All analyses were performed using SPSS software Advanced Models 15.0 (Chicago, IL, USA).

4. RESULTS

Results Section 1: role of endoplasmic reticulum in the differential endurance against redox stress in cortical and spinal astrocytes from new-born SOD1^{G93A} mice

4.1 Purity of WT and SOD1^{G93A} New-born Astrocyte Cell Cultures

In the first set of experiments, we investigated the purity of neonatal astrocytes cultured from the spinal cord of SOD1^{G93A} P2 mouse pups by flow cytometry, labelling cell suspension with antibodies for GFAP or astrocyte cell surface antigen-2 (ACSA2), specific astrocyte markers (Kantzer *et al.,* 2017), and Transmembrane Protein 119 (TMEM119), a specific microglia marker (Bennett *et al.,* 2016).

Figure 4a (g–m) shows that astrocyte preparations indeed express both the astroglial markers GFAP and ACSA2 [Figure 4a (g and k), 95.03 ± 3.38% GFAP positive cells; figure 4a (h and l), 94.46 ± 1.92% ACSA2 positive cells; figure 1a (i), 98.34 ± 1.42% GFAP and ACSA2 positive cells) when compared to the respective unstained controls [Figure 4a (d, e)]. Moreover, cell suspensions showed very low contamination of microglia cells, labelled with TMEM119 (2.42 ± 0.69% TMEM119-positive cells, Figure 4a (j, m)), compared to the respective unstained control (Figure 4a (f)). We also performed confocal microscopy studies staining WT and SOD1^{G93A} spinal cord neonatal astrocytes with antibodies for GFAP and integrin alpha-M/beta-2 (CD11b; specific microglia marker). Representative images reported in Figure 4b (a–f) indicate that both WT and SOD1^{G93A} astrocytes are efficiently stained with GFAP (green fluorescence), while they do not show contamination by microglia cells, labelled with CD11b (red fluorescence). These results indicate that the neonatal astrocyte primary cell culture preparations used here were not contaminated by microglia cells.
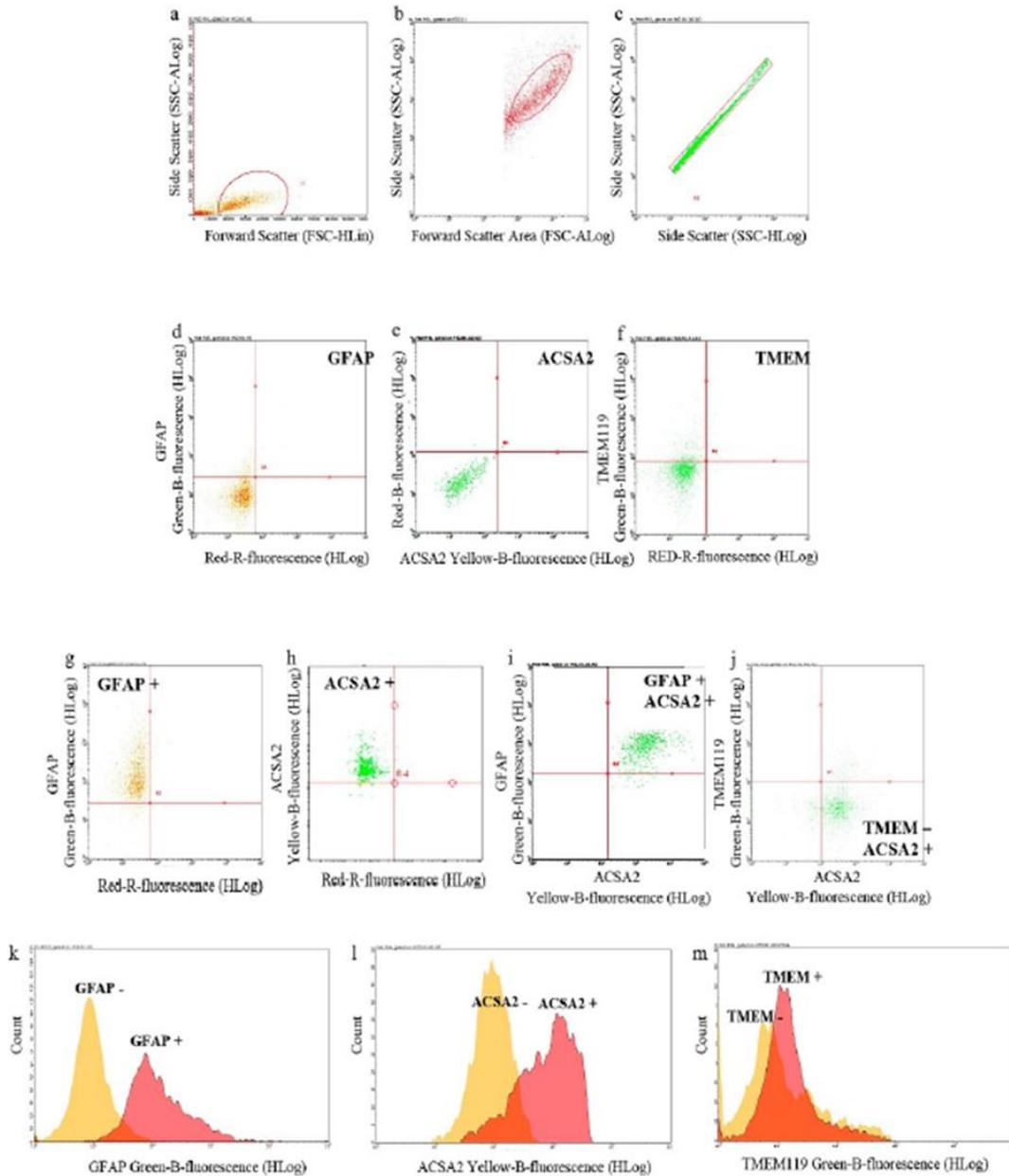
Figure 4a: *Astrocyte cell culture purity*. Spinal cord neonatal astrocyte primary cell cultures were prepared from WT and SOD1[G93A] P2 pups, and their purity has been verified by flow cytometry **(a–m)**. **(a–c)** Representative flow cytometry dot plots of SOD1[G93A] astrocytes showing the cell population gated by (a) side scatter (SSCALog) vs. forward scatter (FSC-HLin), **(b)** SSC-ALog vs. forward scatter (FSC-ALog) and **(c)** SSC-Alog vs. side scatter (SSC-HLog). **(d–f)** Representative dot plots of SOD1[G93A] unstained SOD1[G93A] astrocytes. **(g–j)** Representative dot plots of SOD1[G93A] astrocytes after incubation with fluorophore-conjugated antibodies for **(g)** GFAP (astrocyte marker; green fluorescence), **(h,i)** ACSA2 (astrocyte marker; yellow fluorescence) and **(j)** TMEM119 (microglia marker; green fluorescence). **(k–m)** Representative flow cytometry histogram plots of SOD1[G93A] astrocytes showing the expression of **(k)** GFAP, **(l)** ACSA2 and **(m)** TMEM, compared to the respective unstained controls. For quantization, *n* = 4 biological replicates per group were analysed
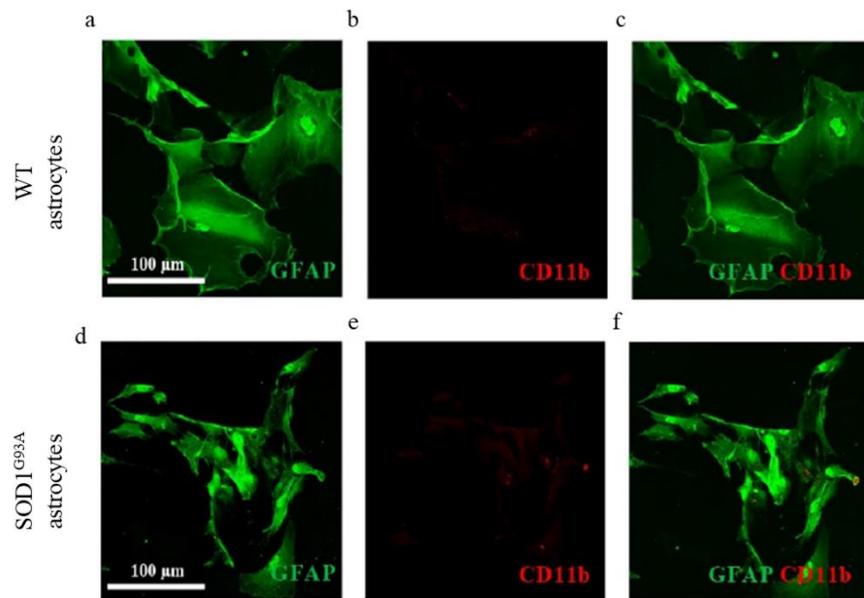
Figure 4b: Astrocyte cell culture purity. Spinal cord neonatal astrocyte primary cell cultures were prepared from WT and SOD1^{G93A} P2 pups, and their purity has been verified by immunofluorescence (**a**–**f**). Representative confocal microscopy images of WT and SOD1^{G93A} spinal cord neonatal astrocyte primary cell cultures stained with selective antibodies for (**a**, **d**) GFAP (green fluorescence) and (**b**, **e**) CD11b (specific microglia marker; red fluorescence); (**c**, **f**) merge panels. For quantization, n = 3 biological replicates per group were analysed, with each value defined in triplicate.

4.2 Redox Stress Response in Cortical and Spinal SOD1^{G93A} New-born Astrocytes

Multiple pathological studies have reported evidence of increased oxidative stress in ALS tissue compared to control (Bonnefont *et al.,* 2000; Siciliano et al., 2002; Rosen *et al*., 1993). MDA evaluates lipid peroxidation. Some studies showed increased oxidative stress in astrocytes, measured as MDA-modified proteins 8 hydroxy-deoxyguanosine, and nitrotyrosine products (Calingasan *et al*., 2005; Ferrante *et al.,* 1997). In this study, astrocytes were isolated from the MC and SC of SOD1^{G93A} mice and WT littermates. In SOD1^{G93A} MC astrocytes, the intensity of H$_2$DCFDA fluorescence was higher than in WT astrocytes, indicating a selective increase in ROS content (Figure 5a), as confirmed by a significant increase in lipid peroxidation evaluated by malondialdehyde (MDA) levels (Figure 5b). The enhanced redox stress at least partially reflected an inadequate response of antioxidant pathways. Indeed, total antioxidant capacity was decreased in MC SOD1^{G93A} astrocytes with respect to their WT counterpart (Figure 5c).

Redox balance was remarkably different in SC cultures. Indeed, H$_2$DCFDA staining intensity and thus ROS content were higher in SC WT astrocytes as compared to MC WT

ones (Figure 5a). This difference was, however, not paralleled by increased lipid peroxidation, suggesting a higher endurance against the redox stress in the spinal district of WT mice (Figure 5b). This pattern was virtually abolished in the experimental ALS model. Indeed, H_2DCFDA fluorescence of SC SOD1^{G93A} astrocytes was markedly increased and became similar to the intensity observed in corresponding MC cultures. Nevertheless, MDA content was only slightly increased (Figure 5a, b). These findings nicely agreed with the behaviour of total antioxidant capacity that was selectively enhanced in mutated SC astrocytes (Figure 5c).
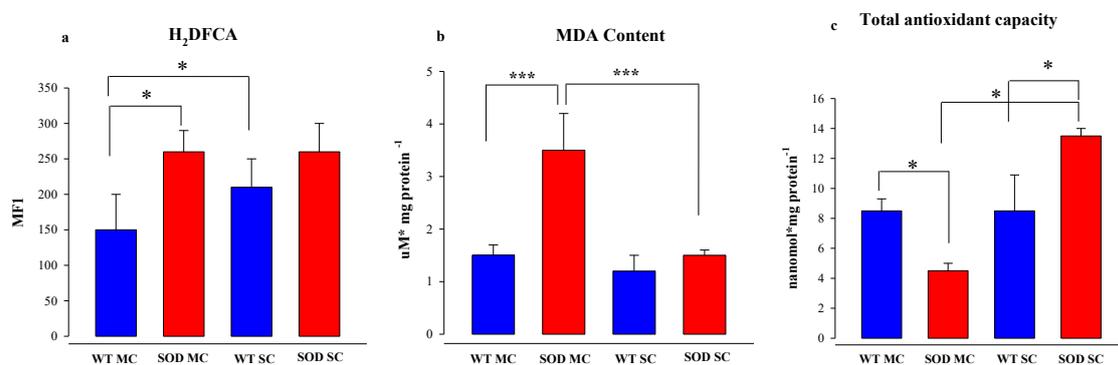

Figure 5: *Astrocyte antioxidant response and oxidative stress.* (**a**) ROS levels measured using H_2DCFDA mean fluorescence index (MFI), (**b**) malondialdehyde content (MDA), (**c**) antioxidant capacity in wildtype (blue) and SOD1^{G93A} (red) astrocytes harvested from MC and SC. Data are shown as the mean ± SD. $n = 3$ experiments per group, with each value defined in triplicate. * $p < 0.05$, *** $p < 0.001$ (WT SC astrocytes vs. WT MC astrocytes and SOD1^{G93A} SC astrocytes vs. SOD1^{G93A} MC astrocytes) (Two-way ANOVA followed by Bonferroni post hoc test).

4.3 Antioxidant Response in Cortical and Spinal SOD1^{G93A} New-born Astrocytes

In eukaryotic cells, ROS scavenging largely involves the availability of NADPH reductive power whose main source is represented by the cytosolic PPP (Riganti *et al.,* 2012). The catalytic function of its triggering enzyme G6PD, evaluated by spectrophotometric assay, was increased in mutated MC astrocytes (p < 0.05, Figure 6a). Then, obtained data suggest an acceleration of cytosolic PPP that should be associated with an enhanced reduction of NADP+ to NADPH. Nevertheless, the overall NADPH content and the NADPH/NADP+ ratio was remarkably decreased in MC astrocytes (Figure 6b, c), suggesting that the high-rate utilization of this reducing cofactor was not counterbalanced by cytosolic PPP, despite the enhanced activity of its triggering enzyme.

This response was at least partially independent of the cytosolic PPP since G6PD activity of WT SC cells was significantly lower than in MC cells and was not affected by SOD1^{G93A}

mutation (Figure 6a). A different behaviour was displayed by H6PD: its activity was undetectable in all cultures except from mutated SC astrocytes in which its activity accounted for 4.97 ± 0.8 Mu/mg of proteins. However, the NADPH content and the NADPH/NADP+ ratio was similarly decreased with respect to mutated MC astrocytes (Figure 6b, c), suggesting that the high-rate utilization of this reducing cofactor was not counterbalanced by cytosolic or reticular PPP activity (Figure 6a-c).
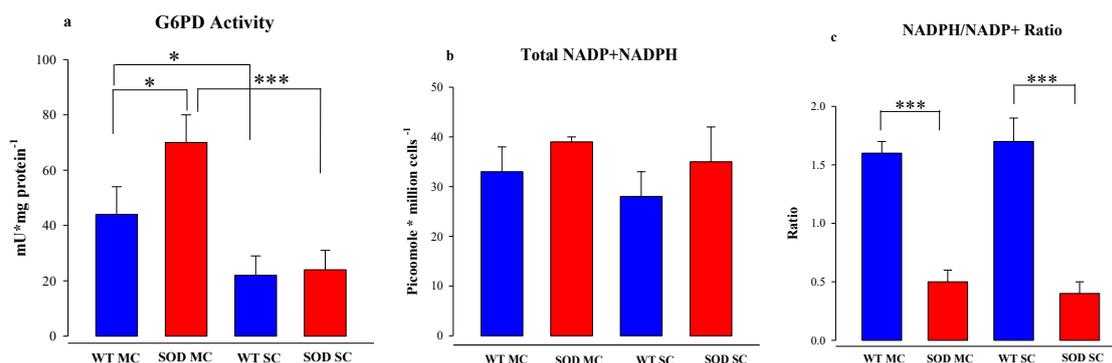

Figure 6: *Astrocyte antioxidant response and oxidative stress.* (**a**) G6PD activity in wildtype (blue) and SOD1[G93A] (red) astrocytes harvested from motor cortex (MC) and spinal cord (SC). (**b**) NADPH level in wildtype (light blue) and SOD1[G93A] (pink) astrocytes and NADP+ level in wildtype (blue) and mutated cells (red). (**c**) NADPH/NADP+ ratio in wildtype (blue) and SOD1[G93A] (red) astrocytes in wildtype (blue) and SOD1[G93A] (red) astrocytes harvested from MC and SC. Data are shown as the mean $\pm$ SD. $n = 3$ experiments per group, with each value defined in triplicate. *$p < 0.05$, *** $p < 0.001$ (WT SC astrocytes vs. WT MC astrocytes and SOD1[G93A] SC astrocytes vs. SOD1[G93A] MC astrocytes) (two-way ANOVA followed by Bonferroni post hoc test).

4.4 Mitochondrial Redox Status in Cortical and Spinal SOD1[G93A] New-born Astrocytes

It is well known that mitochondria play a double role in oxidative stress, representing, at the same time, a main source of ROS and a primary target of ROS-induced damage. We thus estimated the mitochondrial redox status, using Mito-SOX Red, a specific and mitochondrial-targeted detection probe for superoxide radical (O2). As reported in figure 4b, fluorescence intensity was comparable in mutated vs. WT MC or SC cultures. Similarly, the affinity for the mitochondrial probe was only slightly, and not significantly, decreased by SOD1[G93A] mutation in SC astrocytes with respect to both mutated MC and WT SC cells (Figure 7a). A similar conclusion also applied to the evaluation of mitochondrial membrane polarization. Indeed, Mito-Tracker Red staining provided largely variable results without any significant difference among all groups of tested cultures (Figure 7b).

Altogether, these data thus indicated that SOD1^{G93A} mutation is associated with an early enhancement of redox stress that selectively affects MC astrocytes harvested 2 days after birth. However, this oxidative environment seems to not be explained by mitochondrial damage, indicating the possible role of other cell structures or functions in the redox impairment of MC astrocytes.
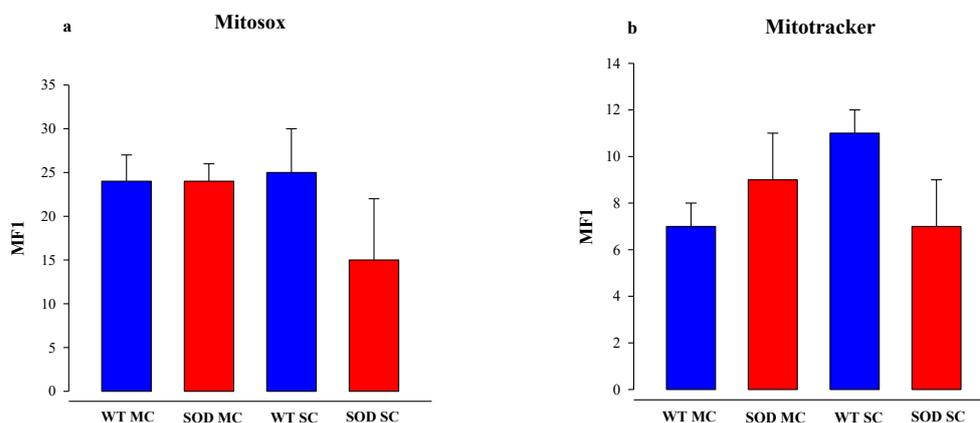

Figure 7: *Astrocyte antioxidant response and oxidative stress.* (**a**) Mean fluorescence intensity (MFI) of MitoSOX and (**b**) MitoTracker in wildtype (blue) and SOD1^{G93A} (red) astrocytes harvested from MC and SC. Data are shown as the mean ± SD. $n = 3$ experiments per group, with each value defined in triplicate. (Two-way ANOVA followed by Bonferroni post hoc test).

4.5 Oxidative Phosphorylation Coupling and Glycolytic Flux in Cortical and Spinal SOD1^{G93A} New-born Astrocytes

To evaluate the mechanisms underlying the apparent mismatch of increased redox damage not paralleled by evident mitochondrial alterations, we extended our evaluation to the respiratory function and glycolytic flux, using the Seahorse technology. In new-born MC astrocytes, SOD1^{G93A} mutation left unaltered both baseline and maximal oxidative phosphorylation (OXPHOS) rates evaluated under control conditions and during respiratory uncoupling by FCCP (Figure 8a, c, e). However, the mutation caused a relative respiratory uncoupling since OCR under ATP-synthase blockade by oligomycin was higher in mutated than in WT MC cultures (Figure 8a, d), suggesting a relative decrease in OXPHOS-linked ATP production. This abnormality was markedly less evident in SC astrocytes, in which SOD1^{G93A} mutation left unaltered basal, ATP-linked, and maximal OCRs (Figure 8b–e).
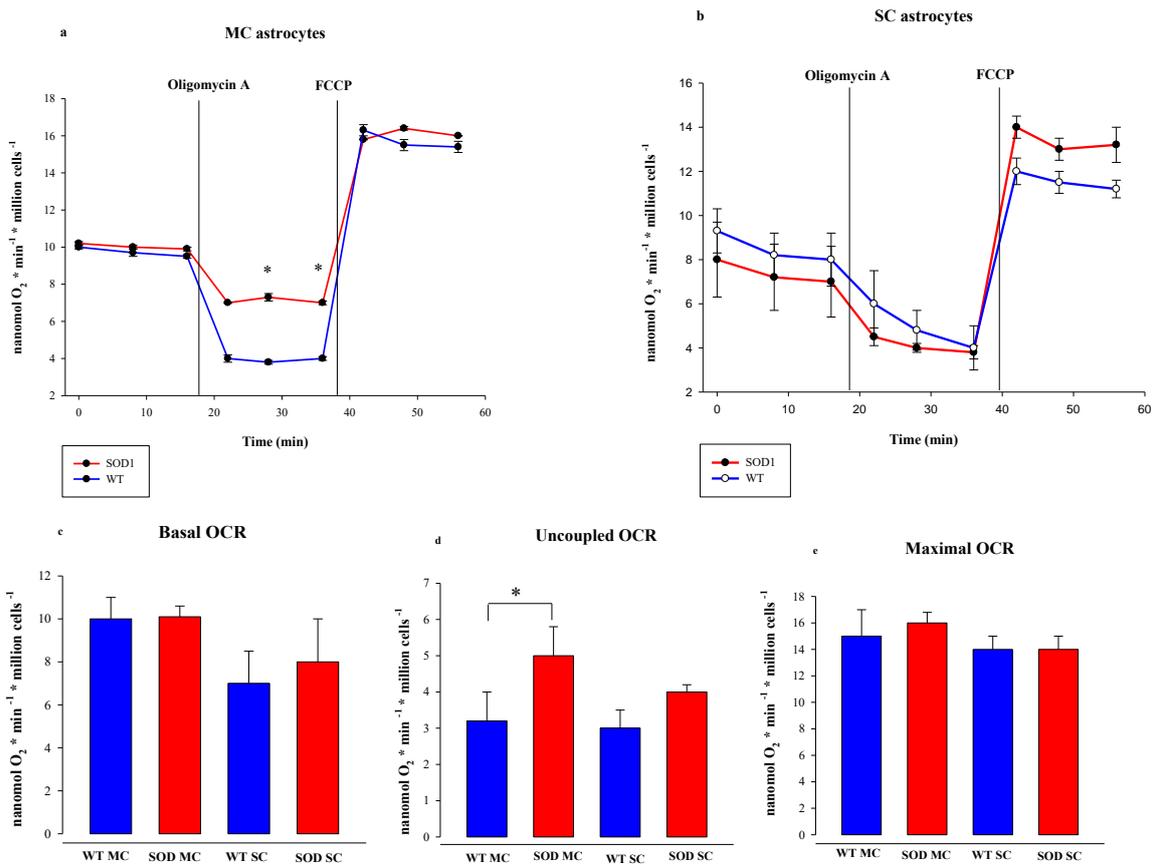
Figure 8: *Mitochondrial energetic function in SOD1^{G93A} astrocytes.* Basal oxygen consumption rate (OCR) measured in presence of glucose (11 mM), glutamine (2 mM) and pyruvate (1 mM) and after sequential injection of the ATP-synthase inhibitor oligomycin A (1 mM) and the ATP synthesis uncoupler FCCP (0.8 μM) in (**a**) motor cortex (MC) and (**b**) spinal cord (SC) astrocytes, in wildtype (blue) and SOD1^{G93A} astrocytes (red). (**c**) Basal, (**d**) uncoupled and (**e**) maximal OCRs in wildtype (blue) and SOD1^{G93A} (red) astrocytes harvested from MC and SC. Data are shown as the mean ± SD. $n = 3$ experiments per group, with each value defined in triplicate. ns = not significant, *$p < 0.05$ vs. corresponding WT astrocytes (Two-way ANOVA followed by Bonferroni post hoc test).

The differential OXPHOS efficiency of the two central nervous system regions was reproduced by the Western blot analysis of electron transport between complexes III and IV. Indeed, SOD1^{G93A} genotype was associated with a significant decrease in total cytochrome c levels in MC astrocytes, as opposed to an increase in SC ones (Figure 9a, b). In addition, complex I activity function was significantly decreased in SOD1^{G93A} MC astrocytes, while it remained unchanged in SC cultures (Figure 9c).
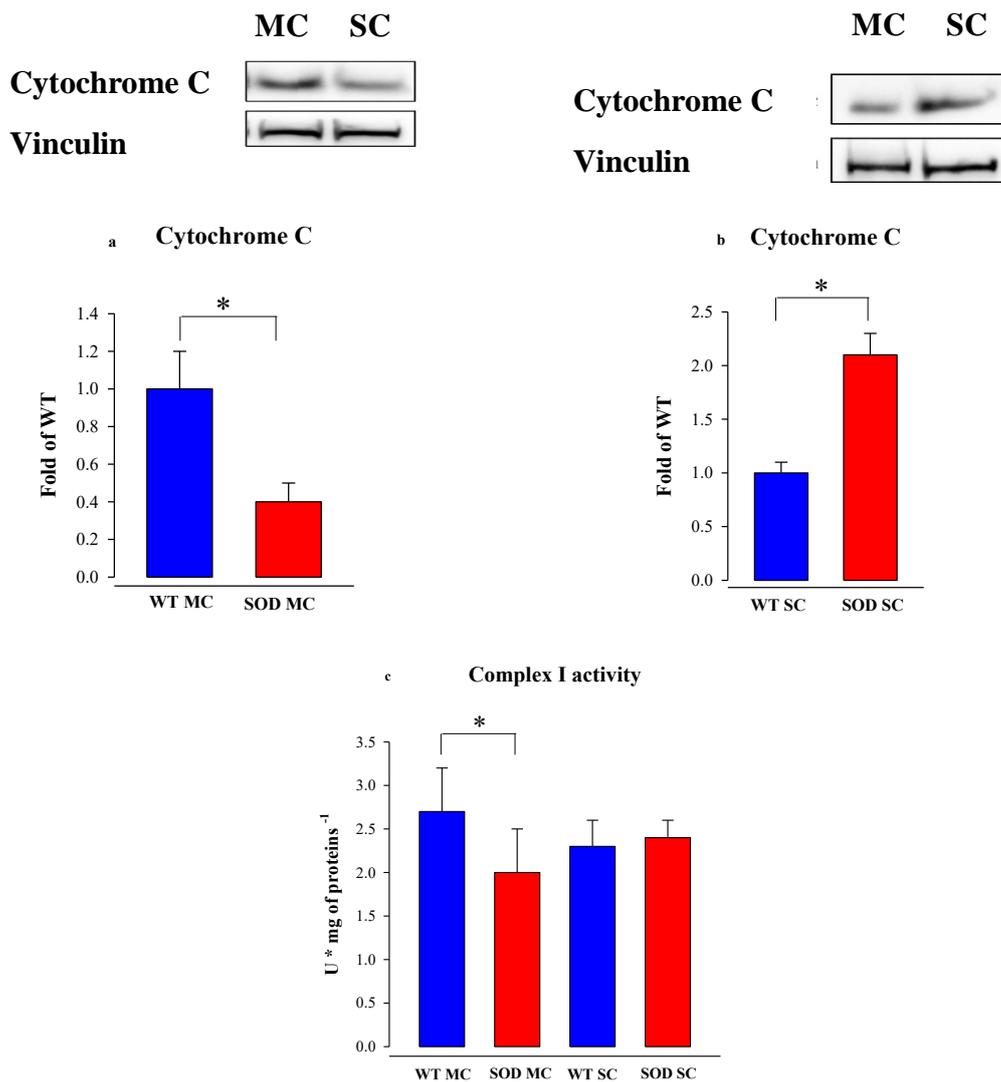
Figure 9: *Mitochondrial energetic function in SOD1^{G93A} astrocytes.* Western blot analysis and relative densitometric quantitative analyses of cytochrome c in MC (**a**) and SC (**b**) astrocytes. (**c**) Complex I activity in wildtype (blue) and SOD1^{G93A} (red) astrocytes harvested from MC and SC. Data are shown as the mean $\pm$ SD. $n = 3$ experiments per group, with each value defined in triplicate. ns = not significant, *$p < 0.05$ vs. corresponding WT astrocytes (One-way ANOVA followed by Bonferroni post hoc test).

Results Section 2: effect of CTEP in pharmacological modulation of mGluR5 receptors on the activation state and metabolic functions of astrocytes obtained from human ALS patients.

4.6 Human Astrocytes Characterization

Human astrocytes were differentiated from fibroblasts derived from two ALS patients carrying the SOD1^{A4V} mutation (patients' number 100 and 102), two C9orf72 mutation (patients' number 78 and 183) and one healthy donor (individual number 155). After four weeks of differentiation protocol to obtain inducible neural progenitor cells (iNPCs), astrocytes were prepared by switching iNPCs medium with astrocyte medium.

To confirm the efficacy of the differentiation protocol, the expression of GFAP, vimentin and CD44, selective markers for astrocytes, was analysed on i-astrocytes obtained from healthy donor by immunofluorescence. i-astrocytes result highly positive to these markers (Meyer *et al.*, 2014). These results confirm that an extensive enrichment in astrocyte-like cells was obtained following the differentiation protocol (Figure 10).
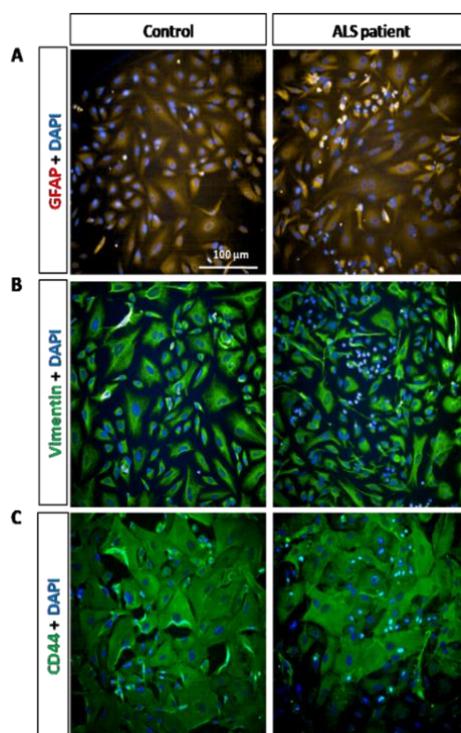

Figure 10: *Immunocytochemical characterization of human astrocytes from control and ALS patients.* Representative images of human astrocytes (i-astrocytes) differentiated from fibroblasts derived from control and ALS patients. i-astrocytes were stained for (A)GFAP (red) and DAPI (blue), (B)Vimentin (green) and DAPI (blue), and (C)CD44 (green) and DAPI (blue). Scale bar: 100 μm

4.7 Effect of CTEP on the expression of proteins characterizing the phenotype of control, C9orf72 and SOD1^{A4V} i-astrocytes

4.7.1 Effect of CTEP on GFAP expression level in control, C9orf72 and SOD1^{A4V} i-astrocytes

Astrogliosis is a key feature of ALS (Rossi *et al.,* 2008, Lasiene and Yamanaka., 2011), often characterized by overexpression of specific astrocytic marker, GFAP (Benninger *et al.,* 2016). GFAP is a monomeric intermediate filament protein found in the astroglial cytoskeleton. This protein is not routinely secreted in blood and is only released after cell death or injury. These characteristics suggest that GFAP may be an ideal marker for activated astrocytes.

Here, the expression of GFAP was quantified in control, C9orf72, and SOD1^{A4V} i-astrocytes by both WB (Figure 11) and immunofluorescence analysis (Figure 12). Figure 11a represents the immunoreactive bands for GFAP in treated and non-treated i-astrocytes. Figure 11b represents the quantification of GFAP expression after the CTEP treatment in i-astrocytes obtained from control, C9orf72, and SOD1^{A4V} patients. The CTEP treatment significantly reduced the expression of GFAP ($P<0.01$) as compared to non-treated i-astrocytes (Figure 11).

The same GFAP expression trend was confirmed by IF analysis (figure 12). Figure 12a shows representative immunocytochemical images of GFAP (green) and GAPDH (red) expression and co-localization (yellow) in control, C9orf72, and SOD1^{A4V} i-astrocytes. Figure 12b reports the quantification of immunocytochemical images and reveal that the expression of GFAP was significantly reduced ($P<0.001$) in CTEP treated C9orf72 and SOD1^{A4V} i-astrocytes, compared to non-treated i-astrocytes.
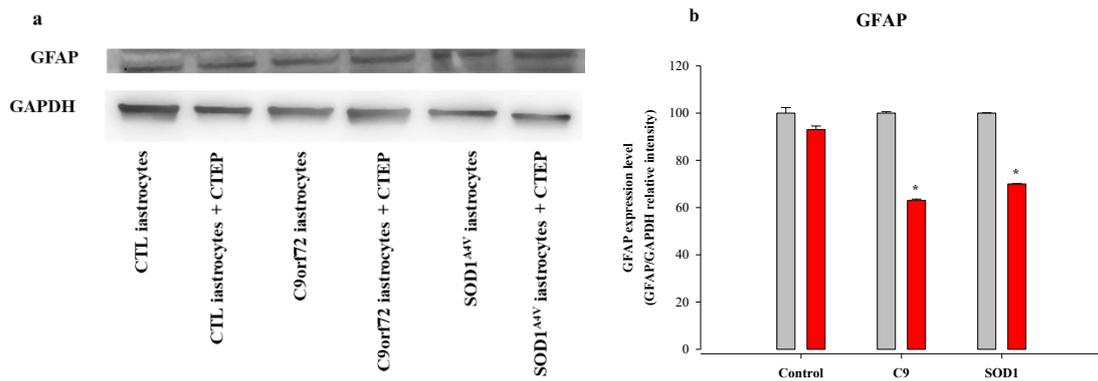
Figure 11: *Western blot quantification of GFAP expression in cell lysates from human astrocytes obtained from control, C9orf72, SOD1^{A4V} and CTEP treatment i-astrocytes*. **(a)** Representative immunoreactive bands for GFAP and GAPDH. **(b)** Quantification of protein expression as per scanned band density in control, C9orf72, SOD1^{A4V} vehicle (Gray) or CTEP-treated (Red) i-astrocytes; Protein expression level was calculated as relative density, normalized to the housekeeping protein GAPDH. Data presented are means ± SD of three independent experiments. *$P<0.001$ vs. non treated i-astrocytes (t-test).
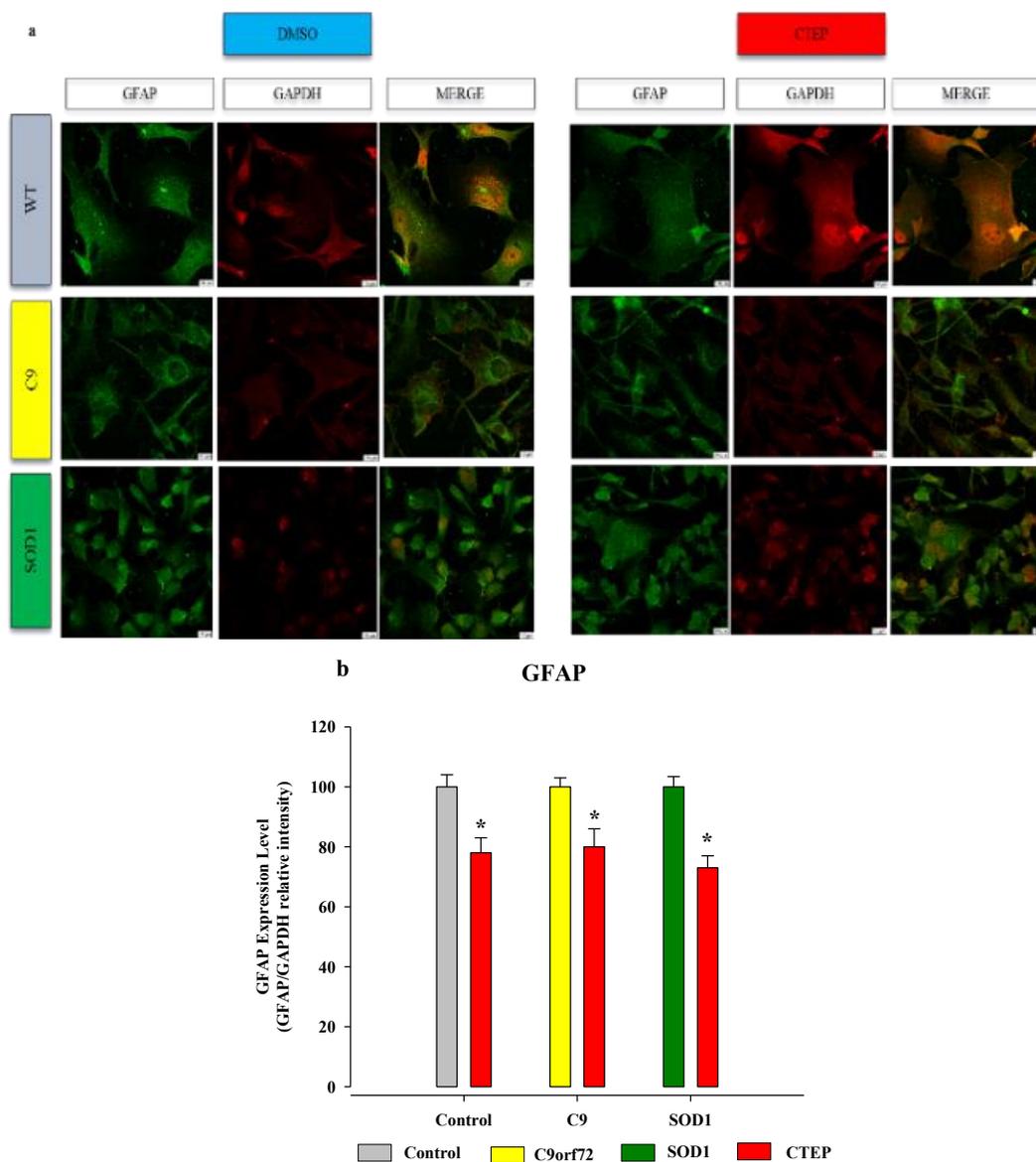
Figure 12: *Immunocytochemical quantification of GFAP expression in i-astrocytes obtained from control, C9orf72, SOD1^{A4V} and CTEP treatment.* (**a**) The panel represents the confocal microscopy immunocytochemical images of GFAP (green) and GAPDH (red) in control, C9orf72 and SOD1^{A4V} vehicle- (left) or CTEP- (right) treated i-astrocytes cultured on coverslip and labelled with the appropriate primary and secondary antibodies. The merge panels represent the co-expression of GFAP and GAPDH. Scale bar: 10 μm. (**b**) Quantification of protein expression, as per relative fluorescence intensity, was performed calculating the co-localization coefficients (Manders *et al.,* 1992) using Image-J software analyses. Data are expressed as relative fluorescence intensity of GFAP normalized respect to the fluorescence intensity of the housekeeping protein GAPDH. The relative intensity of non-treated i-astrocytes is reported as 100. Data presented are means ± SD of three independent experiments run in triplicate (three different coverslips for each experimental condition); statistical analysis was performed by t-test *P<0.001 vs. non treated i-astrocytes.

4.7.2 Effect of CTEP on S100β expression level in control, C9orf72 and SOD1^{A4V} i-astrocytes

In ALS patients, S100β has been shown to increase in cortical and spinal cord astrocytes (Kamo *et al.,* 1987). The protein was also overexpressed in astrocytes in the spinal cord of ALS rodent models (Serrano *et al.,* 2017). It is worth considering that the overexpression of S100β has been observed in a specific subpopulation of astrocytes (Dıaz-Amarilla *et al.,* 2011).

Here, the expression of S100β was quantified in control, C9orf72, and SOD1^{A4V} i-astrocytes by WB (Figure 13) and immunofluorescence analysis (Figure 14). Figure 13a represents the immunoreactive bands for S100β in treated and non-treated i-astrocytes. Figure 13b represents the quantification of S100β expression after the CTEP treatment on i-astrocytes obtained from control, C9orf72, and SOD1^{A4V} patients. CTEP treatment significantly reduced the overexpression of S100β ($P<0.01$) in C9orf72 and SOD1^{A4V} mutated i-astrocytes but not in control i-astrocytes, the reason of this discrepancy is difficult to understand at present (Figure 13).

The same S100β expression trend was confirmed by immunofluorescence except for the control I-astrocytes (figure 14). Figure 14a shows representative immunocytochemical images of S100β (green) and GAPDH (red) expression and co-localization (yellow) in control, C9orf72, and SOD1^{A4V} i-astrocytes. Figure 14b represent the quantification of immunocytochemical images reveal that the expression of S100β was significantly reduced ($P<0.01$) in CTEP treated C9orf72 and SOD1^{A4V} i-astrocytes, compared to non-treated i-astrocytes.
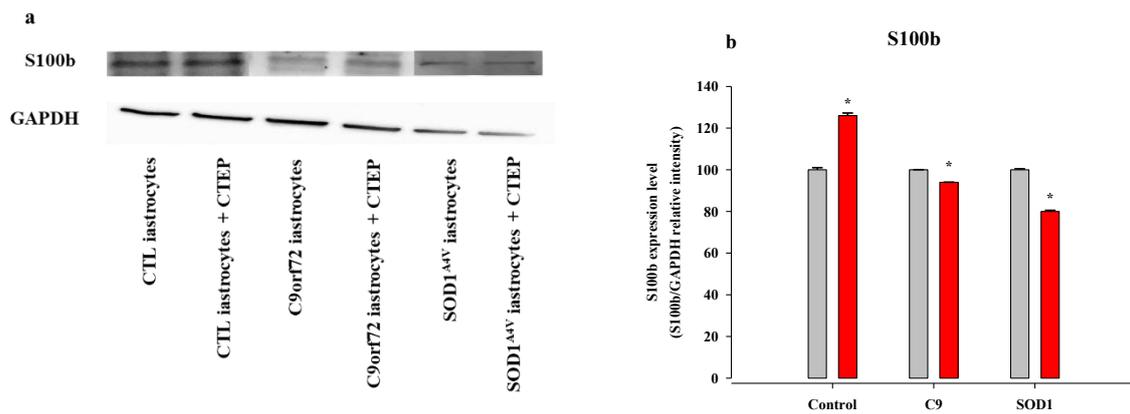
Figure 13: *Western blot quantification of S100β expression in cell lysates from i-astrocytes obtained from control, C9orf72, SOD1^{A4V} and CTEP treatment.* **(a)** Representative immunoreactive bands for S100β and GAPDH; **(b)** Quantification of protein expression as per scanned band density in control, C9orf72, SOD1^{A4V}, vehicle (Gray) or CTEP-treated (Red) i-astrocytes. Protein expression level was calculated as relative density, normalized to the housekeeping protein GAPDH. Data presented are means ± SD of three independent experiments. *P<0.001 vs. non treated i-astrocytes (t-test).
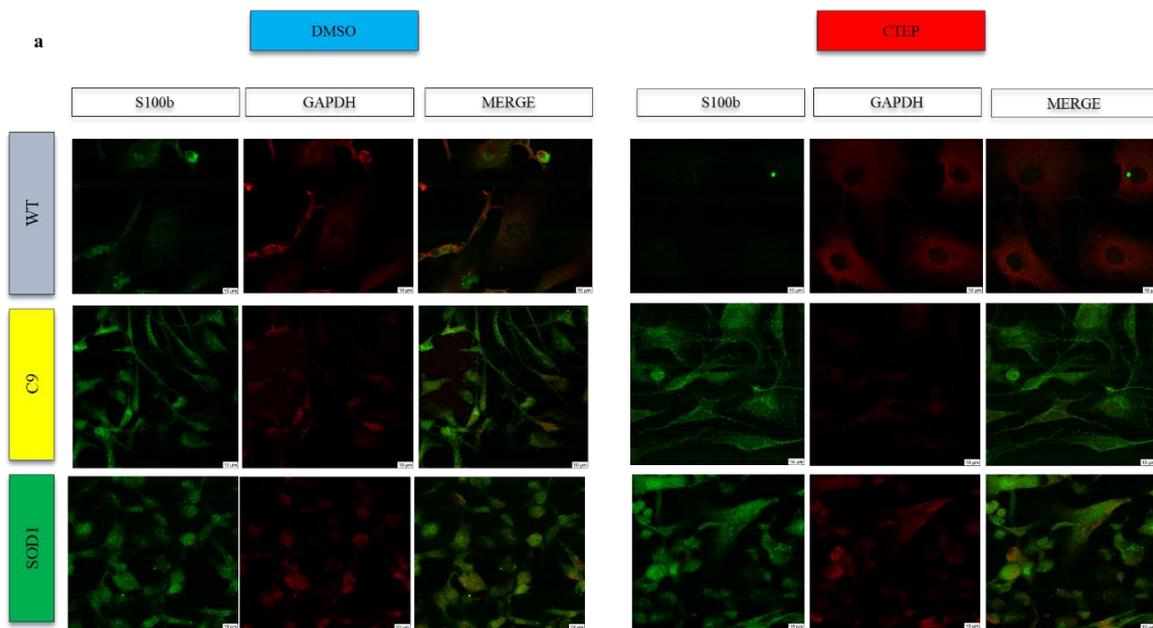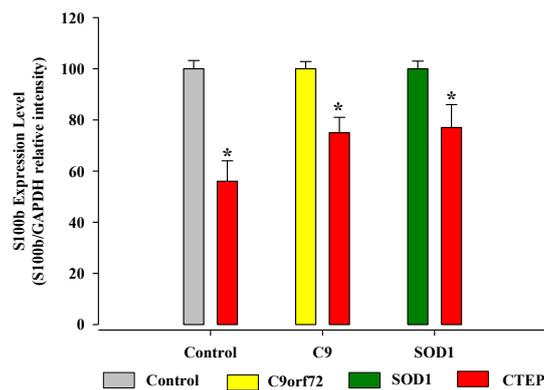
Figure 14: *Immunocytochemical quantification of S100β expression in i-astrocytes obtained from control, C9orf72, SOD1^{A4V} and CTEP treatment.* **(a)** The panel represents the confocal microscopy immunocytochemical images of S100β (green) and GAPDH (red) in control, C9orf72 and SOD1^{A4V} vehicle- (left) or CTEP- (right) treated i-astrocytes cultured on coverslip and labelled with the appropriate primary and secondary antibodies. The merge panels represent the co-expression of S100β and GAPDH. Scale bar: 10 μm. **(b)** Quantification of protein expression, as per relative fluorescence intensity, was performed calculating the co-localization coefficients (Manders *et al.,* 1992) using Image-J software analyses. Data are expressed as relative fluorescence intensity of S100β normalized respect to the fluorescence intensity of the housekeeping protein GAPDH. The relative intensity of non-treated i-astrocytes is reported as 100. Data presented are means ± SD of three independent experiments run in triplicate (three different coverslips for each experimental condition); statistical analysis was performed by t-test *P<0.001 vs. non treated i-astrocytes.

4.7.3 *Effect of CTEP treatment on C3 expression level in control, C9orf72 and SOD1^{A4V} i-astrocytes*

Several lines of evidence indicate that aberrant activation of the complement system in the central nervous may be involved in the pathophysiology of ALS. Within the complement signalling cascade C3 is regarded as potent inflammatory and immunomodulatory peptide with various biological functions. In the CNS their functions include chemotaxis and proliferation of microglia and astrocytes; generation of superoxide radicals; and induction of pro-inflammatory cytokine synthesis. Some of these functions have been observed in neurodegenerative disease, suggesting that these complement factors may play a role in ALS pathogenesis (Kjældgaard *et al.,* 2018).

The expression of C3 was quantified in control, C9orf72, and SOD1^{A4V} i-astrocytes by WB (Figure 15) and IF analysis (Figure 16). Figure 15a represents the C3 immunoreactive bands in treated and non-treated i-astrocytes. Figure 15b represents the quantification of C3 expression after CTEP treatment in i-astrocytes obtained from control, C9orf72, and SOD1^{A4V} patients. Figure 15 shows that CTEP treatment significantly reduced C3 expression (P<0.001) in control, C9orf72, and SOD1^{A4V} i-astrocytes.

The same C3 expression trend was confirmed by immunofluorescence analysis (figure 16). Figure 16a shows representative immunocytochemical images of C3 (green) and GAPDH (green) expression and co-localization (yellow) in control, C9orf72, and SOD1^{A4V} i-astrocytes. Figure 16b reports the quantification of immunocytochemical images and reveal that the C3 expression was significantly reduced (P<0.001) in CTEP treated control, C9orf72 and SOD1^{A4V} i-astrocyte, compared to non-treated i-astrocytes (Figure 16).
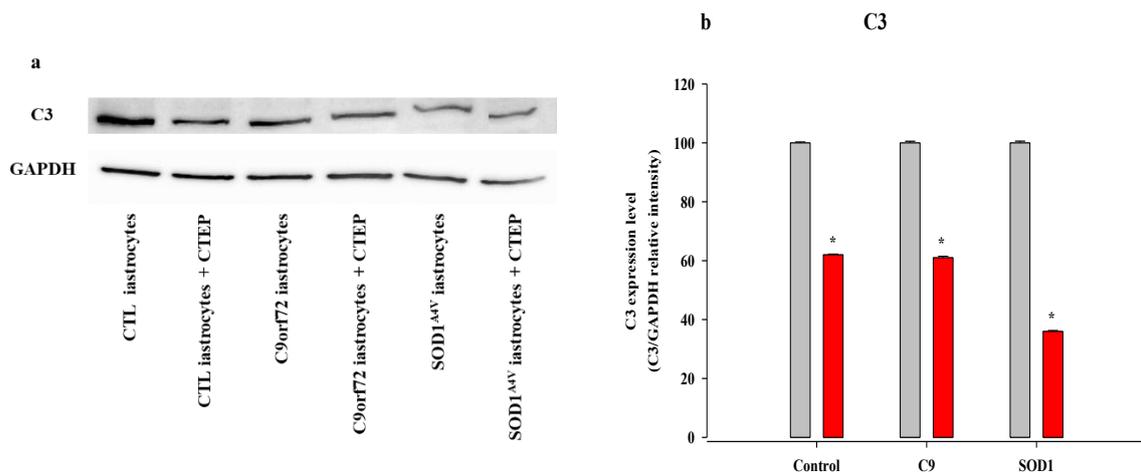
Figure 15: *Western blot quantification of C3 expression in cell lysates from i-astrocytes obtained from control, C9orf72, SOD1^{A4V} and CTEP treatment.* **(a)** Representative immunoreactive bands for C3 and GAPDH; **(b)** Quantification of protein expression as per scanned band density in control, C9orf72, SOD1^{A4V} vehicle (Gray)- or CTEP-treated (Red) i-astrocytes. Protein expression level was calculated as relative density, normalized to the housekeeping protein GAPDH. Data presented are means $\pm$ SD of three independent experiments. *P$<$0.001 vs. Non treated i-astrocytes (t-test).
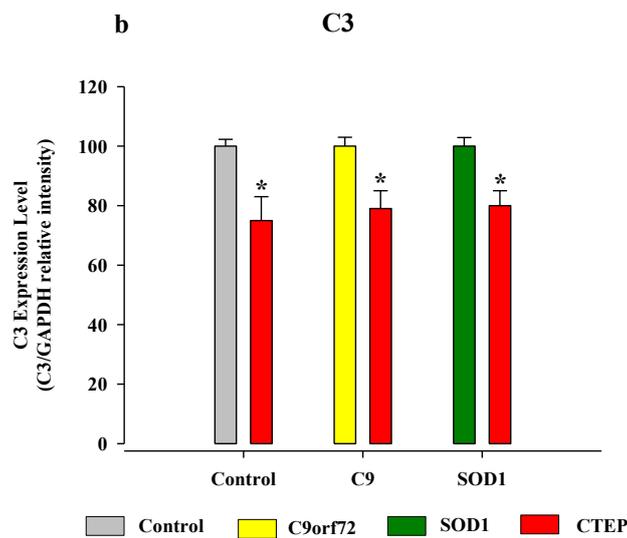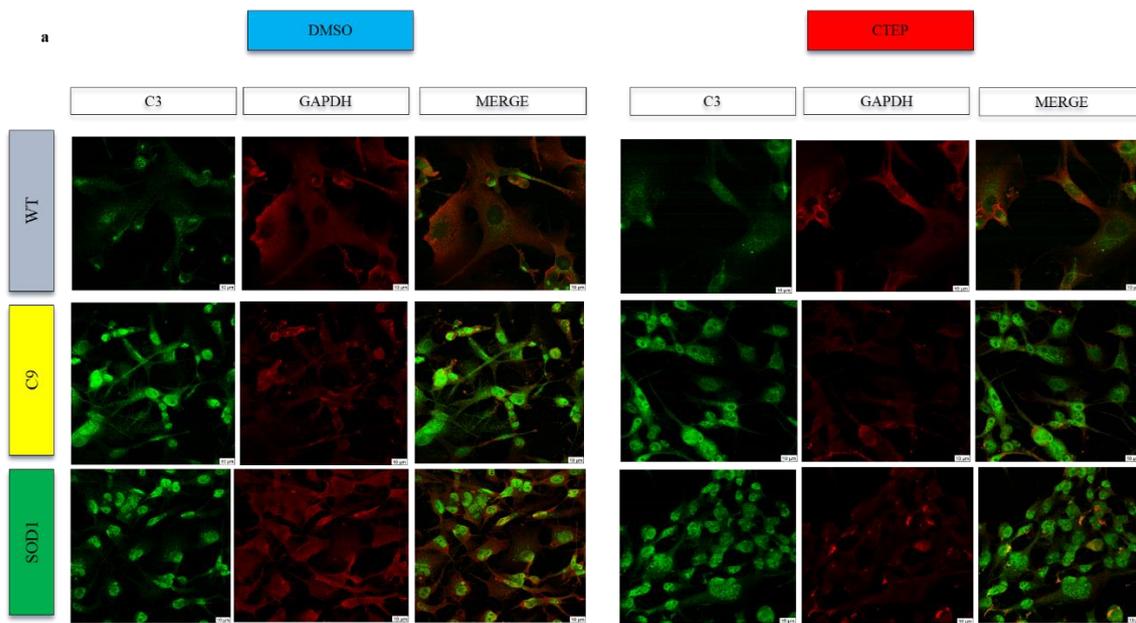
Figure 16: *Immunocytochemical quantification of C3 expression in i-astrocytes obtained from control, C9orf72, SOD1^{A4V} and CTEP treatment.* **(a)** The panel represents the confocal microscopy immunocytochemical images of C3 (green) and GAPDH (red) in control, C9orf72 and SOD1^{A4V} vehicle- (left) or CTEP- (right) treated i-astrocytes cultured on coverslip and labelled with the appropriate primary and secondary antibodies. The merge panels represent the co-expression of C3 and GAPDH. Scale bar: 10 μm. **(b)** Quantification of protein expression, as per relative fluorescence intensity, was performed calculating the co-localization coefficients (Manders *et al.,* 1992) using Image-J software analyses. Data are expressed as relative fluorescence intensity of C3 normalized respect to the fluorescence intensity of the housekeeping protein GAPDH. The relative intensity of non-treated i-astrocytes is reported as 100. Data presented are means ± SD of three independent experiments run in triplicate (three different coverslips for each experimental condition); statistical analysis was performed by t-test *P<0.001 vs. non treated i-astrocytes.

4.7.4 Effect of CTEP treatment on NLRP3 inflammasome expression level in control, C9orf72 and SOD1^{A4V} i-astrocytes

NLRP3 is a protein complex strictly related to inflammation. Its assembly determines the cleavage of IL-1β and IL-18 through caspase-1 and the subsequent conversion of these cytokines into their active form, exacerbating neuroinflammation and inducing cell apoptosis and necroptosis (Mangan *et al.,* 2018).

We here investigated the effect of CTEP treatment on NLRP3 expression in control, C9orf72, and SOD1^{A4V} i-astrocytes by WB (figure 17) and IF (figure 18). Figure 17a represents the immunoreactive bands for NLRP3 in treated and non-treated i-astrocytes. Figure 17b reports the quantification of NLRP3 expression after the CTEP treatment in i-astrocytes obtained from control, C9orf72, and SOD1^{A4V} patients. Figure 17 show that CTEP treatment significantly lowers the expression of NLRP3 in control, C9orf72 and SOD1^{A4V} i-astrocytes as compared to non-treated i-astrocytes ($P<0.001$).

A similar NLRP3 expression trend was confirmed by IF analysis (figure 18). Figure 18a shows representative immunocytochemical images of NLRP3 (green) and GAPDH (red) expression and co-localization (yellow) in control, C9orf72, and SOD1^{A4V} i-astrocytes. Figure 18b reports the quantification of immunocytochemical images and reveal that the expression of NLRP3 (50% decrease; $P<0.01$) in CTEP treated control, and C9orf72-astrocytes but not in mutated SOD1^{A4V} patients, compared to non-treated i-astrocytes
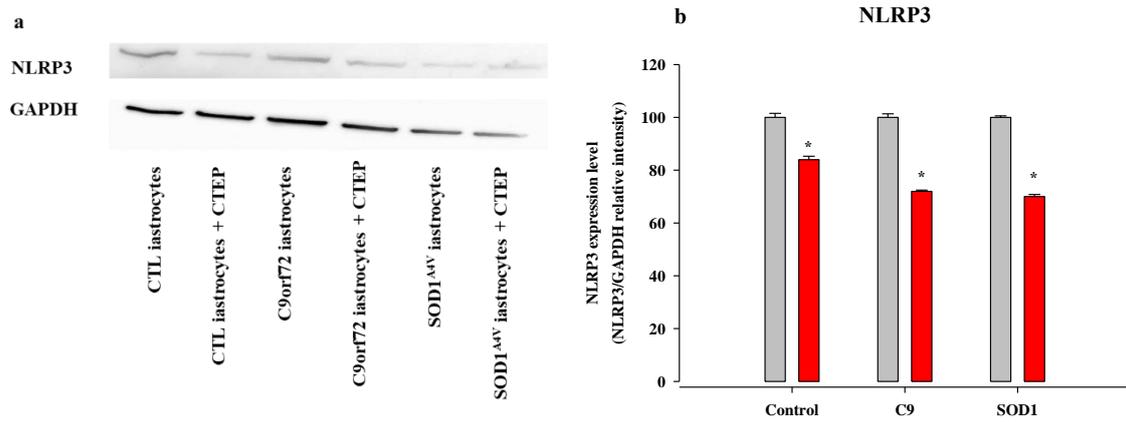
Figure 17: *Western blot quantification of NLRP3 expression in cell lysates from i-astrocytes obtained from control, C9orf72, SOD1^{A4V} and CTEP treatment*. **(a)** Representative immunoreactive bands for NLRP3 and GAPDH; **(b)** Quantification of protein expression as per scanned band density in control, C9orf72, and SOD1^{A4V} vehicle (Gray) or CTEP-treated (Red) i-astrocytes. Protein expression level was calculated as relative density, normalized to the housekeeping protein GAPDH. Data presented are means ± SD of three independent experiments. *P<0.001 vs. Non treated astrocytes (t-test).
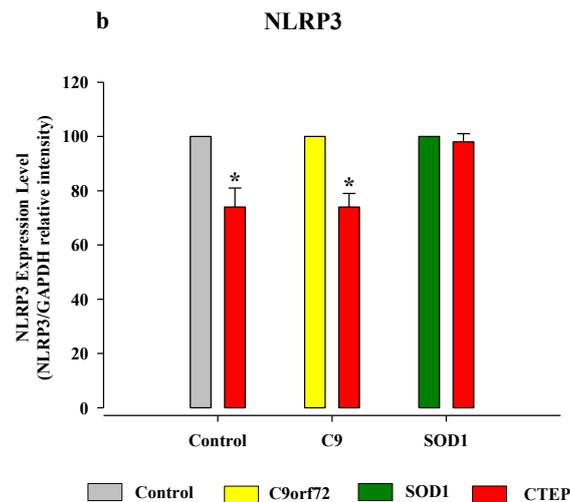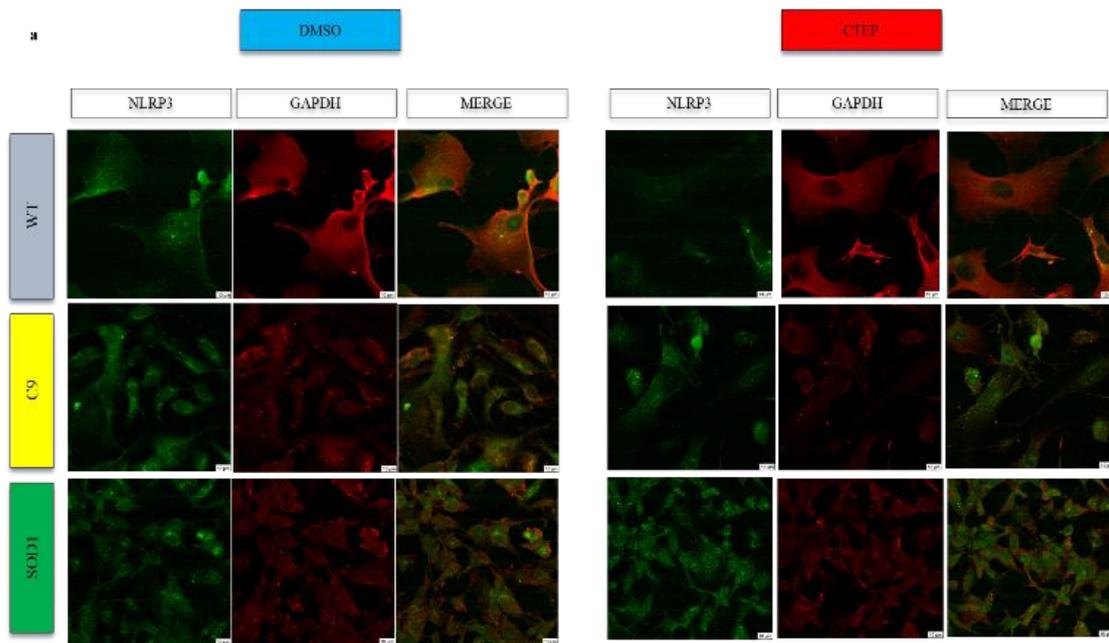
Figure 18: *Immunocytochemical quantification of NLRP3 expression in i-astrocytes obtained from control, C9orf72, SOD1^{A4V} and CTEP treatment.* **(a)** The panel represents the confocal microscopy immunocytochemical images of NLRP3 (green) and GAPDH (red) in control, C9orf72 and SOD1^{A4V} vehicle- (left) or CTEP- (right) treated i-astrocytes cultured on coverslip and labelled with the appropriate primary and secondary antibodies. The merge panels represent the co-expression of NLRP3 and GAPDH. Scale bar: 10 μm. **(b)** Quantification of protein expression, as per relative fluorescence intensity, was performed calculating the co-localization coefficients (Manders *et al.,* 1992) using Image-J software analyses. Data are expressed as relative fluorescence intensity of NLRP3 normalized respect to the fluorescence intensity of the housekeeping protein GAPDH. The relative intensity of non-treated i-astrocytes is reported as 100. Data presented are means ± SD of three independent experiments run in triplicate (three different coverslips for each experimental condition); statistical analysis was performed by t-test *$P < 0.001$ vs. non treated i-astrocytes

4.7.5 CTEP treatment reduce the NRF2 expression in control, C9orf72 and SOD1^{A4V} i-astrocytes

Nrf2 represents a transcriptional factor promoting the transcription of ARE and the synthesis of antioxidant proteins. Therefore, an increased nuclear localization is potentially linked with stronger activation of pathways protecting the cell from oxidative stress (Petri *et al.,* 2012).

The resistance to oxidative stress was measured by quantifying the total cellular expression of Nrf2 in control, C9orf72, and SOD1^{A4V} and CTEP treated i-astrocytes (Figure 19). Figure 19a represents the quantification of NRF2 expression after the CTEP treatment on i-astrocytes obtained from control, C9orf72, and SOD1^{A4V} patients. Figure 19b represents the immunoreactive NRF2 bands in treated and non-treated i-astrocytes. Figure 19 show that CTEP treatment significantly improved the total cellular expression of Nrf2 in C9orf72 and SOD1^{A4V} ($P < 0.001$) i-astrocytes, compared to non-treated i-astrocytes (Figure 19).
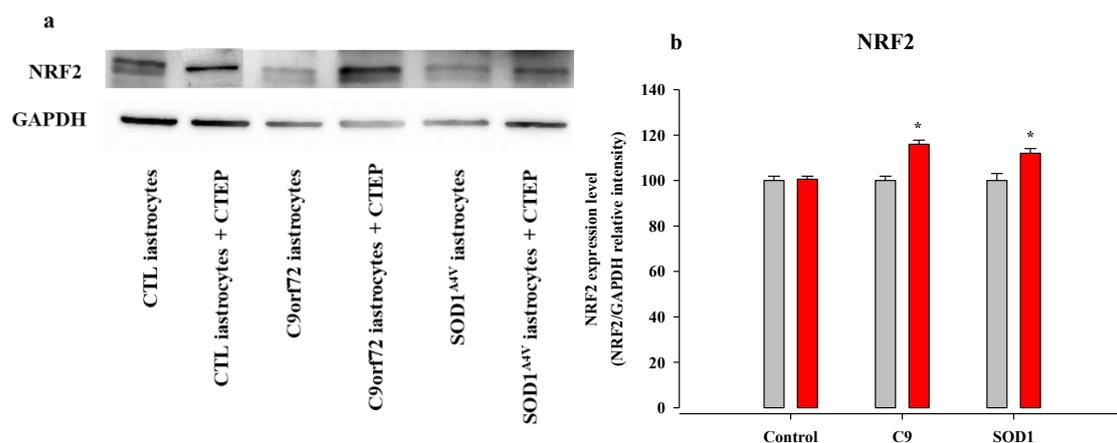

Figure 19: *Western blot quantification of NRF2 expression in cell lysates from i-astrocytes obtained from control, C9orf72, SOD1^{A4V} and CTEP treatment*. (a) Quantification of protein expression as per scanned band density in control, C9orf72, SOD1^{A4V} vehicle (Gray)- or CTEP-treated (Red) i-astrocytes; (b) Representative immunoreactive bands for NRF2 and GAPDH. Protein expression level was calculated as relative density, normalized to the housekeeping protein GAPDH. Data presented are means ± SD of three independent experiments. *P<0.001 vs. Non treated astrocytes (t-test).

### 4.7.6. *Effect of CTEP on the expression level of mGluR5 in control, C9orf72, and SOD1^{A4V} i-astrocytes*

Group-I mGluRs, comprising mGluR1 and mGluR5, are excitatory because of positive coupling to phosphatidylinositol breakdown (Conn and Pin, 1997, De Blasi *et al.,* 2001, Ferraguti *et al.,* 2008). Thus, hyperactivation of glutamate receptors may lead to an excessive increase of intracellular calcium due to either its entry through ionotropic Glu receptors and/or to its release from intracellular stores mediated by Group I mGluRs and contributing to excitotoxicity and cell death. Evidence implicating glutamate -mediated excitotoxicity in ALS is mainly based on the presence of elevated levels of extracellular glutamate in a high percentage of sporadic and familial ALS patients (Perry *et al.,* 1990).

Here, we investigated the effect of CTEP on mGluR5 expression in i-astrocytes obtained from control, C9orf72, and SOD1^{A4V} patients by WB (figure 20) and IF (figure 21) analysis. Figure 20a represents the immunoreactive bands for mGluR5 in treated and non-treated i-astrocytes. Figure 20b represents the quantification of mGluR5 expression after the CTEP treatment on i-astrocytes obtained from control, C9orf72, and SOD1^{A4V} patients. Figure 20 shows that CTEP treatment significantly lowers the expression of mGluR5 in control, C9orf72, and SOD1^{A4V} i-astrocytes as compared to non-treated i-astrocytes ($P<0.001$). The higher reduction in C9 and SOD1^{A4V} i-astrocytes should indicate that the contribution of mGluR5 to excitatory transmission is reduced by CTEP more in in ALS that in control.

The same mGluR5 expression trend was confirmed by IF analysis (figure 21). Figure 21a shows representative immunocytochemical images of mGluR5 (green) and GAPDH (red) expression and co-localization (yellow) in control, C9orf72, and SOD1^{A4V} i-astrocytes. Figure 21b represent the quantification of immunocytochemical images that shows significant reduction in the expression level of mGluR5 in CTEP treated control, C9orf72, and SOD1^{A4V} i-astrocytes as compared to non-treated i-astrocytes (Figure 21).
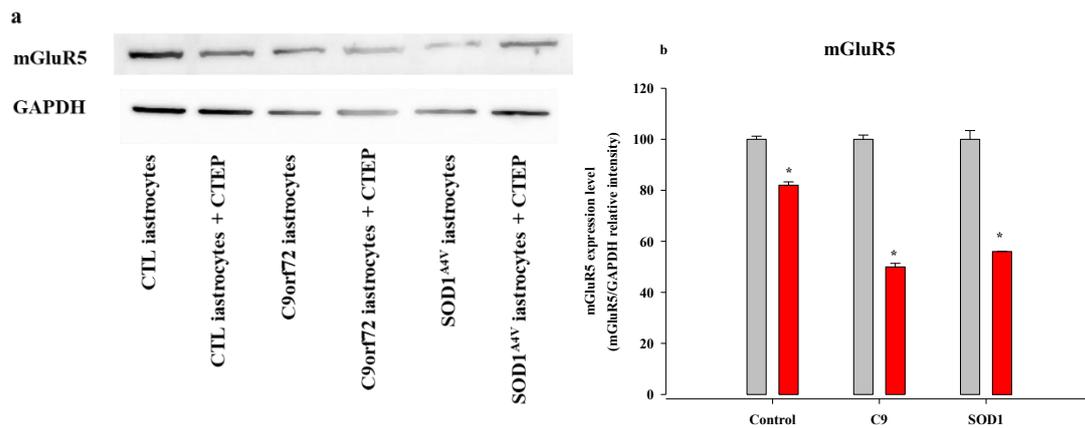
Figure 20: *Western blot quantification of mGluR5 expression in cell lysates from i-astrocytes obtained from control, C9orf72, SOD1^{A4V} and CTEP treatment*. **(a)** Representative immunoreactive bands for mGluR5 and GAPDH; **(b)** Quantification of protein expression as per scanned band density in control, C9orf72, SOD1 vehicle (Gray) or CTEP-treated (Red) i-astrocytes. Protein expression level was calculated as relative density, normalized to the housekeeping protein GAPDH. Data presented are means ± SD of three independent experiments. *P<0.001 vs. non-treated i-astrocytes (t-test).
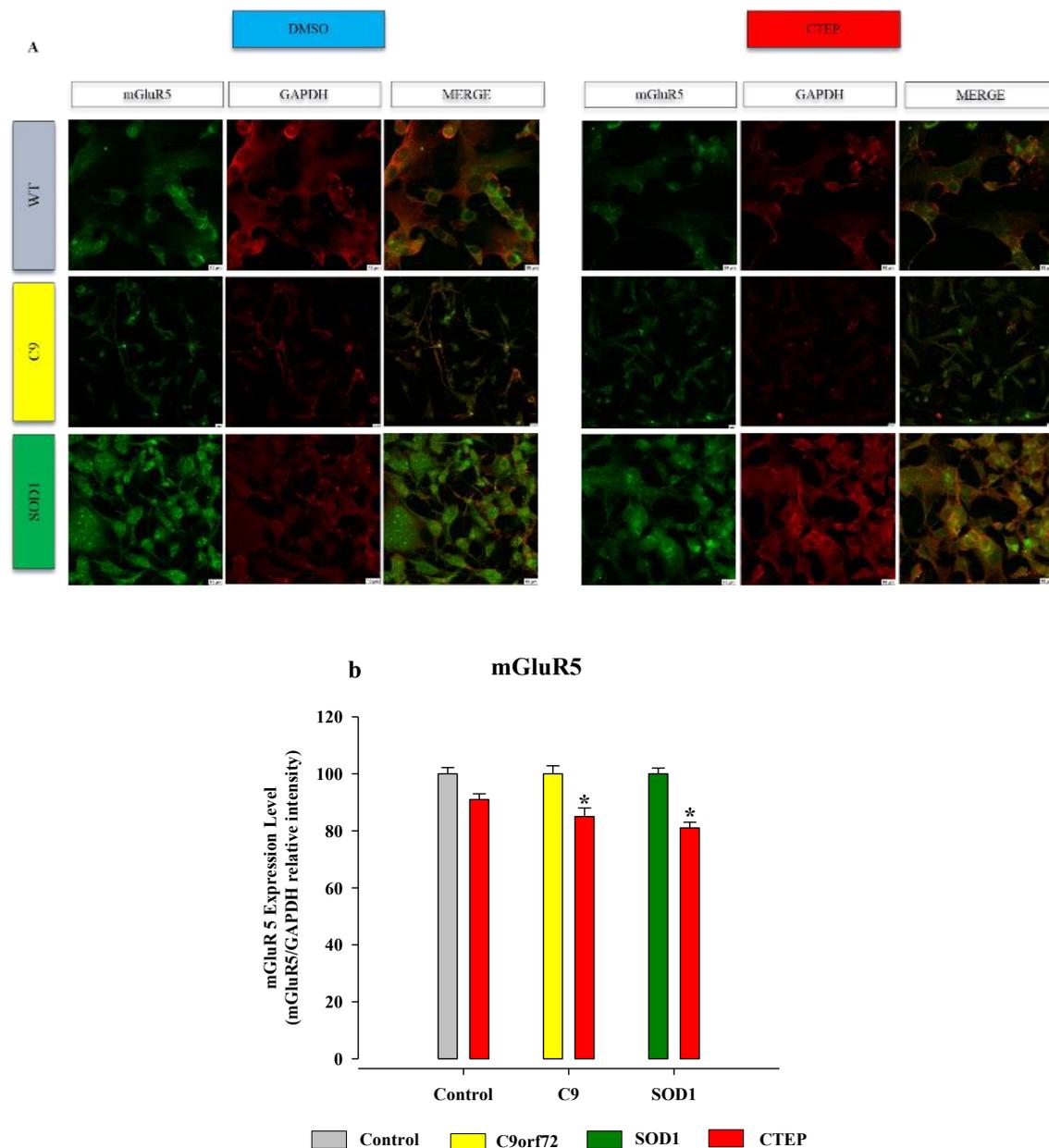
Figure 21: *Immunocytochemical quantification of mGluR5 expression in i-astrocytes obtained from control, C9orf72, SOD1^{A4V} and CTEP treatment*. **(a)** The panel represents the confocal microscopy immunocytochemical images of mGluR5 (green) and GAPDH (red) in control, C9orf72 and SOD1^{A4V} vehicle- (left) or CTEP- (right) treated i-astrocytes cultured on coverslip and labelled with the appropriate primary and secondary antibodies. The merge panels represent the co-expression of mGluR5 and GAPDH. Scale bar: 10 μm. **(b)** Quantification of protein expression, as per relative fluorescence intensity, was performed calculating the co-localization coefficients (Manders *et al.,* 1992) using Image-J software analyses. Data are expressed as relative fluorescence intensity of mGluR5 normalized respect to the fluorescence intensity of the housekeeping protein GAPDH. The relative intensity of non-treated i-astrocytes is reported as 100. Data presented are means $\pm$ SD of three independent experiments run in triplicate (three different coverslips for each experimental condition); statistical analysis was performed by t-test *P<0.001 vs. non treated i-astrocytes

4.8 Effects of CTEP treatment on Lipid Peroxidation and Redox Status in control, C9orf72 and SOD1^{A4V} i-astrocytes

Although the pathogenic mechanisms of the selective loss of MNs in ALS are unknown, there is increasing evidence that oxidative stress-related mitochondrial involvement is a determinant of MN degeneration. Oxidative stress, that includes lipid peroxidation, has been reported in patients with either fALS or sALS. Malondialdehyde (MDA), the oxidative stress biomarker in sALS patients, have been found in urine, cerebrospinal fluid (blood, and tissues) (Siciliano *et al.,* 2002).

We investigated the effect of CTEP on MDA levels in i-astrocytes obtained from control, C9orf72, SOD1^{A4V} patients. Figure 22 shows that i-astrocytes carrying the SOD1^{A4V} or C9orf72 mutation express a higher level of MDA, a marker of lipid peroxidation, compared to control controls. However, a significant reduction of MDA accumulation was observed in patients after CTEP treatment ($p < 0.0001$).

Since oxidative stress is always associated with the cellular antioxidant capacity, the activity of some enzymes involved in the antioxidant response, i.e., G6PD, GR, GP, and catalase, have been assayed. Data show that all enzyme activity was enhanced in i-astrocytes carrying the SOD1^{A4V} and C9orf72 mutation compared to control samples. The treatment with CTEP completely abated the enhancement of the enzyme activity in SOD1^{A4V} and C9orf72 patients ($p < 0.0001$). Interestingly, CTEP treatment seems not to affect the control sample (Figure 22).
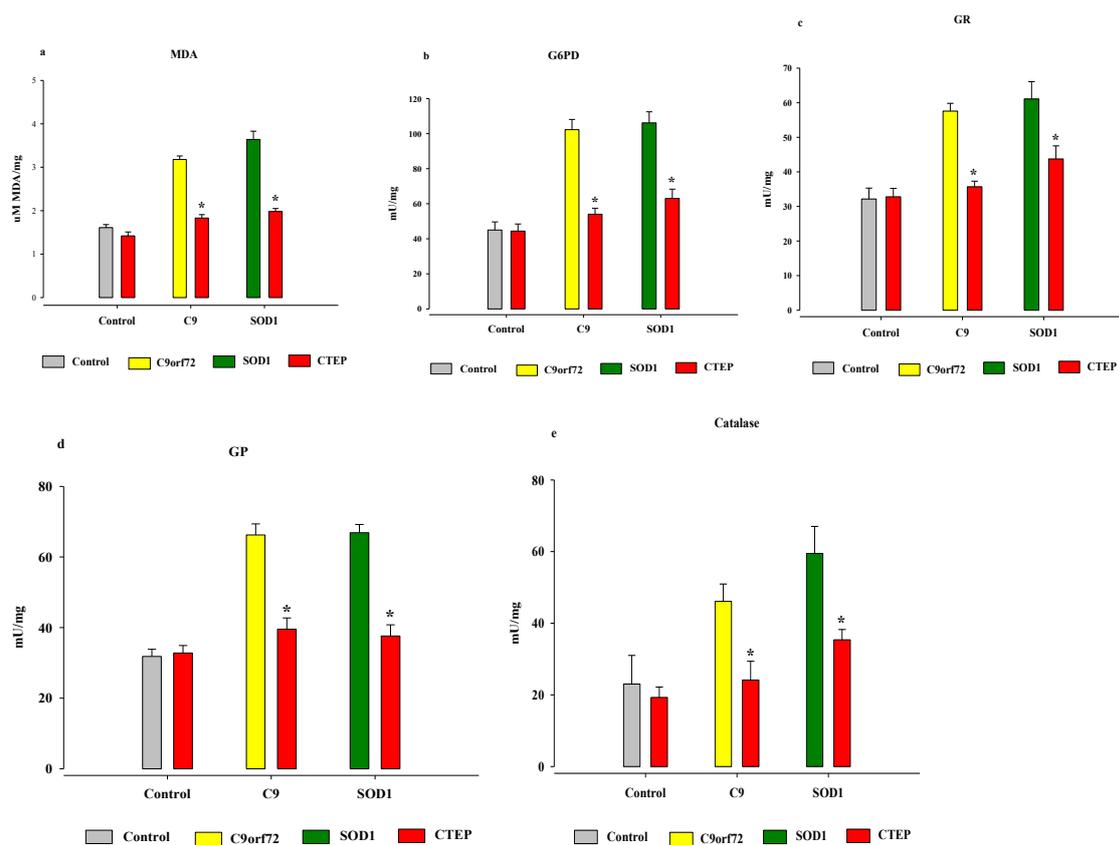
Figure 22: *Oxidative stress production and antioxidant defenses in i-astrocytes obtained from control, C9orf72, SOD1^{A4V} and CTEP treatment.* **(a)** intracellular level of malondialdehyde, marker of lipid peroxidation, and **(b-e)** G6PD, GR, GP, and catalase, markers of endogenous antioxidant enzymatic defenses, activities, in control, C9orf72 and SOD1^{A4V} vehicle- or CTEP-treated i-astrocytes. Data presented are means ± SD of three independent experiments. *P<0.0001 vs. non treated i-astrocytes (t-test).

5. DISCUSSION

5.1 Studies in Mouse Astrocytes

The main finding of our project is the divergent effect of SOD1[G93A] mutation on the redox balance of MC and SC astrocytes cultured for 10 days under standard conditions. This difference was paralleled by the metabolic response since the boost in G6PD activity of MC mutated astrocytes faced the enhancement of H6PD catalytic function in corresponding SC ones. The ER-PPP activation empowered SOD1[G93A] SC astrocytes with the capability to ameliorate the impairment of ER-mitochondria connection that was instead well evident in mutated MC cultures, despite a similar degree of ER enlargement.

In agreement with previous observations in different cells and tissues (Marini *et al.,* 2016; Cossu *et al.,* 2020; Bauckneht *et al.,* 2020), the increase in H6PD catalytic function was indexed by an enhanced FDG uptake. Altogether, these observations indicate that the divergent tracer retention, observed in SC and MC of symptomatic ALS patients, at least partially reflects a selective response of ER metabolism to the redox stress associated with SOD1[G93A] mutation. The link between ER-PPP activation and tolerance to irreversible oxidative stress in the environments surrounding the upper and lower motor neurons configures the reticular redox balance as a possible target to better understand the mechanisms underlying ALS progression.

A study conducted by Sokoloff *et al* in 1977 demonstrated that FDG uptake is an index of overall glucose consumption because after entering the cytosol through GLUT-facilitated transmembrane transport, this is phosphorylated to FDG6P that cannot be recognized by downstream enzymes channelling glucose to glycolysis or cytosolic PPP (Bachelard., 1971) and thus accumulates as a function of overall glucose phosphorylation (G6P). Nevertheless, a measurable FDG loss has been observed in virtually all studied tissues, indicating the hydrolyzation of FDG6P by G6P phosphatase (Sokoloff *et al.,* 1997). The detention of this enzyme within the ER has two important implications. On one side, it implies a carrier able to transfer the polar FDG6P across the reticular membrane (Caracó *et al.,* 2000). On the other side, it implies the presence of an enzymatic function able to prevent the hydrolytic reaction catalysed by G6P-phosphatase. As confirmed by a series of studies (Bánhegyi *et al.,* 2004; Marini *et al.,* 2016; Cossu *et al.,* 2020), H6PD fits these characteristics due to its capability to process FDG6P and its reticular location.

The present data agree with the role of the H6PD reticular PPP in FDG uptake. Indeed, the selective increase in tracer retention of mutated SC astrocytes was associated with an enhancement in H6PD activity and with an invariance of both directly measured glycolytic flux and cytosolic PPP. By contrast, the enhancement of G6PD only occurred in mutated MC cultures and was not associated with any change in FDG uptake, in agreement with the notion that this phosphorylated hexose is not recognized and thus processed by this enzyme (Bachelard., 1971).

The data obtained in this project are in line with previous studies that demonstrated the relationship between SC and brain metabolism in symptomatic ALS patients (Marini *et al.,* 2018). They also confirm that the different FDG uptake of MC and SC reflects a different ER involvement empowering the reaction to the redox stress, thus extending to astrocytes the previous observation in skeletal muscles of SOD1^{G93A} mice. Indeed, the high susceptibility of MC astrocytes to oxidative damage might eventually accelerate their degeneration. Accordingly, the decreased tracer retention observed in the brain cortex of symptomatic ALS patients seems to rather reflect the consequence of cortical atrophy featuring the symptomatic disease phase (Marini *et al.,* 2018). This consideration characterizes FDG retention as a combined index of the metabolic activation of ER in each investigated volume of central nervous tissue, multiplied for the number of cells entailed in it.

In the present study, H6PD activity was considered an important factor in PPP flux within the reticular lumen. This concept was justified by the notion that isolated ER membranes contain the enzymatic asset to manage the full sequence of PPP reactions (Bublitz *et al.,* 1988). This activity is distributed in all mammalian tissues (Sambuceti *et al.,* 2021), although relatively less represented in brain astrocytes (Cossu *et al.,* 2019). In agreement with these previous observations, the H6PD catalytic function remained under the detectability threshold of our method in all cultures except the mutated SC ones. On the other hand, its response confirms the notion that ER is empowered with specific pathways able to overcome the membrane impermeability and the consequent inaccessibility of NADPH reductive power, allowing the regulation of luminal redox balance. The relevance of this empowerment is confirmed by the protective role of ER activation in the SC district against the irreversible consequences of the redox damage induced by SOD1^{G93A} mutation.

Homogenate of MC astrocytes displayed a decreased function of complex-I coupled with lower levels of cytochrome C. However, these abnormalities were only associated with moderate OXPHOS impairment in intact cells. Finally, MitoSOX and MitoTracker staining indicated a scarce contribution of mitochondrial ROS generation. On the other side, SC astrocytes displayed higher ROS levels with respect to MC ones also in WT mice, thus reproducing the finding of a higher O_2- generation in SC naïve motor neurons compared with MC ones (Sullivan *et al.,* 2004). This difference was paralleled by a higher intermembrane distance of ER-mitochondria contacts points in WT cultures that, however, partially prevented the detaching induced by SOD1^{G93A} mutation. Altogether, these data thus suggest the presence of different mechanisms underlying the antioxidant response in SC and MC astrocytes. In other words, the highly oxidative environment in normal SC seems to tailor the metabolic phenotype to prevent the irreversible consequences of the oxidative damage induced by SOD1^{G93A} mutation. Although not fully defined by the present data, the mechanisms underlying this selective endurance should entail the ER-mitochondria connections and the configuration of mitochondria-associated membrane proteins (MAMs), whose role in cellular redox control has been already documented in different cell models (van *et al.,* 2014). In agreement with this hypothesis, the MAM constituent Mfn2 showed an increase in SC astrocytes as opposed to a decrease in MC ones, corroborating the hypothesis of a differential ER involvement in the cellular redox control of these two districts.

5.2 Studies in Human Astrocytes

The present study highlights the role of mGluR5 in reactive phenotype of i-astrocytes derived from iNPCs of controls, C9orf72, and SOD1^{A4V} ALS patients. I demonstrated that the in-vitro treatment with CTEP ameliorated the phenotype of C9orf72 and SOD1 i-astrocytes by reducing; i) the upregulation of mGluR5 expression; ii) the activation state, as demonstrated by the reduced expression of GFAP and S100β; iii) the inflammation state, underlined by the reduced expression of the NRF2 inflammasome complex; iv) the uncoupling between oxygen consumption and ATP synthesis and the impairment of mitochondria function; v) the overexpression of complement C3 protein.

Several lines of evidence demonstrated that mGluR5 is mainly detected at synaptic terminals (Yin and Niswender, 2014), at astrocytes (D'Antoni *et al.,* 2008), microglia (Liu *et al.,* 2009), and at oligodendrocyte progenitor cells (Luyt *et al.,* 2006). These receptors are known

to be involved in the regulation of several cellular processes altered in ALS (Nicoletti *et al.,* 2011; Aronica *et al.,* 2001; Martorana *et al.,* 2012; Anneser *et al.,* 2004a; Anneser *et al.,* 2004b; Rossi *et al.,* 2008; Vergouts *et al.,* 2018). In physiological conditions, astrocytes have a low level of mGluR5 but in ALS patients they show higher expression of these receptors in reactive glial cells (Aronica *et al.,* 2001). Overexpression was also detected in the striatum, hippocampus, frontal cortex, and spinal cord of ALS mice, starting from the pre-symptomatic stages and during the progression of the disease (Martorana *et al.,* 2012; Brownell *et al.,* 2015; Bonifacino *et al.,* 2019b). In astrocyte cultures, the mGluR5 contributes to modulating the glial response to changes in local excitatory tone (D'Antoni *et al.,* 2008; Verkhratsky and Kirchhoff, 2007).

mGluR5 has been suggested to be involved in neuronal growth, regulation of synaptic activity, neuroprotection, and excitotoxicity (Viwatpinyo and Chongthammakun, 2009). Indeed, its activation leads to several effects such as astrocyte proliferation, the release of BDNF (Jean *et al.,* 2008) and glio-transmitters, such as ATP and glutamate (Bezzi and Volterra, 2014; Panatier *et al.,* 2011), increased glutamate uptake (Aronica *et al.,* 2003; Vermeiren *et al.,* 2005) and modulation of inflammatory responses (Shah *et al.,* 2012). This receptor is also reported to be involved in various molecular mechanisms causing astroglial damage (Rossi *et al.,* 2008).

Apart from ALS, similar findings have been reported also in other models of neurological diseases, such as HD (Ribeiro *et al.,* 2014), AD (Hamilton *et al.,* 2016), epilepsy (Ure *et al.,* 2006), and fragile X syndrome (Dolen and Bear, 2008) or in cultured astrocytes exposed to metabolic stress (Paquet *et al.,* 2013). However, notwithstanding the involvement of mGluR5 in ALS and in other neurological disorders, neither the role of astrocyte mGluR5 nor the alteration of signalling pathways have been ever deeply investigated.

In our previous studies carried out in-vivo, both the knocking down (Bonifacino *et al.,* 2017) and the complete knock out (Bonifacino *et al.,* 2019a) of mGluR5 resulted in amelioration of the pathological phenotype of SOD1^{G93A} mice and led to reduced astrogliosis. Similar results were recently obtained after the in-vivo treatment of SOD1^{G93A} mice with CTEP, a mGluR5 allosteric modulators (NAM) (Milanese *et al.,* 2021). In this project, we tried to evaluate the effects of in-vitro CTEP treatment on human astrocytes derived from iNPCs of ALS patients. To this purpose, i-astrocytes were differentiated from iNPCs isolated from

skin fibroblast cells of SOD1^{A4V}, C9orf72 ALS patients and healthy donors were utilized. This is an important aspect of my experiments. Indeed, despite the difficulties of culturing and expanding i-astrocytes from iNPCs, we believe that iNPCs derived i-astrocytes better recapitulate the cellular and molecular modifications of the human disease and complete the data we obtained studying the effect of mGluR5 manipulation in SOD1^{G93A} mouse astrocyte in our laboratory (Torazza *et al.,* manuscript in preparation). The results largely confirmed in human samples, the rodent results that reducing the activity of mGluR5 ameliorates the disease progression in-vivo and the astrocyte phenotype in vitro.

The i-astrocytes obtained from both non-treated SOD1^{A4V}, C9or72 ALS patients and healthy donor showed higher levels of mGluR5 expression as compared to treated i-astrocytes. Thus, CTEP treatment significantly reduced the expression of the receptor protein. Using Western blot, I investigated the total cell expression of the receptor in the cell homogenate but further analyses should be carried out to determine the specific membrane expression of mGluR5, which represents the pharmacologically targetable form of the receptor. In any case, the modulation of the cell status by reducing mGluR5 expression, demonstrated by the experiments discussed below, strongly supports that modulation of mGluR5 total expression likely face the membrane expression of the receptor.

Downregulating mGluR5 also positively affected the reactive state of i-astrocytes. In physiological conditions, astrocyte activation represents the ability of astrocytes to provide a neuroprotective and regenerative defence toward MNs, related to their so-called A2 status. However, in neurodegenerative diseases, such as ALS, this mechanism is exacerbated and astrocytes gain A1-related toxic functions (Verkhratsky and Zorec, 2018).

Astrogliosis is often characterized by overexpression of GFAP and S100β (Benninger *et al.,* 2016). GFAP is a structural component of i-astrocytes cytoskeleton and constitutes the type III intermediate filaments of these cells (Tardy *et al.,* 1990). Its expression is modulated by several factors including cell maturation and environmental challenges (Li *et al.,* 2019). In physiological conditions, GFAP plays an important role in cell communication, BBB formation, and astrocytic plasticity (Kamphuis *et al.,* 2014). However, an abnormal expression and regulation of the protein cause astrocytes activation, characterized by cell proliferation and hypertrophy of the cell body and processes (Li *et al.,* 2019). The upregulation and rearrangements of GFAP can also concur in many neurological diseases,

among which inflammation, ischemic stroke, traumatic brain injury, and neurodegeneration (Hol and Pekny, 2015; Olabarria M and Goldman JE, 2017). S100β is a calcium-binding protein selectively expressed by glial cells. It is involved in several homeostatic functions, such as microtubule assembly, axonal proliferation, astrogliosis, calcium concentration, inflammation, and is often dysregulated in ALS. Accordingly, S100β expression is increased in the CSF of patients affected by the disease, and its levels are directly correlated with the prognosis of the disease and in the cerebral cortex and spinal cord astrocytes and motor neurons of post-mortem ALS patient tissue (Serrano *et al.,* 2017). In line with the literature (Migheli *et al.,* 1999; Benninger *et al.,* 2016), the current experiments demonstrated that i-astrocytes obtained from both non-treated SOD1[A4V,] and C9orf72 ALS patients and healthy donor display an elevated expression of GFAP and S100β related CTEP-treated i-astrocytes. Thus, SOD1[A4V] and C9orf72 CTEP-treated i-astrocytes show a significantly reduced level of GFAP and S100β compared to untreated i-astrocytes.

Several findings have suggested an essential role of the complement system in the pathophysiology of ALS (Kjældgaard *et al.,* 2018). Dysfunctional complement activation also seems to be present during the progression of ALS (Heurich *et al.,* 2011; Woodruff *et al.,* 2014). In the present study, we measured the expression of the component C3 of the complement pathway: non-treated SOD1[A4V] and C9orf72 patients and healthy donors showed higher levels of complement C3 protein as compared with non-treated i-astrocytes. Thus, CTEP significantly decreased the expression of C3 protein in SOD1[A4V] and C9orf72 i-astrocytes.

Another protein strictly related to inflammation is NLRP3. Its activation leads to the cleavage of pro-IL-1β and pro-IL-18 to the respective active forms and, consequently, to their secretion by the cell (Mangan *et al.,* 2018). NLRP3 has been reported to be increased in ALS (Johann *et al.,* 2015; Gugliandolo *et al.,* 2018). In accordance, we detected a dramatic decrease of NLRP3 in CTEP-treated i-astrocytes obtained from both SOD1[A4V], C9orf72 and healthy donors compared to non-treated i-astrocytes.

Another well-recognized parameter in ALS patients is the impairment of the energetic metabolism (Tefera and Borges, 2016). The present study confirmed that iNPCs derived i-astrocytes from SOD1[A4V] and C9orf72 patients are characterized by an increment of oxidative stress, as confirmed by the increased MDA expression in i-astrocytes carrying the

SOD1^{A4V} and C9orf72, despite the increment of the enzymatic activities associated with the cellular antioxidant defences. In other words, data reported in Figure 19 suggest that mutated i-astrocytes can induce an adaptive response against the high level of oxidative stress, activating antioxidant pathways, which, however, is not sufficient to counterbalance oxidative stress production. Noteworthy, CTEP treatment caused a decrement of MDA expression compared to the untreated samples, suggesting that the drug reduced the oxidative stress. This hypothesis is confirmed by the decrement of the activity of the antioxidant enzymes G6PD, GR, GP, and catalase activity.

Altogether, these data highlight a significant improvement with respect to previous studies in the SOD1^{G93A} mouse model. First, they demonstrate that pharmacologically counteracting mGluR5 betters the astrocyte phenotype in ALS patients; second, they suggest that ASL mutations other than SOD1^{G93A} could benefit from the treatment. These considerations will pave the way for a translational application of blocking mGluR5 in patients. Noteworthy, other mGlu5 receptor negative allosteric modulators were studied in human clinical trials to treat fragile X syndrome, depression, levodopa induced, and Huntington's disease (Reilmann *et al.,* 2015; Trenkwalder *et al.,* 2016). Among them, basimglurant, an analogue of CTEP, showed favourable pharmacokinetics and toxicology in human studies (Jaeschke *et al.,* 2015; Lindemann *et al.,* 2015) and was successfully tested for the cure of depression and fragile X syndrome (Quiroz *et al.,* 2016; Youssef *et al.,* 2018).

6. CONCLUSIONS

The results obtained from the animal's study indicate that the activation of cytosolic PPP does not counterbalance the irreversible oxidative damage associated with the SOD1^{G93A} mutation. By contrast, the activation of the ER-PPP provides relative protection despite the marked alteration of this organelle that characterizes the studies in experimental models and specimens from ALS patients. The signals that activate this pathway in SC astrocytes remain to be elucidated. However, their comprehension might configure new pathways to understand ALS progression mechanisms. Data obtained in human studies focussed on investigating the effects of the mGlur5 NAM CTEP in iNPCs derived i-astrocytes, thus recalling the previously obtained data in-vivo SOD1^{G93A}Grm5-/+ and CTEP-treated mice, emphasizing the role of mGluR5 in ALS progression. The downregulation of mGluR5 in iNPCs-derived i-astrocytes determined an amelioration of the reactive state, particularly of the inflammatory phenotype of these cells, and modulated several downstream pathways typically affected in ALS astrocytes. However, these findings demonstrated that mGluR5 can be a target to modulate the astrocyte reactive phenotype suggesting that mGluR5 blockade can reasonably turn out to be effective in counteracting ALS.
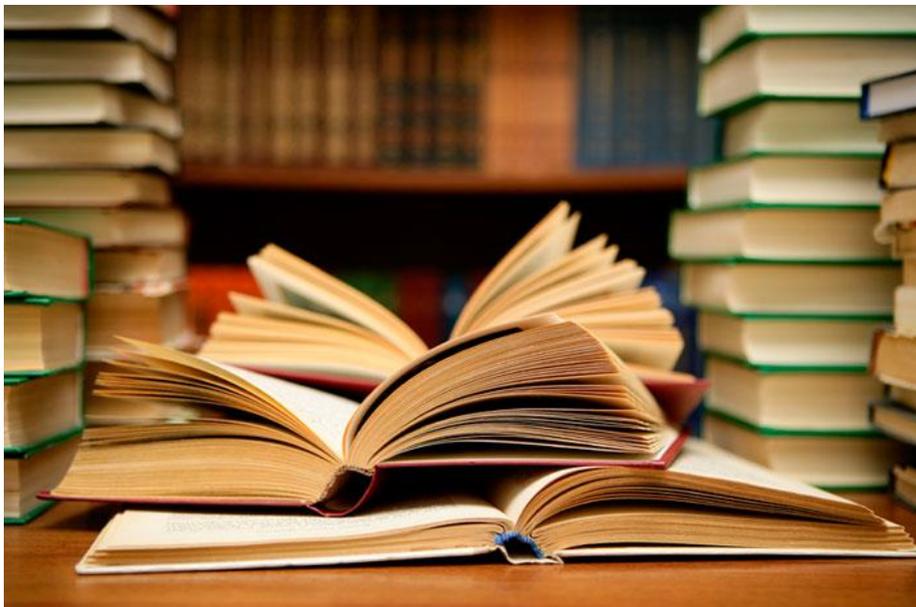
7. BIBLIOGRAPHY

Abd-Elrahman KS, Hamilton A, Hutchinson SR, Liu F, Russell RC, Ferguson SS. mGluR5 antagonism increases autophagy and prevents disease progression in the zQ175 mouse model of Huntington's disease. Science signaling. 2017 Dec 19;10(510):eaan6387.

Ahn JY, Ye K. PIKE GTPase signaling and function. International journal of biological sciences. 2005;1(2):44.

Aizawa H, Sawada J, Hideyama T, Yamashita T, Katayama T, Hasebe N, Kimura T, Yahara O, Kwak S. TDP-43 pathology in sporadic ALS occurs in motor neurons lacking the RNA editing enzyme ADAR2. Acta neuropathologica. 2010 Jul;120(1):75-84.

Al-Chalabi A, Andersen PM, Nilsson P, Chioza B, Andersson JL, Russ C, Shaw CE, Powell JF, Leigh PN: Deletions of the heavy neurofilament subunit tail in amyotrophic lateral sclerosis. Hum. Molec. Genet 1999, 8:157–164.

Al-Chalabi A, Fang F, Hanby MF, *et al*. An estimate of amyotrophic lateral sclerosis heritability using twin data. J Neurol Neurosurg Psychiatry 2010; 81: 1324–1326.

Al-Chalabi A, Hardiman O, Kiernan MC, Chio A, Rix- Brooks B, van den Berg LH. Amyotrophic lateral sclerosis: moving towards a new classification system. Lancet Neurol 2016; 15: 1182–1194.

Al-Chalabi A, Leigh PN. Recent advances in amyotrophic lateral sclerosis. Current opinion in neurology. 2000 Aug 1;13(4):397-405.

Alexianu ME, Kozovska M, Appel SH. Immune reactivity in a mouse model of familial ALS correlates with disease progression. Neurology. 2001 Oct 9;57(7):1282-9.

Allen SP, Hall B, Castelli LM, Francis L, Woof R, Siskos AP, Kouloura E, Gray E, Thompson AG, Talbot K, Higginbottom A. Astrocyte adenosine deaminase loss increases motor neuron toxicity in amyotrophic lateral sclerosis. Brain. 2019 Mar 1;142(3):586-605.

Almad AA, Doreswamy A, Gross SK, Richard JP, Huo Y, Haughey N, Maragakis NJ. Connexin 43 in astrocytes contributes to motor neuron toxicity in amyotrophic lateral sclerosis. Glia. 2016 Jul;64(7):1154-69.

Al-Saif A, Al-Mohanna F, Bohlega S: A mutation in sigma-1 receptor causes juvenile amyotrophic lateral sclerosis. Ann Neurol 2011, 70:913–919.

Andersen PM, Forsgren L, Binzer M, Nilsson P, Ala-Hurula V, Keränen ML, Bergmark L, Saarinen A, Haltia T, Tarvainen I, Kinnunen E. Autosomal recessive adult-onset

amyotrophic lateral sclerosis associated with homozygosity for Asp90Ala CuZn-superoxide dismutase mutation: a clinical and genealogical study of 36 patients. Brain. 1996 Aug 1;119(4):1153-72.

Andersen PM. Amyotrophic lateral sclerosis associated with mutations in the CuZn superoxide dismutase gene. Current neurology and neuroscience reports. 2006 Feb;6(1):37-46.

Anneser JM, Chahli C, Ince PG, Borasio GD, Shaw PJ. Glial proliferation and metabotropic glutamate receptor expression in amyotrophic lateral sclerosis. Journal of Neuropathology & Experimental Neurology. 2004b Aug 1;63(8):831-40.

Anneser JM, Ince PG, Shaw PJ, Borasio GD. Differential expression of mGluR5 in human lumbosacral motoneurons. Neuroreport. 2004 Feb 9;15(2):271-3.

Arai T, Hasegawa M, Akiyama H, Ikeda K, Nonaka T, Mori H, Mann D, Tsuchiya K, Yoshida M, Hashizume Y, Oda T. TDP-43 is a component of ubiquitin-positive tau-negative inclusions in frontotemporal lobar degeneration and amyotrophic lateral sclerosis. Biochemical and biophysical research communications. 2006 Dec 22;351(3):602-11.

Armada-Moreira A, Gomes JI, Pina CC, Savchak OK, Gonçalves-Ribeiro J, Rei N, Pinto S, Morais TP, Martins RS, Ribeiro FF, Sebastião AM. Going the extra (synaptic) mile: excitotoxicity as the road toward neurodegenerative diseases. Frontiers in cellular neuroscience. 2020 Apr 24;14:90.

Aronica E, Catania MV, Geurts J, Yankaya B, Troost D. Immunohistochemical localization of group I and II metabotropic glutamate receptors in control and amyotrophic lateral sclerosis human spinal cord: upregulation in reactive astrocytes. Neuroscience. 2001 Jul 27;105(2):509-20.

Aronica E, Gorter JA, Ijlst-Keizers H, Rozemuller AJ, Yankaya B, Leenstra S, Troost D. Expression and functional role of mGluR3 and mGluR5 in human astrocytes and glioma cells: opposite regulation of glutamate transporter proteins. European Journal of Neuroscience. 2003 May;17(10):2106-18.

Ash PE, Bieniek KF, Gendron TF, Caulfield T, Lin WL, DeJesus-Hernandez M, Van Blitterswijk MM, Jansen-West K, Paul III JW, Rademakers R, Boylan KB.

Unconventional translation of C9ORF72 GGGGCC expansion generates insoluble polypeptides specific to c9FTD/ALS. Neuron. 2013 Feb 20;77(4):639-46.

Atsumi T. The ultrastructure of intramuscular nerves in amyotrophic lateral sclerosis. Acta neuropathologica. 1981 Sep;55(3):193-8.

Aubert A, Costalat R, Magistretti PJ, Pellerin L. Brain lactate kinetics: modeling evidence for neuronal lactate uptake upon activation. Proceedings of the National Academy of Sciences. 2005 Nov 8;102(45):16448-53.

Ayala YM, Zago P, D'Ambrogio A, Xu YF, Petrucelli L, Buratti E, Baralle FE. Structural determinants of the cellular localization and shuttling of TDP-43. Journal of cell science. 2008 Nov 15;121(22):3778-85.

Bachelard HS. Specificity and kinetic properties of monosaccharide uptake into guinea pig cerebral cortex in vitro. Journal of neurochemistry. 1971 Feb;18(2):213-22.

Back SA, Gan X, Li Y, Rosenberg PA, Volpe JJ. Maturation-dependent vulnerability of oligodendrocytes to oxidative stress-induced death caused by glutathione depletion. Journal of Neuroscience. 1998 Aug 15;18(16):6241-53.

Baker M, Mackenzie IR, Pickering-Brown SM, Gass J, Rademakers R, Lindholm C, Snowden J, Adamson J, Sadovnick AD, Rollinson S, Cannon A, Dwosh E, Neary D, Melquist S, Richardson A, Dickson D, Berger Z, Eriksen J, Robinson T, Zehr C, Dickey CA, Crook R, McGowan E, Mann D, Boeve B, Feldman H, Hutton M: Mutations in progranulin cause tau-negative frontotemporal dementia linked to chromosome 17. Nature 2006, 442:916–919.

Balázs R, Miller S, Chun Y, O'Toole J, Cotman CW. Metabotropic glutamate receptor agonists potentiate cyclic AMP formation induced by forskolin or β-adrenergic receptor activation in cerebral cortical astrocytes in culture. Journal of neurochemistry. 1998 Jun;70(6):2446-58.

Banerjee R, Mosley RL, Reynolds AD, Dhar A, Jackson-Lewis V, Gordon PH, Przedborski S, Gendelman HE. Adaptive immune neuroprotection in G93A-SOD1 amyotrophic lateral sclerosis mice. PloS one. 2008 Jul 23;3(7):e2740.

Bánhegyi G, Benedetti A, Fulceri R, Senesi S. Cooperativity between 11β-hydroxysteroid dehydrogenase type 1 and hexose-6-phosphate dehydrogenase in the lumen of the

endoplasmic reticulum. Journal of Biological Chemistry. 2004 Jun 25;279(26):27017-21.

Barker RF, Hopkinson DA: The genetic and biochemical properties of the D-amino acid oxidases in human tissues. Ann Hum Genet 1977, 41:27–42.

Barres BA. The mystery and magic of glia: a perspective on their roles in health and disease. Neuron. 2008 Nov 6;60(3):430-40.

Barton SK, Gregory JM, Chandran S, Turner BJ. Could an Impairment in Local Translation of mRNAs in Glia be Contributing to Pathogenesis in ALS?. Frontiers in molecular neuroscience. 2019 May 21;12:124.

Bauckneht M, Cossu V, Castellani P, Piccioli P, Orengo AM, Emionite L, Di Giulio F, Donegani MI, Miceli A, Raffa S, Borra A. FDG uptake tracks the oxidative damage in diabetic skeletal muscle: An experimental study. Molecular metabolism. 2020 Jan 1;31:98-108.

Bauckneht M, Pastorino F, Castellani P, Cossu V, Orengo AM, Piccioli P, Emionite L, Capitanio S, Yosifov N, Bruno S, Lazzarini E. Increased myocardial 18F-FDG uptake as a marker of Doxorubicin-induced oxidative stress. Journal of Nuclear Cardiology. 2020 Dec;27(6):2183-94.

Bäumer D, Hilton D, Paine SM, Turner MR, Lowe J, Talbot K, Ansorge O: Juvenile ALS with basophilic inclusions is a FUS proteinopathy with FUS mutations. Neurology 2010, 75:611 -618.

Beaulieu JM, Nguyen MD, Julien JP: Late onset of motor neurons in mice overexpressing wild-type peripherin. J Cell Biol 1999, 147:531–544.

Beers DR, Henkel JS, Zhao W, Wang J, Appel SH. CD4+ T cells support glial neuroprotection, slow disease progression, and modify glial morphology in an animal model of inherited ALS. Proceedings of the National Academy of Sciences. 2008 Oct 7;105(40):15558-63.

Beers DR, Zhao W, Liao B, Kano O, Wang J, Huang A, Appel SH, Henkel JS. Neuroinflammation modulates distinct regional and temporal clinical responses in ALS mice. Brain, behavior, and immunity. 2011 Jul 1;25(5):1025-35.

Bélanger M, Allaman I, Magistretti PJ. Brain energy metabolism: focus on astrocyte-neuron metabolic cooperation. Cell metabolism. 2011 Dec 7;14(6):724-38.

Belly A, Bodon G, Blot B, Bouron A, Sadoul R, Goldberg Y: CHMP2B mutants linked to frontotemporal dementia impair maturation of dendritic spines. J Cell Sci 2010, 123:2943–2954.

Ben-Ami M, Bassan M, Sorani K. Method for Treatment of Amyotrophic Lateral Sclerosis using Talampanel. 2009 US0258863

Bennett ML, Bennett FC, Liddelow SA, Ajami B, Zamanian JL, Fernhoff NB, Mulinyawe SB, Bohlen CJ, Adil A, Tucker A, Weissman IL. New tools for studying microglia in the mouse and human CNS. Proceedings of the National Academy of Sciences. 2016 Mar 22;113(12):E1738-46.

Benninger F, Glat MJ, Offen D, Steiner I, 2016. Glial fibrillary acidic protein as a marker of astrocytic activation in the cerebrospinal fluid of patients with amyotrophic lateral sclerosis. J Clin Neurosci. 26: 75-78. Astroglial signalling in health and disease. Neuroscience letters. 2019 Jan 10;689:1-4.

Benoit M, Desnues B, Mege JL. Macrophage polarization in bacterial infections. The Journal of Immunology. 2008 Sep 15;181(6):3733-9.

Bensimon G, Lacomblez L, Meininger V. A controlled trial of riluzole in amyotrophic lateral sclerosis. ALS/ Riluzole Study Group. N Engl J Med 1994; 330: 585– 591.

Bercier V, Hubbard JM, Fidelin K, *et al*. Dynactin1 depletion leads to neuromuscular synapse instability and functional abnormalities. Mol Neurodegener 2019; 14: 27.

Berry JD, Shefner JM, Conwit R, Schoenfeld D, Keroack M, Felsenstein D, Krivickas L, David WS, Vriesendorp F, Pestronk A, Caress JB, J. K, Simpson E, Rosenfeld J, Pascuzzi R, Glass J, Rezania K, Rothstein JD, Greenblatt DJ, Cudkowicz ME, Consortium. NA. Design and initial results of a multi-phase randomized trial of ceftriaxone in amyotrophic lateral sclerosis. PLoS One. 2013; 8(4).

Bezzi P, Volterra A. Imaging exocytosis and recycling of synaptic-like microvesicles in astrocytes. Cold Spring Harbor Protocols. 2014 May 1;2014(5):pdb-rot081711.

Bigio EH. C9ORF72, the new gene on the block, causes C9FTD/ALS: new insights provided by neuropathology.

Blokhuis AM, Koppers M, Groen EJ, van den Heuvel DM, Modigliani SD, Anink JJ, Fumoto K, van Diggelen F, Snelting A, Sodaar P, Verheijen BM. Comparative

interactomics analysis of different ALS-associated proteins identifies converging molecular pathways. Acta neuropathologica. 2016 Aug;132(2):175-96.

Boeynaems S, Bogaert E, Van Damme P, Van Den Bosch L. Inside out: the role of nucleocytoplasmic transport in ALS and FTLD. Acta Neuropathol 2016; 132: 159–173.

Boillée S, Yamanaka K, Lobsiger CS, Copeland NG, Jenkins NA, Kassiotis G, Kollias G, Cleveland DW. Onset and progression in inherited ALS determined by motor neurons and microglia. Science. 2006 Jun 2;312(5778):1389-92.

Bonifacino T, Cattaneo L, Gallia E, Puliti A, Melone M, Provenzano F, Bossi S, Musante I, Usai C, Conti F, Bonanno G. In-vivo effects of knocking-down metabotropic glutamate receptor 5 in the SOD1G93A mouse model of amyotrophic lateral sclerosis. Neuropharmacology. 2017 Sep 1;123:433-45.

Bonifacino T, Musazzi L, Milanese M, Seguini M, Marte A, Gallia E, Cattaneo L, Onofri F, Popoli M, Bonanno G. Altered mechanisms underlying the abnormal glutamate release in amyotrophic lateral sclerosis at a pre-symptomatic stage of the disease. Neurobiology of disease. 2016 Nov 1;95:122-33.

Bonifacino T, Provenzano F, Gallia E, Ravera S, Torazza C, Bossi S, Ferrando S, Puliti A, Van Den Bosch L, Bonanno G, Milanese M. In-vivo genetic ablation of metabotropic glutamate receptor type 5 slows down disease progression in the SOD1G93A mouse model of amyotrophic lateral sclerosis. Neurobiology of disease. 2019 Sep 1;129:79-92.

Bonifacino T, Rebosio C, Provenzano F, Torazza C, Balbi M, Milanese M, Raiteri L, Usai C, Fedele E, Bonanno G. Enhanced function and overexpression of metabotropic glutamate receptors 1 and 5 in the spinal cord of the SOD1G93A mouse model of amyotrophic lateral sclerosis during disease progression. International journal of molecular sciences. 2019 Jan;20(18):4552.

Bonifacino T, Rebosio C., Provenzano F., Torazza C., Balbi M., Milanese M., Raiteri L. Usai C., Fedele E., Bonanno G. Enhanced function and overexpression of metabotropic glutamate receptors 1 and 5 in the spinal cord of the SOD1G93A mouse model of amyotrophic lateral sclerosis during disease progression. Int. J. Mol. Sci. 20: 4552-4571, 2019.

Bonifacino T., Cattaneo L., Gallia E., Puliti A, Melone M, Provenzano F, Bossi S., Musante I., Usai C., Conti F., Bonanno G., Milanese M. In-vivo effects of knocking-down metabotropic glutamate receptor 5 in the SOD1G93A mouse model of amyotrophic lateral sclerosis. Neuropharmacology 123: 433-445, 2017.

Bosco DA, Lemay N, Ko HK, Zhou H, Burke C, Kwiatkowski TJ Jr, Sapp P, McKenna-Yasek D, Brown RH Jr, Hayward LJ: Mutant FUS proteins that cause amyotrophic lateral sclerosis incorporate into stress granules. Hum Mol Genet 2010, 19:4160–4175.

Boston-Howes W, Gibb SL, Williams EO, Pasinelli P, Brown Jr RH, Trotti D. Caspase-3 cleaves and inactivates the glutamate transporter EAAT2. Journal of Biological Chemistry. 2006 May 19;281(20):14076-84.

Bowling AC, Beal MF. Bioenergetic and oxidative stress in neurodegenerative diseases. Life sciences. 1995 Feb 24;56(14):1151-71.

Brettschneider J, Arai K, Del Tredici K, Toledo JB, Robinson JL, Lee EB, Kuwabara S, Shibuya K, Irwin DJ, Fang L, Van Deerlin VM. TDP-43 pathology and neuronal loss in amyotrophic lateral sclerosis spinal cord. Acta neuropathologica. 2014 Sep 1;128(3):423-37.

Brockington A: Expression of vascular endothelial growth factor and its receptors in the central nervous system in amyotrophic lateral sclerosis. J Neuropathol Exp Neurol 2006, 65:26–36.

Brooks BR, Miller RG, Swash M, Munsat TL. El Escorial revisited: revised criteria for the diagnosis of amyotrophic lateral sclerosis. Amyotroph Lateral Scler Other Motor Neuron Disord 2000; 1: 293–299.

Brown HA, Murphy RC. Working towards an exegesis for lipids in biology. Nat Chem Biol. 2009 Sep;5(9):602-6.

Brown IR. Heat shock proteins and protection of the nervous system. Ann N Y Acad Sci. 2007; 1113:147–158.

Brown RH, Al-Chalabi A. Amyotrophic lateral sclerosis. N Engl J Med 2017; 377: 162–172.

Browne SE, Yang L, DiMauro JP, Fuller SW, Licata SC, Beal MF. Bioenergetic abnormalities in discrete cerebral motor pathways presage spinal cord pathology in the

G93A SOD1 mouse model of ALS. Neurobiology of disease. 2006 Jun 1;22(3):599-610.

Brownell AL, Kuruppu D, Kil KE, Jokivarsi K, Poutiainen P, Zhu A, Maxwell M. PET imaging studies show enhanced expression of mGluR5 and inflammatory response during progressive degeneration in ALS mouse model expressing SOD1-G93A gene. Journal of neuroinflammation. 2015 Dec;12(1):1-8.

Bruijn LI, Becher MW, Lee MK, Anderson KL, Jenkins NA, Copeland NG, Sisodia SS, Rothstein JD, Borchelt DR, Price DL, Cleveland DW. ALS-linked SOD1 mutant G85R mediates damage to astrocytes and promotes rapidly progressive disease with SOD1-containing inclusions. Neuron. 1997 Feb 1;18(2):327-38.

Bublitz C, Steavenson S. The pentose phosphate pathway in the endoplasmic reticulum. Journal of Biological Chemistry. 1988 Sep 15;263(26):12849-53.

Buratti E, Baralle FE: The multiple roles of TDP-43 in pre-mRNA processing and gene expression regulation. RNA Biol 2010, 7:420–429.

Buratti E, De Conti L, Stuani C, Romano M, Baralle M, Baralle F. Nuclear factor TDP-43 can affect selected microRNA levels. FEBS J 2010; 277: 2268–2281.

Cadenas E, Davies KJ. Mitochondrial free radical generation, oxidative stress, and aging. Free radical biology and medicine. 2000 Aug 1;29(3-4):222-30.

Cai H, Shim H, Lai C, Xie C, Lin X, Yang WJ, Chandran J: ALS2/alsin knockout mice and motor neuron diseases. Neurodegener Dis 2008, 5:359–366.

Camargo N, Goudriaan A, van Deijk AL, Otte WM, Brouwers JF, Lodder H, Gutmann DH, Nave KA, Dijkhuizen RM, Mansvelder HD, Chrast R. Oligodendroglial myelination requires astrocyte-derived lipids. PLoS biology. 2017 May 26;15(5):e1002605.

Canzi L, Castellaneta V, Navone S, Nava S, Dossena M, Zucca I, Mennini T, Bigini P, Parati EA. Human skeletal muscle stem cell antiinflammatory activity ameliorates clinical outcome in amyotrophic lateral sclerosis models. Mol Med. 2012; 18:401–411.

Cappelli E, Degan P, Bruno S, Pierri F, Miano M, Raggi F, Farruggia P, Mecucci C, Crescenzi B, Naim V, Dufour C. The passage from bone marrow niche to bloodstream triggers the metabolic impairment in Fanconi Anemia mononuclear cells. Redox biology. 2020 Sep 1;36:101618.

Caraci F, Battaglia G, Sortino MA, Spampinato S, Molinaro G, Copani A, Nicoletti F, Bruno V. Metabotropic glutamate receptors in neurodegeneration/neuroprotection: still a hot topic?. Neurochemistry international. 2012 Sep 1;61(4):559-65.

Caracó C, Aloj L, Chen LY, Chou JY, Eckelman WC. Cellular release of [18F] 2-fluoro-2-deoxyglucose as a function of the glucose-6-phosphatase enzyme system. Journal of Biological Chemistry. 2000 Jun 16;275(24):18489-94.

Cardona AE, Pioro EP, Sasse ME, Kostenko V, Cardona SM, Dijkstra IM, Huang D, Kidd G, Dombrowski S, Dutta R, Lee JC. Control of microglial neurotoxicity by the fractalkine receptor. Nature neuroscience. 2006 Jul;9(7):917-24.

Carrera-Juliá S, Moreno ML, Barrios C, de la Rubia Ortí JE, Drehmer E. Antioxidant alternatives in the treatment of amyotrophic lateral sclerosis: a comprehensive review. Frontiers in physiology. 2020 Feb 6;11:63.

Carrì MT, Grignaschi G, Bendotti C. Targets in ALS: designing multidrug therapies. Trends Pharmacol Sci. 2006; 27(5):267–273.

Carriedo SG, Sensi SL, Yin HZ, Weiss JH. AMPA exposures induce mitochondrial Ca2+ overload and ROS generation in spinal motor neurons in vitro. Journal of Neuroscience. 2000 Jan 1;20(1):240-50.

Carriedo SG, Yin HZ, Weiss JH. Motor neurons are selectively vulnerable to AMPA/kainate receptor-mediated injury in vitro. Journal of Neuroscience. 1996 Jul 1;16(13):4069-79.

Carriedo SG. Sensi SL, Yin HZ, Weiss JH. AMPA exposures induce mitochondrial Ca.;2:240-50.

Cereda C, Leoni E, Milani P, Pansarasa O, Mazzini G, Guareschi S, Alvisi E, Ghiroldi A, Diamanti L, Bernuzzi S, Ceroni M. Altered intracellular localization of SOD1 in leukocytes from patients with sporadic amyotrophic lateral sclerosis. PLoS One. 2013 Oct 14;8(10):e75916.

Chance PF, Rabin BA, Ryan SG, Ding Y, Scavina M, Crain B, Griffin JW, Cornblath DR: Linkage of the gene for an autosomal dominant form of juvenile amyotrophic lateral sclerosis to chromosome 9q34. Am J Hum Genet 1998, 62:633–640.

Chen HJ, Anagnostou G, Chai A, Withers J, Morris A, Adhikaree J, Pennetta G, de Belleroche JS: Characterization of the properties of a novel mutation in VAPB in familial amyotrophic lateral sclerosis. J Biol Chem 2010, 285:40266–40281.

Chen Y, Yang M, Deng J, Chen X, Ye Y, Zhu L, Liu J, Ye H, Shen Y, Li Y, Rao EJ, Fushimi K, Zhou X, Bigio EH, Mesulam M, Xu Q, Wu JY: Expression of human FUS protein in Drosophila leads to progressive neurodegeneration. Protein Cell 2011, 2:477–486.

Chen Y-Z, Bennett CL, Huynh HM, Blair IP, Puls I, Irobi J, Dierick I, Abel A, Kennerson ML, Rabin BA, Nicholson GA, Auer-Grumbach M, Wagner K, De Jonghe P, Griffin JW, Fischbeck KH, Timmerman V, Cornblath DR, Chance PF: DNA/RNA helicase gene mutations in a form of juvenile amyotrophic lateral sclerosis (ALS4). Am J Hum Genet 2004, 74:1128–1135.

Cherry JD, Olschowka JA, O'Banion MK. Neuroinflammation and M2 microglia: the good, the bad, and the inflamed. Journal of neuroinflammation. 2014 Dec;11(1):1-5.

Chiò A, Calvo A, Moglia C, Mazzini L, Mora G. Phenotypic heterogeneity of amyotrophic lateral sclerosis: a population-based study. Journal of Neurology, Neurosurgery & Psychiatry. 2011 Jul 1;82(7):740-6.

Chiu IM, Chen A, Zheng Y, Kosaras B, Tsiftsoglou SA, Vartanian TK, Brown RH, Carroll MC. T lymphocytes potentiate endogenous neuroprotective inflammation in a mouse model of ALS. Proceedings of the National Academy of Sciences. 2008 Nov 18;105(46):17913-8.

Choi DW. Glutamate neurotoxicity and diseases of the nervous system. Neuron. 1988 Oct 1;1(8):623-34.

Chow CY, Zhang Y, Dowling JJ, Jin N, Adamska M, Shiga K, Szigeti K, Shy ME, Li J, Zhang X, Lupski JR, Weisman LS, Meisler MH: Mutation of FIG 4 causes neurodegeneration in the pale tremor mouse and patients with CMT4J. Nature 2007, 448:68–72.

Ciesler J, Sari Y. Neurotrophic peptides: potential drugs for treatment of amyotrophic lateral sclerosis and Alzheimer's disease. Open journal of neuroscience. 2013 Apr 8;3.

Cirulli ET, Lasseigne BN, Petrovski S, *et al*. Exome sequencing in amyotrophic lateral sclerosis identifies risk genes and pathways. Science 2015; 347: 1436–1441.

Cohen TJ, Hwang AW, Unger T, Trojanowski JQ, Lee VM. Redox signalling directly regulates TDP-43 via cysteine oxidation and disulphide cross-linking. The EMBO journal. 2012 Mar 7;31(5):1241-52.

Cohen TJ. An acetylation switch controls TDP-43 function and aggregation propensity. Nat Commun. 2015 Jan 5;6:5845.

Collingridge GL. Excitatory amino acid receptors in the vertebrate central nervous system. Pharmacol. Rev.. 1989;41:143-210.

Conn PJ, Pin JP. Pharmacology and functions of metabotropic glutamate receptors. Annual review of pharmacology and toxicology. 1997 Apr;37(1):205-37.

Contestabile A. Amyotrophic lateral sclerosis: from research to therapeutic attempts and therapeutic perspectives. Curr Med Chem. 2011; 18(36):5655–5665.

Corcia P, Camu W, Halimi JM, Vourc'h P, Antar C, Vedrine S, Giraudeau B, De Toffol B, Andres CR. SMN1 gene, but not SMN2, is a risk factor for sporadic ALS. Neurology. 2006 Oct 10;67(7):1147-50.

Corcia P, Mayeux-Portas V, Khoris J, de Toffol B, Autret A, Muh JP, Camu W, Andres C, French ALS Research Group: Amyotrophic Lateral Sclerosis. Abnormal SMN1 gene copy number is a susceptibility factor for amyotrophic lateral sclerosis. Ann Neurol 2002, 51:243–246.

Corona JC, Tapia R. AMPA receptor activation, but not the accumulation of endogenous extracellular glutamate, induces paralysis and motor neuron death in rat spinal cord in vivo. Journal of neurochemistry. 2004 May;89(4):988-97.

Corrado L, Carlomagno Y, Falasco L, Mellone S, Godi M, Cova E, Cereda C, Testa L, Mazzini L, D'Alfonso S: A novel peripherin gene (PRPH) mutation identified in one sporadic amyotrophic lateral sclerosis patient. Neurobiol Aging 2011, 32(552):e1–e6.

Corti O, Blomgren K, Poletti A, Beart PM. Autophagy in neurodegeneration: New insights underpinning therapy for neurological diseases. Journal of Neurochemistry. 2020 Aug;154(4):354-71.

Cossu V, Bauckneht M, Bruno S, Orengo AM, Emionite L, Balza E, Castellani P, Piccioli P, Miceli A, Raffa S, Borra A. The Elusive Link Between Cancer FDG Uptake and Glycolytic Flux Explains the Preserved Diagnostic Accuracy of PET/CT in Diabetes. Translational oncology. 2020 May 1;13(5):100752.

Cossu V, Bonanomi M, Bauckneht M, Ravera S, Righi N, Miceli A, Morbelli S, Orengo AM, Piccioli P, Bruno S, Gaglio D. Two high-rate pentose-phosphate pathways in cancer cells. Scientific reports. 2020 Dec 17;10(1):1-9.

Cossu V, Marini C, Piccioli P, Rocchi A, Bruno S, Orengo AM, Emionite L, Bauckneht M, Grillo F, Capitanio S, Balza E. Obligatory role of endoplasmic reticulum in brain FDG uptake. European journal of nuclear medicine and molecular imaging. 2019 May;46(5):1184-96.

Couillard-Després S, Zhu Q, Wong PC, Price DL, Cleveland DW, Julien JP: Protective effect of neurofilament heavy gene overexpression in motor neuron disease induced by mutant superoxide dismutase. Proc Natl Acad Sci USA 1998, 95:9626–9630.

Cox LE, Ferraiuolo L, Goodall EF, Heath PR, Higginbottom A, Mortiboys H, Hollinger HC, Hartley JA, Brockington A, Burness CE, Morrison KE, Wharton SB, Grierson AJ, Ince PG, Kirby J, Shaw PJ: Mutations in CHMP2B in lower motor neuron predominant amyotrophic lateral sclerosis (ALS). PLoS One 2010, 5:e9872.

Coyle JT, Puttfarcken P. Oxidative stress, glutamate, and neurodegenerative disorders. Science. 1993 Oct 29;262(5134):689-95.

Csala M, Bánhegyi G, Benedetti A. Endoplasmic reticulum: a metabolic compartment. FEBS letters. 2006 Apr 17;580(9):2160-5.

Csordas G. Renken C, Varnai P, Walter L, Weaver D, Buttle KF, Balla T, Mannella CA, Hajnóczky G. Structural and functional features and significance of the physical linkage between ER and mitochondria. J Cell Biol. 2006;174:915-21.

Cudkowicz ME, Shefner JM, Simpson E, Grasso D, Yu H, Zhang H, Shui A, Schoenfeld D, Brown RH, Wieland S, Barber JR, Consortium NA. Arimoclomol at dosages up to 300 mg/day is well tolerated and safe in Amyotrophic Lateral Sclerosis. Muscle Nerve. 2008; 38(1):837–844.

D'Antoni S, Berretta A, Bonaccorso CM, Bruno V, Aronica E, Nicoletti F, Catania MV, 2008. Metabotropic glutamate receptors in glial cells. Neurochemistry Research, 33: 2436-2443.

Da Cruz S, Cleveland DW: Understanding the role of TDP-43 and FUS/TLS in ALS and beyond. Curr Opin Neurobiol 2011, 21:904–919.

Dafinca R, Scaber J, Ababneh NA, Lalic T, Weir G, Christian H, Vowles J, Douglas AG, Fletcher-Jones A, Browne C, Nakanishi M. C9orf72 hexanucleotide expansions are associated with altered endoplasmic reticulum calcium homeostasis and stress granule formation in induced pluripotent stem cell-derived neurons from patients with

amyotrophic lateral sclerosis and frontotemporal dementia. Stem cells. 2016 Aug;34(8):2063-78.

D'Ambrosi N, Cozzolino M, Carrì MT. Neuroinflammation in amyotrophic lateral sclerosis: role of redox (dys) regulation. Antioxidants & redox signaling. 2018 Jul 1;29(1):15-36.

D'Antoni S, Berretta A, Seminara G, Longone P, Giuffrida-Stella AM, Battaglia G, Sortino MA, Nicoletti F, Catania MV. A prolonged pharmacological blockade of type-5 metabotropic glutamate receptors protects cultured spinal cord motor neurons against excitotoxic death. Neurobiology of disease. 2011 Jun 1;42(3):252-64.

Danzeisen R, Schwalenstoecker B, Gillardon F, Buerger E, Krzykalla V, Klinder K, Schild L, Hengerer B, Ludolph AC, Dorner-Ciossek C, Kussmaul L. Targeted antioxidative and neuroprotective properties of the dopamine agonist pramipexole and its nondopaminergic enantiomer SND919CL2x [(+)2-amino-4,5,6,7-tetrahydro-6-Lpropylamino-benzathiazole dihydrochloride]. J Pharmacol Exp Ther. 2006; 316(1):189–199.

Daoud H, Rouleau GA: Motor neuron disease: a role for ubiquilin 2 mutations in neurodegeneration. Nat Rev Neurol 2011, 7:599–600.

De Blasi A, Conn PJ, Pin JP, Nicoletti F. Molecular determinants of metabotropic glutamate receptor signaling. Trends in pharmacological sciences. 2001 Mar 1;22(3):114-20.

de Carvalho M, Dengler R, Eisen A, *et al*. Electrodiagnostic criteria for diagnosis of ALS. Clin Neurophysiol 2008; 119: 497–503.

De Vos KJ, Hafezparast M. Neurobiology of axonal transport defects in motor neuron diseases: opportunities for translational research? Neurobiol Dis 2017; 105: 283–299.

DeJesus-Hernandez M, Mackenzie IR, Boeve BF, Boxer AL, Baker M, Rutherford NJ, Nicholson AM, Finch NA, Flynn H, Adamson J, Kouri N, Wojtas A, Sengdy P, Hsiung GY, Karydas A, Seeley WW, Josephs KA, Coppola G, Geschwind DH, Wszolek ZK, Feldman H, Knopman DS, Petersen RC, Miller BL, Dickson DW, Boylan KB, Graff-Radford NR, Rademakers R: Expanded GGGGCC hexanucleotide repeat in noncoding region of C9ORF72 causes chromosome 9p-linked FTD and ALS. Neuron 2011, 72:245–256.

DeJesus-Hernandez M, Mackenzie IR, Boeve BF, *et al*. Expanded GGGGCC hexanucleotide repeat in noncoding region of C9ORF72 causes chromosome 9p-linked FTD and ALS. Neuron 2011; 72: 245–256.

Deng H-X, Chen W, Hong S-T, Boycott KM, Gorrie GH, Siddique N, Yang Y, Fecto F, Shi Y, Zhai H, Jiang H, Hirano M, Rampersaud E, Jansen GH, Donkervoort S, Bigio EH, Brooks BR, Ajroud K, Sufit RL, Haines JL, Mugnaini E, Pericak-Vance MA, Siddique T: Mutations in UBQLN2 cause dominant X-linked juvenile and adult-ons*et al*S and ALS/dementia. Nature 2011, 477:211–215.

Deng HX, Chen W, Hong ST, *et al*. Mutations in UBQLN2 cause dominant X-linked juvenile and adult-ons*et al*S and ALS/dementia. Nature 2011; 477: 211–215.

Deng HX, Hentati A, Tainer JA, Iqbal Z, Cayabyab A, Hung WY, Getzoff ED, Hu P, Herzfeldt B, Roos RP, Warner C. Amyotrophic Lateral Ssclerosis and Structural Defects in Cu, Zn Superoxide Dismutase. Science. 1993 Aug 20;261(5124):1047-51.

Deng J, Yang M, Chen Y, Chen X, Liu J, Sun S, Cheng H, Li Y, Bigio EH, Mesulam M, Xu Q. FUS interacts with HSP60 to promote mitochondrial damage. PLoS genetics. 2015 Sep 3;11(9):e1005357.

Dewil M, Van Den Bosch L, Robberecht W. Microglia in amyotrophic lateral sclerosis. Acta neurologica belgica. 2007 Sep 1;107(3):63.

Díaz-Amarilla P, Olivera-Bravo S, Trias E, Cragnolini A, Martínez-Palma L, Cassina P, Beckman J, Barbeito L. Phenotypically aberrant astrocytes that promote motoneuron damage in a model of inherited amyotrophic lateral sclerosis. Proceedings of the National Academy of Sciences. 2011 Nov 1;108(44):18126-31.

Dimos JT, Rodolfa KT, Niakan KK, Weisenthal LM, Mitsumoto H, Chung W, Croft GF, Saphier G, Leibel R, Goland R, Wichterle H, Henderson CE, Eggan K. Induced pluripotent stem cells generated from patients with ALS can be differentiated into motor neurons. Science. 2008; 321(5893):1218–1221.

Doble A. The role of excitotoxicity in neurodegenerative disease: implications for therapy. Pharmacology & therapeutics. 1999 Mar 1;81(3):163-221.

Doi H, Koyano S, Suzuki Y, Nukina N, Kuroiwa Y: The RNA-binding protein FUS/TLS is a common aggregate-interacting protein in polyglutamine diseases. Neurosci Res 2010, 66:131–133.

Dolen G, Bear MF. A role for metabotropic glutamate receptor 5 (mGluR5) in the pathogenesis of fragile X syndrome. Neuroscience Research. 2009(65):S27.

Dormann D, Rodde R, Edbauer D, Bentmann E, Fischer I, Hruscha A, Than ME, Mackenzie IR, Capell A, Schmid B, Neumann M, Haass C: ALS-associated fused in sarcoma (FUS) mutations disrupt transportin-mediated nuclear import. EMBO J 2010, 29:2841–2857.

Doumazane E, Scholler P, Zwier JM, Trinquet E, Rondard P, Pin JP. A new approach to analyze cell surface protein complexes reveals specific heterodimeric metabotropic glutamate receptors. The FASEB Journal. 2011 Jan;25(1):66-77.

Duan W, Li X, Shi J, Guo Y, Li Z, Li C. Mutant TAR DNA-binding protein-43 induces oxidative injury in motor neuron-like cell. Neuroscience. 2010 Sep 15;169(4):1621-9.

Dupuis L, Pradat PF, Ludolph AC, Loeffler JP. Energy metabolism in amyotrophic lateral sclerosis. The Lancet Neurology. 2011 Jan 1;10(1):75-82.

Dvorak HF, Brown LF, Detmar M, Dvorak AM Am J Pathol. 1995 May; 146(5):1029-39.

Dykens JA. Isolated cerebral and cerebellar mitochondria produce free radicals when exposed to elevated CA2+ and Na+: implications for neurodegeneration. Journal of neurochemistry. 1994 Aug;63(2):584-91.

Elden AC, Kim HJ, Hart MP, Chen-Plotkin AS, Johnson BS, Fang X, Armakola M, Geser F, Greene R, Lu MM, Padmanabhan A, Clay-Falcone D, McCluskey L, Elman L, Juhr D, Gruber PJ, Rüb U, Auburger G, Trojanowski JQ, Lee VM, Van Deerlin VM, Bonini NM, Gitler AD: Ataxin-2 intermediate-length polyglutamine expansions are associated with increased risk for ALS. Nature 2010, 466:1069–1075.

Engl E, Attwell D. Non-signalling energy use in the brain. The Journal of physiology. 2015 Aug 15;593(16):3417-29.

Ezzi SA, Urushitani M, Julien JP. Wild-type superoxide dismutase acquires binding and toxic properties of ALS-linked mutant forms through oxidation. Journal of neurochemistry. 2007 Jul;102(1):170-8.

Farmer K, Abd-Elrahman KS, Derksen A, Rowe EM, Thompson AM, Rudyk CA, Prowse NA, Dwyer Z, Bureau SC, Fortin T, Ferguson SS. mGluR5 allosteric modulation promotes neurorecovery in a 6-OHDA-toxicant model of Parkinson's disease. Molecular Neurobiology. 2020 Mar;57(3):1418-31.

Faulkner JR, Herrmann JE, Woo MJ, Tansey KE, Doan NB, Sofroniew MV. Reactive astrocytes protect tissue and preserve function after spinal cord injury. Journal of neuroscience. 2004 Mar 3;24(9):2143-55.

Fazal A, Parker F, Palmer AM, Croucher MJ. Characterisation of the actions of group I metabotropic glutamate receptor subtype selective ligands on excitatory amino acid release and sodium-dependent re-uptake in rat cerebrocortical minislices. Journal of neurochemistry. 2003 Sep;86(6):1346-58.

Fecto F, Yan J, Vemula SP, *et al*. SQSTM1 mutations in familial and sporadic amyotrophic lateral sclerosis. Arch Neurol 2011; 68: 1440–1446.

Ferraguti F, Crepaldi L, Nicoletti F. Metabotropic glutamate 1 receptor: current concepts and perspectives. Pharmacological reviews. 2008 Dec 1;60(4):536-81.

Ferraiuolo L, Meyer K, Sherwood TW, Vick J, Likhite S, Frakes A, Miranda CJ, Braun L, Heath PR, Pineda R, Beattie CE. Oligodendrocytes contribute to motor neuron death in ALS via SOD1-dependent mechanism. Proceedings of the National Academy of Sciences. 2016 Oct 18;113(42):E6496-505.

Ferri A, Cozzolino M, Crosio C, Nencini M, Casciati A, Gralla EB, Rotilio G, Valentine JS, Carri MT. Familial ALS-superoxide dismutases associate with mitochondria and shift their redox potentials. Proceedings of the National Academy of Sciences. 2006 Sep 12;103(37):13860-5.

Finegan E, Chipika RH, Li Hi Shing S, Hardiman O, Bede P. Pathological crying and laughing in motor neuron disease: pathobiology, screening, intervention. Front Neurol 2019; 10: 260.

Fomin V, Richard P, Hoque M, Li C, Gu Z, Fissore-O'Leary M, Tian B, Prives C, Manley JL. The C9ORF72 gene, implicated in amyotrophic lateral sclerosis and frontotemporal dementia, encodes a protein that functions in control of endothelin and glutamate signaling. Molecular and cellular biology. 2018 Nov 15;38(22).

Foran E, Bogush A, Goffredo M, Roncaglia P, Gustincich S, Pasinelli P, Trotti D. Motor neuron impairment mediated by a sumoylated fragment of the glial glutamate transporter EAAT2. Glia. 2011 Nov;59(11):1719-31.

Forsberg K, Andersen PM, Marklund SL, Brännström T. Glial nuclear aggregates of superoxide dismutase-1 are regularly present in patients with amyotrophic lateral sclerosis. Acta neuropathologica. 2011 May;121(5):623-34.

Franklin RJ. Regenerating CNS myelin—from mechanisms to experimental medicines. Nature Reviews Neuroscience. 2017 Dec;18(12):753.

Freischmidt A, Wieland T, Richter B, *et al*. Haploinsufficiency of TBK1 causes familial ALS and fronto-temporal dementia. Nat Neurosci 2015; 18: 631–636.

French HM, Reid M, Mamontov P, Simmons RA, Grinspan JB. Oxidative stress disrupts oligodendrocyte maturation. Journal of neuroscience research. 2009 Nov 1;87(14):3076-87.

G. Kantzer C, Boutin C, Herzig ID, Wittwer C, Reiß S, Tiveron MC, Drewes J, Rockel TD, Ohlig S, Ninkovic J, Cremer H. Anti-ACSA-2 defines a novel monoclonal antibody for prospective isolation of living neonatal and adult astrocytes. Glia. 2017 Jun;65(6):990-1004.

Gallardo G, Barowski J, Ravits J, Siddique T, Lingrel JB, Robertson J, Steen H, Bonni A. An α2-Na/K ATPase/α-adducin complex in astrocytes triggers non–cell autonomous neurodegeneration. Nature neuroscience. 2014 Dec;17(12):1710-9.

Geissmann F, Auffray C, Palframan R, Wirrig C, Ciocca A, Campisi L, Narni-Mancinelli E, Lauvau G. Blood monocytes: distinct subsets, how they relate to dendritic cells, and their possible roles in the regulation of T-cell responses. Immunology and cell biology. 2008 Jul;86(5):398-408.

Gendron TF, Petrucelli L: Rodent models of TDP-43 proteinopathy: investigating the mechanisms of TDP-43-mediated neurodegeneration. J Mol Neurosci 2011, 45:486–499.

Ghazi-Noori S, Froud KE, Mizielinska S, Powell C, Smidak M, Fernandez De Marco M, O'Malley C, Farmer M, Parkinson N, Fisher EM, Asante EA, Brandner S, Collinge J, Isaacs AM: Progressive neuronal inclusion formation and axonal degeneration in CHMP2B mutant transgenic mice. Brian 2012, 135(Pt 3):819–832.

Gibb SL, Boston-Howes W, Lavina ZS, Gustincich S, Brown Jr RH, Pasinelli P, Trotti D. A caspase-3-cleaved fragment of the glial glutamate transporter EAAT2 is sumoylated and targeted to promyelocytic leukemia nuclear bodies in mutant SOD1-linked

amyotrophic lateral sclerosis. Journal of Biological Chemistry. 2007 Nov 2;282(44):32480-90. [CrossRef] [PubMed]

Giordano G, Cole TB, Furlong CE, Costa LG: Paraoxonase 2 (PON2) in the mouse central nervous system: a neuroprotective role? Toxicol Appl Pharmacol 2011, 256:369–378.

Giribaldi F, Milanese M, Bonifacino T, Rossi PI, Di Prisco S, Pittaluga A, Tacchetti C, Puliti A, Usai C, Bonanno G. Group I metabotropic glutamate autoreceptors induce abnormal glutamate exocytosis in a mouse model of amyotrophic lateral sclerosis. Neuropharmacology. 2013 Mar 1;66:253-63.

Gispert S, Twells R, Orozco G, Brice A, Weber J, Heredero L, Scheufler K, Riley B, Allotey R, Nothers C, Hillermann R. Chromosomal assignment of the second locus for autosomal dominant cerebellar ataxia (SCA2) to chromosome 12q23–24.1. Nature genetics. 1993 Jul;4(3):295-9.

Gomes C, Cunha C, Nascimento F, Ribeiro JA, Vaz AR, Brites D. Cortical neurotoxic astrocytes with early ALS pathology and miR-146a deficit replicate gliosis markers of symptomatic SOD1G93A mouse model. Molecular neurobiology. 2019 Mar;56(3):2137-58.

Gordon PH. Amyotrophic lateral sclerosis: pathophysiology, diagnosis and management. CNS Drugs. 2011; 25(11):1–15.

Gorter RP, Stephenson J, Nutma E, Anink J, de Jonge JC, Baron W, Jahreiβ MC, Belien JA, van Noort JM, Mijnsbergen C, Aronica E. Rapidly progressive amyotrophic lateral sclerosis is associated with microglial reactivity and small heat shock protein expression in reactive astrocytes. Neuropathology and applied neurobiology. 2019 Aug;45(5):459-75.

Greenway MJ, Alexander MD, Ennis S, Traynor BJ, Corr B, Frost E, Green A, Hardiman O: A novel candidate region for ALS on chromosome 14q11.2. Neurology 2004, 63:1936–1938.

Gribkoff VK, Bozik ME. KNS-760704 [(6R)-4,5,6,7-tetrahydro-N6-propyl-2, 6-benzothiazolediamine dihydrochloride monohydrate] for the treatment of amyotrophic lateral sclerosis. CNS Neurosci Ther. 2008; 14(3):215–226.

Grieshammer U, Lewandoski M, Prevette D, Oppenheim RW, Martin GR. Muscle-specific cell ablation conditional upon Cre-mediated DNA recombination in transgenic mice leads to massive spinal and cranial motoneuron loss. Dev Biol. 1998; 197(2):234–247.

Grohmann K, Schuelke M, Diers A, Hoffmann K, Lucke B, Adams C, Bertini E, Leonhardt-Horti H, Muntoni F, Ouvrier R, Pfeufer A, Rossi R, Van Maldergem L, Wilmshurst JM, Wienker TF, Sendtner M, Rudnik-Schöneborn S, Zerres K, Hübner C: Mutations in the gene encoding immunoglobulin mu- binding protein 2 cause spinal muscular atrophy with respiratory distress type 1. Nat Genet 2001, 29:75–77.

Gros-Louis F, Kriz J, Kabashi E, McDearmid J, Millecamps S, Urushitani M, Lin L, Dion P, Zhu Q, Drapeau P, Julien JP, Rouleau GA: Als2 mRNA splicing variants detected in KO mice rescue severe motor dysfunction phenotype in Als2 knock-down zebrafish. Hum Mol Genet 2008, 17:2691–2702.

Gros-Louis F, Soucy G, Larivière R, Julien JP. Intracerebroventricular infusion of monoclonal antibody or its derived Fab fragment against misfolded forms of SOD1 mutant delays mortality in a mouse model of ALS. J Neurochem. 2010; 113(5):1188–1199.

Gruchot J, Weyers V, Göttle P, Förster M, Hartung HP, Küry P, Kremer D. The molecular basis for remyelination failure in multiple sclerosis. Cells. 2019 Aug;8(8):825.

Gruzman A, Wood WL, Alpert E, Prasad MD, Miller RG, Rothstein JD, Bowser R, Hamilton R, Wood TD, Cleveland DW, Lingappa VR. Common molecular signature in SOD1 for both sporadic and familial amyotrophic lateral sclerosis. Proceedings of the National Academy of Sciences. 2007 Jul 24;104(30):12524-9.

Gugliandolo A, Giacoppo S, Bramanti P, Mazzon E. NLRP3 inflammasome activation in a transgenic amyotrophic lateral sclerosis model. Inflammation. 2018 Feb;41(1):93-103.

Guo H, Lai L, Butchbach ME, Stockinger MP, Shan X, Bishop GA, Lin CL. Increased expression of the glial glutamate transporter EAAT2 modulates excitotoxicity and delays the onset but not the outcome of ALS in mice. Human molecular genetics. 2003 Oct 1;12(19):2519-32.

Gupta R, Lan M, Mojsilovic-Petrovic J, Choi WH, Safren N, Barmada S, Lee MJ, Kalb R. The proline/arginine dipeptide from hexanucleotide repeat expanded C9ORF72 inhibits the proteasome. Eneuro. 2017 Jan;4(1).

Gurney ME. Pu H, Chiu AY, Dal Canto MC, Polchow CY, Alexander DD, Caliendo J, Hentati A, Kwon YW, Deng HX, Chen W, Zhai P, Sufit RL, and Siddique T. Motor neuron degeneration in mice that express a human Cu, Zn superoxide dismutase mutation. Science. 1994;264:1772-5.

Gurney ME: The use of transgenic mouse models of amyotrophic lateral sclerosis in preclinical drug studies. J Neurol Sci 1997, 152(Suppl 1): S67–S73.

Guttenplan KA, Weigel MK, Adler DI, Couthouis J, Liddelow SA, Gitler AD, Barres BA. Knockout of reactive astrocyte activating factors slows disease progression in an ALS mouse model. Nature communications. 2020 Jul 27;11(1):1-9.

Hadano S, Hand CK, Osuga H, Yanagisawa Y, Otomo A, Devon RS, Miyamoto N, Showguchi-Miyata J, Okada Y, Singaraja R, Figlewicz DA, Kwiatkowski T, Hosler BA, Sagie T, Skaug J, Nasir J, Brown RH Jr, Scherer SW, Rouleau GA, Hayden MR, Ikeda JE: A gene encoding a putative GTPase regulator is mutated in familial amyotrophic lateral sclerosis 2. Nature Genet 2001, 29:166–173.

Haidet-Phillips AM, Hester ME, Miranda CJ, Meyer K, Braun L, Frakes A, Song S, Likhite S, Murtha MJ, Foust KD, Rao M. Astrocytes from familial and sporadic ALS patients are toxic to motor neurons. Nature biotechnology. 2011 Sep;29(9):824-8.

Halliwell B, Gutteridge JMC. Oxygen toxicity, oxygen radicals, transition metals and disease. Biochem J. 1984 Apr 1;219(1):1-14.

Halliwell B. Biochemistry of oxidative stress. Biochem. Soc. Trans. 2007, 35, 1147–1150.

Halliwell B. Reactive Species and Antioxidants. Redox Biology Is a Fundamental Theme of Aerobic Life. Plant Physiol. 2006, 141, 312–322.

Hamby ME, Sofroniew MV. Reactive astrocytes as therapeutic targets for CNS disorders. Neurotherapeutics. 2010 Oct 1;7(4):494-506.

Hamilton A, Vasefi M, Vander Tuin C, McQuaid RJ, Anisman H, Ferguson SS. Chronic pharmacological mGluR5 inhibition prevents cognitive impairment and reduces pathogenesis in an Alzheimer disease mouse model. Cell reports. 2016 May 31;15(9):1859-65.

Hao Z, Wang R, Ren H, Wang G. Role of the C9ORF72 gene in the pathogenesis of amyotrophic lateral sclerosis and frontotemporal dementia. Neuroscience Bulletin. 2020 Aug 29:1-4.

Hardiman O and van den Berg LH. Edaravone: a new treatment for ALS on the horizon? Lancet Neurol. 2017 Jul;16(7):490-491.

Hardiman O, Al-Chalabi A, Chio A, *et al*. Amyotrophic lateral sclerosis. Nat Rev Dis Primers 2017; 3: 17085.

Hariri RJ, Gurney JP. Treatment of Amyotrophy Lateral Sclerosis Using Placental Stem Cells. 2013 WO05547.

Harper JM, Krishnan C, Darman JS, Deshpande DM, Peck S, Shats I, Backovic S, Rothstein JD, Kerr DA. Axonal growth of embryonic stem cell-derived motoneurons in vitro and in motoneuron-injured adult rats. Proc Natl Acad Sci U S A. 2004; 101(18):7123–7128.

Hautbergue GM, Castelli LM, Ferraiuolo L, Sanchez-Martinez A, Cooper-Knock J, Higginbottom A, Lin YH, Bauer CS, Dodd JE, Myszczynska MA, Alam SM. SRSF1-dependent nuclear export inhibition of C9ORF72 repeat transcripts prevents neurodegeneration and associated motor deficits. Nature communications. 2017 Jul 5;8(1):1-8.

Hayward C, Colville S, Swingler RJ, Brock DJ: Molecular genetic analysis of the APEX nuclease gene in amyotrophic lateral sclerosis. Neurology 1999, 52:1899–1901.

He BP, Wen W, Strong MJ. Activated microglia (BV-2) facilitation of TNF-α-mediated motor neuron death in vitro. Journal of neuroimmunology. 2002 Jul 1;128(1-2):31-8.

Hefferan MP, Galik J, Kakinohana O, Sekerkova G, Santucci C, Marsala S, Navarro R, Hruska- Plochan M, Johe K, Feldman E, Cleveland DW, Marsala M. Human neural stem cell replacement therapy for amyotrophic lateral sclerosis by spinal transplantation. PLoS One. 2012; 7(8).

Henkel JS, Beers DR, Siklós L, Appel SH. The chemokine MCP-1 and the dendritic and myeloid cells it attracts are increased in the mSOD1 mouse model of ALS. Molecular and Cellular Neuroscience. 2006 Mar 1;31(3):427-37.

Hensley K, Floyd RA, Gordon B, Mou S, Pye QN, Stewart C, West M, Williamson K. Temporal patterns of cytokine and apoptosis-related gene expression in spinal cords of the G93A-SOD1 mouse model of amyotrophic lateral sclerosis. Journal of neurochemistry. 2002 Jul;82(2):365-74.

Hentati A, Ouahchi K, Pericak-Vance MA, Nijhawan D, Ahmad A, Yang Y, Rimmler J, Hung W, Schlotter B, Ahmed A, Ben Hamida M, Hentati F, Siddique T: Linkage of a

commoner form of recessive amyotrophic lateral sclerosis to chromosome 15q15-q22 markers. Neurogenetics 1998, 2:55–60.

Hermans E, CHALLISS RJ. Structural, signalling and regulatory properties of the group I metabotropic glutamate receptors: prototypic family C G-protein-coupled receptors. Biochemical Journal. 2001 Nov 1;359(3):465-84.

Heurich B, El Idrissi NB, Donev RM, Petri S, Claus P, Neal J, Morgan BP, Ramaglia V. Complement upregulation and activation on motor neurons and neuromuscular junction in the SOD1 G93A mouse model of familial amyotrophic lateral sclerosis. Journal of neuroimmunology. 2011 Jun 1;235(1-2):104-9.

Higgins CM, Jung C, Ding H, Xu Z. Mutant Cu, Zn superoxide dismutase that causes motoneuron degeneration is present in mitochondria in the CNS. Journal of Neuroscience. 2002 Mar 15;22(6):RC215-.

Hoch-Kraft P, Trotter J, Gonsior C. Missing in Action: Dysfunctional RNA Metabolism in Oligodendroglial Cells as a Contributor to Neurodegenerative Diseases?. Neurochemical research. 2020 Mar;45(3):566-79.

Höhn A, Tramutola A, Cascella R. Proteostasis failure in neurodegenerative diseases: focus on oxidative stress. Oxidative Medicine and Cellular Longevity. 2020 Mar 27;2020.

Holzbaur ELF, Tokito MK: Localization of the DCTN1 gene encoding p150 (Glued) to human chromosome 2p13 by fluorescence in situ hybridization. Genomics 1996, 31:398–399.

Hong K, Li Y, Duan W, Guo Y, Jiang H, Li W, Li C. Full-length TDP-43 and its C-terminal fragments activate mitophagy in NSC34 cell line. Neuroscience letters. 2012 Nov 21;530(2):144-9.

Horner RD, Kamins KG, Feussner JR, Grambow SC, Hoff-Lindquist J, Harati Y, Mitsumoto H, Pascuzzi R, Spencer PS, Tim R, Howard D, Smith TC, Ryan MA, Coffman CJ, Kasarskis EJ: Occurrence of amyotrophic lateral sclerosis among Gulf War veterans. Neurology 2003, 61:742–749.

Hosler BA, Siddique T, Sapp PC, Sailor W, Huang MC, Hossain A, Daube JR, Nance M, Fan C, Kaplan J, Hung WY, McKenna-Yasek D, Haines JL, Pericak-Vance MA, Horvitz HR, Brown RH Jr: Linkage of familial amyotrophic lateral sclerosis with frontotemporal dementia to chromosome 9q21-q22. JAMA 2000, 284:1664–1669.

Houamed KM, Kuijper JL, Gilbert TL, Haldeman BA, O'Hara PJ, Mulvihill ER, Almers W, Hagen FS. Cloning, expression, and gene structure of a G protein-coupled glutamate receptor from rat brain. Science. 1991 May 31;252(5010):1318-21.

Howland DS, Liu J, She Y, Goad B, Maragakis NJ, Kim B, Erickson J, Kulik J, DeVito L, Psaltis G, DeGennaro LJ. Focal loss of the glutamate transporter EAAT2 in a transgenic rat model of SOD1 mutant-mediated amyotrophic lateral sclerosis (ALS). Proceedings of the National Academy of Sciences. 2002 Feb 5;99(3):1604-9.

Hubert GW, Paquet M, Smith Y. Differential subcellular localization of mGluR1a and mGluR5 in the rat and monkey substantia nigra. Journal of Neuroscience. 2001 Mar 15;21(6):1838-47.

Ikeda JE, Osuga I, Kasunori T. Therapeutic Agent for Amyotrophic lateral Sclerosis. 2011 US0105517

Ilieva H, Polymenidou M, Cleveland DW. Non–cell autonomous toxicity in neurodegenerative disorders: ALS and beyond. Journal of Cell Biology. 2009 Dec 14;187(6):761-72.

Imbert G, Saudou F, Yvert G, Devys D, Trottier Y, Garnier JM, Weber C, Mandel JL, Cancel G, Abbas N, Dürr A. Cloning of the gene for spinocerebellar ataxia 2 reveals a locus with high sensitivity to expanded CAG/glutamine repeats. Nature genetics. 1996 Nov;14(3):285-91.

Ingre C, Roos PM, Piehl F, Kamel F, Fang F. Risk factors for amyotrophic lateral sclerosis. Clin Epidemiol 2015; 7: 181–193.

Ishii T, Kawakami E, Endo K, Misawa H, Watabe K. Formation and spreading of TDP-43 aggregates in cultured neuronal and glial cells demonstrated by time-lapse imaging. PLoS One. 2017 Jun 9;12(6):e0179375.

Ishikawa H, Yasui K, Oketa Y, Suzuki M, Ono S: Increased expression of valosin-containing protein in the skin of patients with amyotrophic lateral sclerosis. J Clin Neurosci 2012, 19:522–526.

Israelson A, Arbel N, Da Cruz S, Ilieva H, Yamanaka K, Shoshan-Barmatz V, Cleveland DW. Misfolded mutant SOD1 directly inhibits VDAC1 conductance in a mouse model of inherited ALS. Neuron. 2010 Aug 26;67(4):575-87.

Ito Y, Ofengeim D, Najafov A, Das S, Saberi S, Li Y, Hitomi J, Zhu H, Chen H, Mayo L, Geng J. RIPK1 mediates axonal degeneration by promoting inflammation and necroptosis in ALS. Science. 2016 Aug 5;353(6299):603-8.

Jackson M, Llado J, Rothstein JD. Therapeutic developments in the treatment of amyotrophic lateral sclerosis. Expert Opin Investig Drugs. 2002; 11(10):1343–1364.

Jaiswal MK. Riluzole and edaravone: A tale of two amyotrophic lateral sclerosis drugs. Med Res Rev. 2019 Mar;39(2):733-748.

Jean YY, Lercher LD, Dreyfus CF. Glutamate elicits release of BDNF from basal forebrain astrocytes in a process dependent on metabotropic receptors and the PLC pathway. Neuron glia biology. 2008 Feb;4(1):35-42.

Jenkins TM, Alix JJP, Fingret J, *et al*. Correction to: Longitudinal multi-modal muscle-based biomarker assessment in motor neuron disease. J Neurol 2020; 267: 257–258.

Johann S, Heitzer M, Kanagaratnam M, Goswami A, Rizo T, Weis J, Troost D, Beyer C. NLRP3 inflammasome is expressed by astrocytes in the SOD1 mouse model of ALS and in human sporadic ALS patients. Glia. 2015 Dec;63(12):2260-73.

Johnson JO, Mandrioli J, Benatar M, Abramzon Y, Van Deerlin VM, Trojanowski JQ, Gibbs JR, Brunetti M, Gronka S, Wuu J, Ding J, McCluskey L, Martinez-Lage M, Falcone D, Hernandez DG, Arepalli S, Chong S, Schymick JC, Rothstein J, Landi F, Wang YD, Calvo A, Mora G, Sabatelli M, Monsurrò MR, Battistini S, Salvi F, Spataro R, Sola P, Borghero G, Consortium ITALSGEN, Galassi G, Scholz SW, Taylor JP, Restagno G, Chiò A, Traynor BJ: Exome sequencing reveals VCP mutations as a cause of familial ALS. Neuron 2010, 68:857–864.

Johnson JO, Mandrioli J, Benatar M, *et al*. Exome sequencing reveals VCP mutations as a cause of familial ALS. Neuron 2010; 68: 857–864.

Johnston CA, Stanton BR, Turner MR, *et al*. Amyotrophic lateral sclerosis in an urban setting: a population based study of inner city London. J Neurol 2006; 253: 1642–1643.

Joyce PI, Fratta P, Fisher EM, Acevedo-Arozena A: SOD1 and TDP- 43 animal models of amyotrophic lateral sclerosis: recent advances in understanding disease toward the development of clinical treatments. Mamm Genome 2011, 22:420–448.

Juneja T, Pericak-Vance MA, Laing NG, Dave S, Siddique T. Prognosis in familial amyotrophic lateral sclerosis: progression and survival in patients with glu100gly and ala4val mutations in Cu, Zn superoxide dismutase. Neurology. 1997 Jan 1;48(1):55-7.

Kabashi E, Valdmanis PN, Dion P, *et al*. TARDBP mutations in individuals with sporadic and familial amyotrophic lateral sclerosis. Nat Genet 2008; 40: 572–574.

Kalmar B, Novoselov S, Gray A, Cheetham ME, Margulis B, Greensmith L. Late stage treatment with arimoclomol delays disease progression and prevents protein aggregation in the SOD1 mouse model of ALS. J Neurochem. 2008; 107(2):339–350.

Kamo H, Haebara H, Akiguchi I, Kameyama M, Kimura H, McGeer PL. A distinctive distribution of reactive astroglia in the precentral cortex in amyotrophic lateral sclerosis. Acta neuropathologica. 1987 Mar 1;74(1):33-8.

Kanekura K, Hashimoto Y, Niikura T, Aiso S, Matsuoka M, Nishimoto I: Alsin, the product of ALS2 gene, suppresses SOD1 mutant neurotoxicity through RhoGEF domain by interacting with SOD1 mutants. J Biol Chem 2004, 279:19247–19256.

Kang SH, Li Y, Fukaya M, Lorenzini I, Cleveland DW, Ostrow LW, Rothstein JD, Bergles DE. Degeneration and impaired regeneration of gray matter oligodendrocytes in amyotrophic lateral sclerosis. Nature neuroscience. 2013 May;16(5):571-9.

Karussis D, Karageorgiou C, Vaknin-Dembinsky A, Gowda-Kurkalli B, Gomori JM, Kassis I, Bulte JW, Petrou P, Ben-Hur T, Abramsky O, Slavin S. Safety and immunological effects of mesenchymal stem cell transplantation in patients with multiple sclerosis and amyotrophic lateral sclerosis. Arch Neurol. 2010; 67(10):1187–1194.

Kawamata H, Manfredi G. Mitochondrial dysfunction and intracellular calcium dysregulation in ALS. Mechanisms of ageing and development. 2010 Jul 1;131(7-8):517-26.

Kaye FJ, Shows TB: Assignment of ubiquilin2 (UBQLN2) to human chromosome xp11: 23– > p11.1 by Gene Bridge radiation hybrids. Cytogenet Cell Genet 2000, 89:116–117.

Ke YD, van Hummel A, Stevens CH, Gladbach A, Ippati S, Bi M, Lee WS, Krüger S, van der Hoven J, Volkerling A, Bongers A. Short-term suppression of A315T mutant human TDP-43 expression improves functional deficits in a novel inducible transgenic mouse model of FTLD-TDP and ALS. Acta neuropathologica. 2015 Nov;130(5):661-78.

Kenny PJ, Chen SA, Kitamura O, Markou A, Koob GF. Conditioned withdrawal drives heroin consumption and decreases reward sensitivity. Journal of Neuroscience. 2006 May 31;26(22):5894-900.

Khalfallah Y, Kuta R, Grasmuck C, Prat A, Durham HD, Velde CV. TDP-43 regulation of stress granule dynamics in neurodegenerative disease-relevant cell types. Scientific reports. 2018 May 15;8(1):1-3.

Kieran D, Kalmar B, Dick JR, Riddoch-Contreras J, Burnstock G, Greensmith L. Treatment with arimoclomol, a coinducer of heat shock proteins, delays disease progression in ALS mice. Nat Med. 2004; 10(4):402–405.

Kim JH, Marton J, Ametamey SM, Cumming P. A Review of molecular imaging of glutamate receptors. Molecules. 2020 Jan;25(20):4749.

Kim RB, Irvin CW, Tilva KR, Mitchell CS. State of the field: an informatics-based systematic review of the SOD1-G93A amyotrophic lateral sclerosis transgenic mouse model. Amyotrophic Lateral Sclerosis and Frontotemporal Degeneration. 2016 Feb 17;17(1-2):1-4.

Kim S, Chung AY, Na JE, Lee SJ, Jeong SH, Kim E, Sun W, Rhyu IJ, Park HC. Myelin degeneration induced by mutant superoxide dismutase 1 accumulation promotes amyotrophic lateral sclerosis. Glia. 2019 Oct;67(10):1910-21.

Kjældgaard AL, Pilely K, Olsen KS, Pedersen SW, Lauritsen AØ, Møller K, Garred P. Amyotrophic lateral sclerosis: The complement and inflammatory hypothesis. Molecular immunology. 2018 Oct 1;102:14-25.

Klein SM, Behrstock S, McHugh J, Hoffmann K, Wallace K, Suzuki M, Aebischer P, Svendsen CN. GDNF delivery using human neural progenitor cells in a rat model of ALS. Hum Gene Ther. 2005; 16(4):509–521.

Koga S, Lin WL, Walton RL, Ross OA, Dickson DW. TDP-43 pathology in multiple system atrophy: colocalization of TDP-43 and α-synuclein in glial cytoplasmic inclusions. Neuropathology and applied neurobiology. 2018 Dec;44(7):707-21.

Korac J, Schaeffer V, Kovacevic I, Clement AM, Jungblut B, Behl C, Terzic J, Dikic I: Ubiquitin-independent function of optineurin in autophagic clearance of protein aggregates. J Cell Sci 2013, 126:580–592.

Kreft H, Jetz W. Global patterns and determinants of vascular plant diversity. Proceedings of the National Academy of Sciences. 2007 Apr 3;104(14):5925-30.

Kriegstein A, Alvarez-Buylla A. The glial nature of embryonic and adult neural stem cells. Annual review of neuroscience. 2009 Jul 21;32:149-84.

Kruger NJ. The Bradford method for protein quantitation. The protein protocols handbook. 2009:17-24.

Kwiatkowski TJ, Bosco DA, Leclerc AL, Tamrazian E, Vanderburg CR, Russ C, Davis A, Gilchrist J, Kasarskis EJ, Munsat T, Valdmanis P. Mutations in the FUS/TLS gene on chromosome 16 cause familial amyotrophic lateral sclerosis. Science. 2009 Feb 27;323(5918):1205-8.

La Spada AR, Taylor JP. Repeat expansion disease: progress and puzzles in disease pathogenesis. Nature Reviews Genetics. 2010 Apr;11(4):247-58.

Lagier-Tourenne C, Polymenidou M, Cleveland DW. TDP-43 and FUS/TLS: emerging roles in RNA processing and neurodegeneration. Human molecular genetics. 2010 Apr 15;19(R1):R46-64.

Lai C, Lin X, Chandran J, Shim H, Yang WJ, Cai H: The G59S mutation in p150(glued) causes dysfunction of dynactin in mice. J Neurosci 2007, 27:13982–13990.

Laird FM, Farah MH, Ackerley S, Hoke A, Maragakis N, Rothstein JD, Griffin J, Price DL, Martin LJ, Wong PC: Motor neuron disease occurring in a mutant dynactin mouse model is characterized by defects in vesicular trafficking. J Neurosci 2008, 28:1997–2005.

Lambrechts D, Poesen K, Fernández-Santiago R, Al-Chalabi A, Del Bo R, Van Vught PW, Khan S, Marklund SL, Brockington A, van Marion I, Anneser J, Shaw C, Ludolph AC, Leigh NP, Comi GP, Gasser T, Shaw PJ, Morrison KE, Andersen PM, Van den Berg LH, Thijs V, Siddique T, Robberecht W, Carmeliet P: Meta-analysis of vascular endothelial growth factor variations in amyotrophic lateral sclerosis: increased susceptibility in male carriers of the -2578AA genotype. J Med Genet 2009, 46:840–846.

Lanson NA Jr, Pandey UB: FUS-related proteinopathies: lessons from animal models. Brain Res 2012, 1462:3–15.

Le Ber I, De Septenville A, Millecamps S, *et al*. TBK1 mutation frequencies in French frontotemporal dementia and amyotrophic lateral sclerosis cohorts. Neurobiol Aging 2015; 36: 3116.e5–3116.e8.

Lee Y, Morrison BM, Li Y, Lengacher S, Farah MH, Hoffman PN, Liu Y, Tsingalia A, Jin L, Zhang PW, Pellerin L. Oligodendroglia metabolically support axons and contribute to neurodegeneration. Nature. 2012 Jul;487(7408):443-8.

Lefebvre S, Bürglen L, Reboullet S, Clermont O, Burlet P, Viollet L, Benichou B, Cruaud C, Millasseau P, Zeviani M, Le Paslier D. Identification and characterization of a spinal muscular atrophy-determining gene. Cell. 1995 Jan 13;80(1):155-65.

Lefebvre S, Burlet P, Liu Q, Bertrandy S, Clermont O, Munnich A, Dreyfuss G, Melki J: Correlation between severity and SMN protein level in spinal muscular atrophy. Nat Genet 1997, 16:265–269.

Leigh PN, Whitwell H, Garofalo O, Buller J, Swash M, Martin JE, Gallo JM, Weller RO, Anderton BH. Ubiquitin-immunoreactive intraneuronal inclusions in amyotrophic lateral sclerosis: morphology, distribution, and specificity. Brain. 1991 Apr 1;114(2):775-88.

Lepore AC, Rauck B, Dejea C, Pardo AC, Rao MS, Rothstein JD, Maragakis NJ. Focal transplantation–based astrocyte replacement is neuroprotective in a model of motor neuron disease. Nature neuroscience. 2008 Nov;11(11):1294-301.

Levine TP, Daniels RD, Gatta AT, Wong LH, Hayes MJ. The product of C9orf72, a gene strongly implicated in neurodegeneration, is structurally related to DENN Rab-GEFs. Bioinformatics. 2013 Feb 15;29(4):499-503.

Li B, Guo YS, Sun MM, Dong H, Wu SY, Wu DX, Li CY. The NADPH oxidase is involved in lipopolysaccharide-mediated motor neuron injury. Brain research. 2008 Aug 21;1226:199-208.

Li Q, Spencer NY, Pantazis NJ, Engelhardt JF: Alsin and SOD1(G93A) proteins regulate endosomal reactive oxygen species production by glial cells and proinflammatory pathways responsible for neurotoxicity. J Biol Chem 2011, 286:40151–40162.

Liddelow S, Barres B. SnapShot: astrocytes in health and disease. Cell. 2015 Aug 27;162(5):1170-.

Liddelow SA, Guttenplan KA, Clarke LE, Bennett FC, Bohlen CJ, Schirmer L, Bennett ML, Münch AE, Chung WS, Peterson TC, Wilton DK. Neurotoxic reactive astrocytes are induced by activated microglia. Nature. 2017 Jan;541(7638):481-7.

Lindemann L, Jaeschke G, Michalon A, Vieira E, Honer M, Spooren W, Porter R, Hartung T, Kolczewski S, Büttelmann B, Flament C. CTEP: a novel, potent, long-acting, and orally bioavailable metabotropic glutamate receptor 5 inhibitor. Journal of Pharmacology and Experimental Therapeutics. 2011 Nov 1;339(2):474-86.

Lino MM, Schneider C, Caroni P. Accumulation of SOD1 mutants in postnatal motoneurons does not cause motoneuron pathology or motoneuron disease. Journal of Neuroscience. 2002 Jun 15;22(12):4825-32.

Lipton SA, Rosenberg PA. Excitatory amino acids as a final common pathway for neurologic disorders. New England Journal of Medicine. 1994 Mar 3;330(9):613-22.

Liu HN, Sanelli T, Horne P, Pioro EP, Strong MJ, Rogaeva E, Bilbao J, Zinman L, Robertson J. Lack of evidence of monomer/misfolded superoxide dismutase-1 in sporadic amyotrophic lateral sclerosis. Annals of Neurology: Official Journal of the American Neurological Association and the Child Neurology Society. 2009 Jul;66(1):75-80.

Liu J, Wang F. Role of neuroinflammation in amyotrophic lateral sclerosis: cellular mechanisms and therapeutic implications. Frontiers in Immunology. 2017 Aug 21;8:1005.

Lloyd AF, Miron VE. The pro-remyelination properties of microglia in the central nervous system. Nature Reviews Neurology. 2019 Aug;15(8):447-58.

Logroscino G, Traynor BJ, Hardiman O, *et al*. Incidence of amyotrophic lateral sclerosis in Europe. J Neurol Neurosurg Psychiatry 2010; 81: 385–390.

Lopate G, Baloh RH, Al-Lozi MT, Miller TM, Fernandes Filho JA, Ni O, Leston A, Florence J, Schierbecker J, Allred P: Familial ALS with extreme phenotypic variability due to the I113T SOD1 mutation. Amyotroph Lateral Scler 2010, 11:232–236.

Luigetti M, Lattante S, Zollino M, Conte A, Marangi G, Del Grande A, Sabatelli M: SOD1 G93D sporadic amyotrophic lateral sclerosis (SALS) patient with rapid progression and concomitant novel ANG variant. Neurobiol Aging 1924, 2011:32.

Luo XG, Chen SD. The changing phenotype of microglia from homeostasis to disease. Translational neurodegeneration. 2012 Dec;1(1):1-3.

Luty AA, Kwok JB, Dobson-Stone C, Loy CT, Coupland KG, Karlström H, Sobow T, Tchorzewska J, Maruszak A, Barcikowska M, Panegyres PK, Zekanowski C, Brooks WS, Williams KL, Blair IP, Mather KA, Sachdev PS, Halliday GM, Schofield PR: Sigma nonopioid intracellular receptor 1 mutations cause frontotemporal lobar degeneration-motor neurondisease. Ann Neurol 2010, 68:639–649.

Luyt K, Va´radi A, Durant CF, Molna´r E, 2006. Oligodendroglial metabotropic glutamate receptors are developmentally regulated and involved in the prevention of apoptosis. Journal of Neurochemistry, 99: 641-656.

Mackenzie IR, Ansorge O, Strong M, Bilbao J, Zinman L, Ang LC, Baker M, Stewart H, Eisen A, Rademakers R, Neumann M. Pathological heterogeneity in amyotrophic lateral sclerosis with FUS mutations: two distinct patterns correlating with disease severity and mutation. Acta neuropathologica. 2011 Jul 1;122(1):87-98.

Mackenzie IR, Arzberger T, Kremmer E, Troost D, Lorenzl S, Mori K, Weng SM, Haass C, Kretzschmar HA, Edbauer D, Neumann M. Dipeptide repeat protein pathology in C9ORF72 mutation cases: clinico-pathological correlations. Acta neuropathologica. 2013 Dec 1;126(6):859-79.

Mackenzie IR, Bigio EH, Ince PG, Geser F, Neumann M, Cairns NJ, Kwong LK, Forman MS, Ravits J, Stewart H, Eisen A, McClusky L, Kretzschmar HA, Monoranu CM, Highley JR, Kirby J, Siddique T, Shaw PJ, Lee VM, Trojanowski JQ: Pathological TDP-43 distinguishes sporadic amyotrophic lateral sclerosis from amyotrophic lateral sclerosis with SOD1 mutations. Ann Neurol 2007, 61:427–434.

Mackenzie IR, Nicholson AM, Sarkar M, Messing J, Purice MD, Pottier C, Annu K, Baker M, Perkerson RB, Kurti A, Matchett BJ. TIA1 mutations in amyotrophic lateral sclerosis and frontotemporal dementia promote phase separation and alter stress granule dynamics. Neuron. 2017 Aug 16;95(4):808-16.

Mackenzie IR, Rademakers R, Neumann M. TDP-43 and FUS in amyotrophic lateral sclerosis and frontotemporal dementia. Lancet Neurol 2010; 9: 995–1007.

Madill M, McDonagh K, Ma J, Vajda A, McLoughlin P, O'Brien T, Hardiman O, Shen S. Amyotrophic lateral sclerosis patient iPSC-derived astrocytes impair autophagy via non-cell autonomous mechanisms. Molecular brain. 2017 Dec;10(1):1-2.

Magistretti PJ. Neuron–glia metabolic coupling and plasticity. Journal of Experimental Biology. 2006 Jun 15;209(12):2304-11.

Magrane J, Cortez C, Gan WB, Manfredi G. Abnormal mitochondrial transport and morphology are common pathological denominators in SOD1 and TDP43 ALS mouse models. Human molecular genetics. 2014 Mar 15;23(6):1413-24.

Mahmoud S, Gharagozloo M, Simard C, Gris D. Astrocytes maintain glutamate homeostasis in the CNS by controlling the balance between glutamate uptake and release. Cells. 2019 Feb;8(2):184.

Mangan MS, Olhava EJ, Roush WR, Seidel HM, Glick GD, Latz E. Targeting the NLRP3 inflammasome in inflammatory diseases. Nature reviews Drug discovery. 2018 Aug;17(8):588-606.

Manjaly ZR, Scott KM, Abhinav K, *et al*. The sex ratio in amyotrophic lateral sclerosis: a population-based study. Amyotroph Lateral Scler 2010; 11: 439–442.

Marco Milanese, Tiziana Bonifacino, Carola Torazza, Francesca Provenzano, Mandeep Kumar, Silvia Ravera, Arianna Roberta Zerbo, Giulia Frumento, Matilde Balbi, T. P. Nhung Nguyen, Nadia Bertola, Sara Ferrando, Maurizio Viale, Aldo Profumo, Giambattista Bonanno. Blocking glutamate mGlu5 receptors with the negative allosteric modulator CTEP improves disease course in SOD1G93A mouse model of amyotrophic lateral sclerosis. Br. J. Pharmacol 178 (18), 3747-3764, 2021.

Margaret Hunter, Ian Robinson. Motor Neurone Disease: Assessment and Management. London, UK: National Clinical Guideline Centre, 2016. https://www.ncbi.nlm.nih.gov/books/NBK349620/

Marin B, Boumediene F, Logroscino G, *et al*. Variation in worldwide incidence of amyotrophic lateral sclerosis: a meta-analysis. Int J Epidemiol 2017; 46: 57–74.

Marini C, Cistaro A, Campi C, Calvo A, Caponnetto C, Nobili FM, Fania P, Beltrametti MC, Moglia C, Novi G, Buschiazzo A. A PET/CT approach to spinal cord metabolism in amyotrophic lateral sclerosis. European journal of nuclear medicine and molecular imaging. 2016 Oct;43(11):2061-71.

Marini C, Cossu V, Bonifacino T, Bauckneht M, Torazza C, Bruno S, Castellani P, Ravera S, Milanese M, Venturi C, Carlone S. Mechanisms underlying the predictive power of high skeletal muscle uptake of FDG in amyotrophic lateral sclerosis. EJNMMI research. 2020 Dec;10(1):1-6.

Marini C, Morbelli S, Cistaro A, Campi C, Caponnetto C, Bauckneht M, Bellini A, Buschiazzo A, Calamia I, Beltrametti MC, Margotti S. Interplay between spinal cord and cerebral cortex metabolism in amyotrophic lateral sclerosis. Brain. 2018 Aug 1;141(8):2272-9.

Marini C, Ravera S, Buschiazzo A, Bianchi G, Orengo AM, Bruno S, Bottoni G, Emionite L, Pastorino F, Monteverde E, Garaboldi L. Discovery of a novel glucose metabolism in cancer: The role of endoplasmic reticulum beyond glycolysis and pentose phosphate shunt. Scientific reports. 2016 Apr 28;6(1):1-3.

Markovinovic A, Cimbro R, Ljutic T, Kriz J, Rogelj B, Munitic I. Optineurin in amyotrophic lateral sclerosis: multifunctional adaptor protein at the crossroads of different neuroprotective mechanisms. Progress in neurobiology. 2017 Jul 1;154:1-20.

Martin LJ. Mitochondrial pathobiology in ALS. Journal of bioenergetics and biomembranes. 2011 Dec 1;43(6):569-79.

Martinez FO, Sica A, Mantovani A, Locati M. Macrophage activation and polarization. Front Biosci. 2008 Jan 1;13(1):453-61.

Martorana F, Brambilla L, Valori CF, Bergamaschi C, Roncoroni C, Aronica E, Volterra A, Bezzi P, Rossi D. The BH4 domain of Bcl-XL rescues astrocyte degeneration in amyotrophic lateral sclerosis by modulating intracellular calcium signals. Human molecular genetics. 2012 Feb 15;21(4):826-40.

Maruyama H, Morino H, Ito H, *et al*. Mutations of optineurin in amyotrophic lateral sclerosis. Nature 2010; 465: 223–226.

Maruyama H, Morino H, Ito H, Izumi Y, Kato H, Watanabe Y, Kinoshita Y, Kamada M, Nodera H, Suzuki H, Komure O, Matsuura S, Kobatake K, Morimoto N, Abe K, Suzuki N, Aoki M, Kawata A, Hirai T, Kato T, Ogasawara K, Hirano A, Takumi T, Kusaka H, Hagiwara K, Kaji R, Kawakami H: Mutations of optineurin in amyotrophic lateral sclerosis. Nature 2010, 465:223–226.

Masu M, Tanabe Y, Tsuchida K, Shigemoto R, Nakanishi S. Sequence and expression of a metabotropic glutamate receptor. Nature. 1991 Feb;349(6312):760-5.

Mattiazzi M, D'Aurelio M, Gajewski CD, Martushova K, Kiaei M, Beal MF, Manfredi G. Mutated human SOD1 causes dysfunction of oxidative phosphorylation in mitochondria of transgenic mice. Journal of biological chemistry. 2002 Aug 16;277(33):29626-33.

Mazzini L, Vercelli A, Ferrero I, Boido M, Cantello R, Fagioli F. Transplantation of mesenchymal stem cells in ALS. Prog Brain Res. 2012; 201:333–359.

McGeer EG, McGeer PL. Pharmacologic approaches to the treatment of amyotrophic lateral sclerosis. BioDrugs. 2005; 19(1):31–37.

Mejzini R, Flynn LL, Pitout IL, Fletcher S, Wilton SD, Akkari PA. ALS genetics, mechanisms, and therapeutics: where are we now?. Frontiers in neuroscience. 2019 Dec 6;13:1310.

Menke RA, Proudfoot M, Wuu J, Andersen PM, Talbot K, Benatar M, Turner MR. Increased functional connectivity common to symptomatic amyotrophic lateral sclerosis and those at genetic risk. Journal of Neurology, Neurosurgery & Psychiatry. 2016 Jun 1;87(6):580-8.

Mersiyanova IV, Perepelov AV, Polyakov AV, Sitnikov VF, Dadali EL, Oparin RB, Petrin AN, Evgrafov OV: A new variant of Charcot-Marie-Tooth disease type 2 is probably the result of a mutation in the neurofilament-light gene. Am J Hum Gene 2000, 67:37-46.

Meyer K, Ferraiuolo L, Miranda CJ, Likhite S, McElroy S, Renusch S, Ditsworth D, Lagier-Tourenne C, Smith RA, Ravits J, Burghes AH. Direct conversion of patient fibroblasts demonstrates non-cell autonomous toxicity of astrocytes to motor neurons in familial and sporadic ALS. Proceedings of the National Academy of Sciences. 2014 Jan 14;111(2):829-32.

Miceli A, Cossu V, Marini C, Castellani P, Raffa S, Donegani MI, Bruno S, Ravera S, Emionite L, Orengo AM, Grillo F. 18F-Fluorodeoxyglucose Positron Emission Tomography Tracks the Heterogeneous Brain Susceptibility to the Hyperglycemia-Related Redox Stress. International journal of molecular sciences. 2020 Jan;21(21):8154.

Michell RH, Dove SK: A protein complex that regulates PtdIns(3,5)P2 levels. EMBO J 2009, 28:86–97.

Migheli A, Cordera S, Bendotti C, Atzori C, Piva R, Schiffer D. S-100β protein is upregulated in astrocytes and motor neurons in the spinal cord of patients with amyotrophic lateral sclerosis. Neuroscience letters. 1999 Feb 12;261(1-2):25-8.

Milanese M, Bonifacino T, Torazza C, Provenzano F, Kumar M, Ravera S, Zerbo AR, Frumento G, Balbi M, Nguyen TN, Bertola N. Blocking glutamate mGlu5 receptors with the negative allosteric modulator CTEP improves disease course in SOD1G93A mouse model of amyotrophic lateral sclerosis. British journal of pharmacology. 2021 Sep;178(18):3747-64.

Milanese M, Giribaldi F, Melone M, Bonifacino T, Musante I, Carminati E, Rossi PI, Vergani L, Voci A, Conti F, Puliti A. Knocking down metabotropic glutamate receptor 1 improves survival and disease progression in the SOD1G93A mouse model of amyotrophic lateral sclerosis. Neurobiology of disease. 2014 Apr 1;64:48-59.

Milanese M, Zappettini S, Onofri F, Musazzi L, Tardito D, Bonifacino T, Messa M, Racagni G, Usai C, Benfenati F, Popoli M. Abnormal exocytotic release of glutamate in a mouse model of amyotrophic lateral sclerosis. Journal of neurochemistry. 2011 Mar;116(6):1028-42.

Millecamps S, Salachas F, Cazeneuve C, Gordon P, Bricka B, Camuzat A, Guillot-Noël L, Russaouen O, Bruneteau G, Pradat PF, Le Forestier N, Vandenberghe N, Danel-Brunaud V, Guy N, Thauvin-Robinet C, Lacomblez L, Couratier P, Hannequin D, Seilhean D, Le Ber I, Corcia P, Camu W, Brice A, Rouleau G, LeGuern E, Meininger V: SOD1, ANG, VAPB, TARDBP, and FUS mutations in familial amyotrophic lateral sclerosis: genotype-phenotype correlations. J Med Genet 2010, 47:554–560.

Miller RG, Mitchell JD, Moore DH. Riluzole for amyotrophic lateral sclerosis (ALS)/motor neuron disease (MND). Cochrane Database Syst Rev. 2012 Mar 14;(3):CD001447.

Mitchell J, Paul P, Chen HJ, Morris A, Payling M, Falchi M, Habgood J, Panoutsou S, Winkler S, Tisato V, Hajitou A, Smith B, Vance C, Shaw C, Mazarakis ND, de Belleroche J: Familial amyotrophic lateral sclerosis is associated with a mutation in D-amino acid oxidase. Proc Natl Acad Sci USA 2010, 107:7556–7561.

Mitsumoto H, Brooks BR, Silani V. Clinical trials in amyotrophic lateral sclerosis: why so many negative trials and how can trials be improved? Lancet Neurol 2014; 13: 1127–1138.

Mizielinska S, Lashley T, Norona FE, Clayton EL, Ridler CE, Fratta P, Isaacs AM. C9orf72 frontotemporal lobar degeneration is characterised by frequent neuronal sense and antisense RNA foci. Acta neuropathologica. 2013 Dec;126(6):845-57.

Mizuno Y, Fujita Y, Takatama M, Okamoto K: Peripherin partially localizes in Bunina bodies in amyotrophic lateral sclerosis. J Neurol Sci 2011, 302:14–18.

Mordes DA, Prudencio M, Goodman LD, Klim JR, Moccia R, Limone F, Pietilainen O, Chowdhary K, Dickson DW, Rademakers R, Bonini NM. Dipeptide repeat proteins activate a heat shock response found in C9ORF72-ALS/FTLD patients. Acta neuropathologica communications. 2018 Dec;6(1):1-3.

Moreira M-C, Klur S, Watanabe M, Nemeth AH, Le Ber I, Moniz J-C, Tranchant C, Aubourg P, Tazir M, Schöls L, Pandolfo P, Schulz JB, Pouget J, Calvas P, Shizuka-Ikeda M, Shoji M, Tanaka M, Izatt L, Shaw CE, M'Zahem A, Dunne E, Bomont P, Benhassine T, Bouslam N, Stevanin G, Brice A, Guimarães J, Mendonça P, Barbot C, Coutinho P, Sequeiros J, Dürr A, Warter JM, Koenig M: Senataxin, the ortholog of a yeast RNA helicase, is mutant in ataxia-ocular apraxia 2. Nature Genet. 2004, 36:225–227.

Mori K, Weng SM, Arzberger T, May S, Rentzsch K, Kremmer E, Schmid B, Kretzschmar HA, Cruts M, Van Broeckhoven C, Haass C. The C9orf72 GGGGCC repeat is translated into aggregating dipeptide-repeat proteins in FTLD/ALS. Science. 2013 Mar 15;339(6125):1335-8.

Morita M, Al-Chalabi A, Andersen PM, Hosler B, Sapp P, Englund E, Mitchell JE, Habgood JJ, de Belleroche J, Xi J, Jongjaroenprasert W, Horvitz HR, Gunnarsson LG, Brown RH Jr: A locus on chromosome 9p confers susceptibility to ALS and frontotemporal dementia. Neurology 2006, 66:839–844.

Moroni F, Cozzi A, Lombardi G, Sourtcheva S, Leonardi P, Carfì M, Pellicciari R. Presynaptic mGlu1 type receptors potentiate transmitter output in the rat cortex. European journal of pharmacology. 1998 Apr 24;347(2-3):189-95.

Morrison BM, Lee Y, Rothstein JD. Oligodendroglia: metabolic supporters of axons. Trends in cell biology. 2013 Dec 1;23(12):644-51.

Moujalled D, Grubman A, Acevedo K, Yang S, Ke YD, Moujalled DM, Duncan C, Caragounis A, Perera ND, Turner BJ, Prudencio M. TDP-43 mutations causing amyotrophic lateral sclerosis are associated with altered expression of RNA-binding protein hnRNP K and affect the Nrf2 antioxidant pathway. Human molecular genetics. 2017 May 1;26(9):1732-46.

Muly EC, Maddox M, Smith Y. Distribution of mGluR1α and mGluR5 immunolabeling in primate prefrontal cortex. Journal of Comparative Neurology. 2003 Dec 22;467(4):521-35.

Munch C, Sedlmeier R, Meyer T, *et al*. Point mutations of the p150 subunit of dynactin (DCTN1) gene in ALS. Neurology 2004; 63: 724–726

Münch C, Sedlmeier R, Meyer T, Homberg V, Sperfeld AD, Kurt A, Prudlo J, Peraus G, Hanemann CO, Stumm G, Ludolph AC: Point mutations of the p150 subunit of dynactin (DCTN1) gene in ALS. Neurology 2004, 63:724–726.

Murmu RP, Martin E, Rastetter A, Esteves T, Muriel MP, El Hachimi KH, Denora PS, Dauphin A, Fernandez JC, Duyckaerts C, Brice A, Darios F, Stevanin G: Cellular distribution and subcellular localization of spatacsin and spastizin, two proteins involved in hereditary spastic paraplegia. Mol Cell Neurosci 2011, 47:191–202.

Murray ME, DeJesus-Hernandez M, Rutherford NJ, Baker M, Duara R, Graff-Radford NR, Wszolek ZK, Ferman TJ, Josephs KA, Boylan KB, Rademakers R. Clinical and neuropathologic heterogeneity of c9FTD/ALS associated with hexanucleotide repeat expansion in C9ORF72. Acta neuropathologica. 2011 Dec;122(6):673-90.

Musante V, Neri E, Feligioni M, Puliti A, Pedrazzi M, Conti V, Usai C, Diaspro A, Ravazzolo R, Henley JM, Battaglia G. Presynaptic mGlu1 and mGlu5 autoreceptors facilitate glutamate exocytosis from mouse cortical nerve endings. Neuropharmacology. 2008 Sep 1;55(4):474-82.

Nagai M, Re DB, Nagata T, Chalazonitis A, Jessell TM, Wichterle H, Przedborski S. Astrocytes expressing ALS-linked mutated SOD1 release factors selectively toxic to motor neurons. Nature neuroscience. 2007 May;10(5):615-22.

Naon D, Zaninello M, Giacomello M, Varanita T, Grespi F, Lakshminaranayan S, Serafini A, Semenzato M, Herkenne S, Hernández-Alvarez MI, Zorzano A. Critical reappraisal confirms that Mitofusin 2 is an endoplasmic reticulum–mitochondria tether. Proceedings of the National Academy of Sciences. 2016 Oct 4;113(40):11249-54.

Naon D, Zaninello M, Giacomello M, Varanita T, Grespi F, Lakshminaranayan S, Serafini A, Semenzato M, Herkenne S, Hernández-Alvarez MI, Zorzano A. Critical reappraisal confirms that Mitofusin 2 is an endoplasmic reticulum–mitochondria tether. Proceedings of the National Academy of Sciences. 2016 Oct 4;113(40):11249-54.

Nave KA. Myelination and support of axonal integrity by glia. Nature. 2010 Nov;468(7321):244-52.

Nave KA. Myelination and the trophic support of long axons. Nature Reviews Neuroscience. 2010 Apr;11(4):275-83.

Neumann M, Sampathu DM, Kwong LK, Truax AC, Micsenyi MC, Chou TT, Bruce J, Schuck T, Grossman M, Clark CM, McCluskey LF. Ubiquitinated TDP-43 in frontotemporal lobar degeneration and amyotrophic lateral sclerosis. Science. 2006 Oct 6;314(5796):130-3.

Neymotin A, Calingasan NY, Wille E, Naseri N, Petri S, Damiano M, Liby KT, Risingsong R, Sporn M, Beal MF, Kiaei M. Neuroprotective effect of Nrf2/ARE activators, CDDO ethylamide and CDDO trifluoroethylamide, in a mouse model of amyotrophic lateral sclerosis. Free RadicBiol Med. 2011 Jul 1;51(1):88-96.

Nguyen MD, D'Aigle T, Gowing G, Julien JP, Rivest S. Exacerbation of motor neuron disease by chronic stimulation of innate immunity in a mouse model of amyotrophic lateral sclerosis. Journal of Neuroscience. 2004 Feb 11;24(6):1340-9.

Nicholls DG, Budd SL. Mitochondria and neuronal survival. Physiological reviews. 2000 Jan 1;80(1):315-60.

Nicoletti F, Bockaert J, Collingridge GL, Conn PJ, Ferraguti F, Schoepp DD, Wroblewski JT, Pin JP, 2011. Metabotropic glutamate receptors: from the workbench to the bedside. Neuropharmacology, 60 (7-8): 1017-1041.

Nicolini C, Fahnestock M. The valproic acid-induced rodent model of autism. Experimental neurology. 2018 Jan 1;299:217-27.

Nimmerjahn A, Kirchhoff F, Helmchen F. Resting microglial cells are highly dynamic surveillants of brain parenchyma in vivo. Science. 2005 May 27;308(5726):1314-8.

Nishimura AL, Mitne-Neto M, Silva HC, Richieri-Costa A, Middleton S, Cascio D, Kok F, Oliveira JR, Gillingwater T, Webb J, Skehel P, Zatz M: A mutation in the vesicle-trafficking protein VAPB causes late-onset spinal muscular atrophy and amyotrophic lateral sclerosis. Am J Hum Genet 2004, 75:822–831.

Nishimura K, Sano M, Ohtaka M, Furuta B, Umemura Y, Nakajima Y, Ikehara Y, Kobayashi T, Segawa H, Takayasu S, Sato H. Development of defective and persistent Sendai virus vector: a unique gene delivery/expression system ideal for cell reprogramming. Journal of Biological Chemistry. 2011 Feb 11;286(6):4760-71.

Niven E, Newton J, Foley J, *et al*. Validation of the Edinburgh cognitive and behavioural amyotrophic lateral sclerosis screen (ECAS): a cognitive tool for motor disorders. Amyotroph Lateral Scler Frontotemporal Degener 2015; 16: 172–179.

Novelli A, Reilly JA, Lysko PG, Henneberry RC. Glutamate becomes neurotoxic via the N-methyl-D-aspartate receptor when intracellular energy levels are reduced. Brain research. 1988 Jun 7;451(1-2):205-12.

Nowicka N, Juranek J, Juranek JK, Wojtkiewicz J. Risk Factors and Emerging Therapies in Amyotrophic Lateral Sclerosis. Int. J. Mol. Sci. 2019, 20, 2616.

Nutma E, van Gent D, Amor S, Peferoen LA. Astrocyte and oligodendrocyte cross-talk in the central nervous system. Cells. 2020 Mar;9(3):600.

O'Connor DM, Boulis NM. Cellular and molecular approaches to motor neuron therapy in amyotrophic lateral sclerosis and spinal muscular atrophy. Neurosci Lett. 2012; 527(2):78–84.

Okamoto K, Hirai S, Shoji M, Senoh Y, Yamazaki T. Axonal swellings in the corticospinal tracts in amyotrophic lateral sclerosis. Acta neuropathologica. 1990 Jun;80(2):222-6.

Olney JW. Neurotoxicity of excitatory amino acids. Kainic acid as a tool in neurobiology. 1978.

Onesto E, Colombrita C, Gumina V, Borghi MO, Dusi S, Doretti A, Fagiolari G, Invernizzi F, Moggio M, Tiranti V, Silani V. Gene-specific mitochondria dysfunctions in human TARDBP and C9ORF72 fibroblasts. Acta neuropathologica communications. 2016 Dec;4(1):1-4.

Oosthuyse B, Moons L, Storkebaum E, Beck H, Nuyens D, Brusselmans K, Van Dorpe J, Hellings P, Gorselink M, Heymans S, Theilmeier G, Dewerchin M, Laudenbach V, Vermylen P, Raat H, Acker T, Vleminckx V, Van Den Bosch L, Cashman N, Fujisawa H, Drost MR, Sciot R, Bruyninckx F, Hicklin DJ, Ince C, Gressens P, Lupu F, Plate KH, Robberecht W, Herbert JM, Collen D, Carmeliet P: Deletion of the hypoxia-response element in the vascular endothelial growth factor promoter causes motor neuron degeneration. Nat Genet 2001, 28:131–138.

Orlacchio A, Babalini C, Borreca A, Patrono C, Massa R, Basaran S, Munhoz RP, Rogaeva EA, St George-Hyslop PH, Bernardi G, Kawarai T: SPATACSIN mutations cause autosomal recessive juvenile amyotrophic lateral sclerosis. Brain 2010, 133:591–598.

Otomo A, Kunita R, Suzuki-Utsunomiya K, Mizumura H, Onoe K, Osuga H, Hadano S, Ikeda JE: ALS2/alsin deficiency in neurons leads to mild defects in macropinocytosis and axonal growth. Biochem Biophys Res Commun 2008, 370:87–92.

Padhi AK, Kumar H, Vasaikar SV, Jayaram B, Gomes J: Mechanisms of loss of functions of human angiogenin variants implicated in amyotrophic lateral sclerosis. PLoS One 2012, 7:e32479.

Paizs M, Tortarolo M, Bendotti C, Engelhardt JI, Siklós L. Talampanel reduces the level of motoneuronal calcium in transgenic mutant SOD1 mice only if applied presymptomatically. Amyotroph Lateral Scler. 2011; 12(5):340–344.

Paluzzi S, Alloisio S, Zappettini S, Milanese M, Raiteri L, Nobile M, Bonanno G. Adult astroglia is competent for Na+/Ca2+ exchanger-operated exocytotic glutamate release triggered by mild depolarization. Journal of neurochemistry. 2007 Nov;103(3):1196-207.

Pandya NJ, Klaassen RV, van der Schors RC, Slotman JA, Houtsmuller A, Smit AB, Li KW. Group 1 metabotropic glutamate receptors 1 and 5 form a protein complex in mouse hippocampus and cortex. Proteomics. 2016 Oct;16(20):2698-705.

Pandya RS, Mao LL, Zhou EW, Bowser R, Zhu Z, Zhu Y, Wang X. Neuroprotection for amyotrophic lateral sclerosis: role of stem cells, growth factors, and gene therapy. Cent Nerv Syst Agents Med Chem. 2012; 12(1):15–27.

Pansarasa O, Bordoni M, Diamanti L, Sproviero D, Gagliardi S, Cereda C. SOD1 in amyotrophic lateral sclerosis:"ambivalent" behavior connected to the disease. International journal of molecular sciences. 2018 May;19(5):1345.

Papadeas ST, Kraig SE, O'Banion C, Lepore AC, Maragakis NJ. Astrocytes carrying the superoxide dismutase 1 (SOD1G93A) mutation induce wild-type motor neuron degeneration in vivo. Proceedings of the National Academy of Sciences. 2011 Oct 25;108(43):17803-8.

Paquet M, Ribeiro FM, Guadagno J, Esseltine JL, Ferguson SS, Cregan SP. Role of metabotropic glutamate receptor 5 signaling and homer in oxygen glucose deprivation-mediated astrocyte apoptosis. Molecular brain. 2013 Dec;6(1):1-1.

Parvizi J, Anderson SW, Martin CO, Damasio H, Damasio AR. Pathological laughter and crying: a link to the cerebellum. Brain 2001; 124: 1708–1719.

Pascuzzi RM, Shefner J, Chappell AS, Bjerke JS, Tamura R, Chaudhry V, Clawson L, Haas L, Rothstein JD. A phase II trial of talampanel in subjects with amyotrophic lateral sclerosis. Amyotroph Lateral Scler. 2010; 11(3):266–271.

Pasinelli P, Brown RH: Molecular biology of amyotrophic lateral sclerosis: insights from genetics. Nat Rev Neurosci 2006, 7:710–723.

Pasinetti GM. Treatment of Amyotrophic Lateral Sclerosis with nimesulide. 2006 US0041022 a1.

Pattee GL, Post GR, Gerber RE, Bennett JPJ. Reduction of oxidative stress in amyotrophi lateral sclerosis following pramipexole treatment. Amyotroph Lateral Scler Other Motor Neuron Disord. 2003; 4(2):90–95.

Payne BA, Chinnery PF. Mitochondrial dysfunction in aging: much progress but many unresolved questions. Biochimica et Biophysica Acta (BBA)-Bioenergetics. 2015 Nov 1;1847(11):1347-53.

Peavy RD, Conn PJ. Phosphorylation of mitogen-activated protein kinase in cultured rat cortical glia by stimulation of metabotropic glutamate receptors. Journal of neurochemistry. 1998 Aug;71(2):603-12.

Pegoretti V, Swanson KA, Bethea JR, Probert L, Eisel UL, Fischer R. Inflammation and Oxidative Stress in Multiple Sclerosis: Consequences for Therapy Development. Oxidative Medicine and Cellular Longevity. 2020 May 12;2020.

Perry TL, Krieger C, Hansen S, Eisen A. Amyotrophic lateral sclerosis: amino acid levels in plasma and cerebrospinal fluid. Annals of neurology. 1990 Jul;28(1):12-7.

Petri S, Körner S, Kiaei M. Nrf2/ARE signaling pathway: key mediator in oxidative stress and potential therapeutic target in ALS. Neurology research international. 2012 Oct;2012.

Petri S, Körner S, Kiaei M. Nrf2/ARE Signaling Pathway: Key Mediator in Oxidative Stress and Potential Therapeutic Target in ALS. Neurol Res Int. 2012;2012:878030.

Phukan J, Pender NP, Hardiman O. Cognitive impairment in amyotrophic lateral sclerosis. Lancet Neurol 2007; 6: 994–1003.

Picher-Martel V, Valdmanis PN, Gould PV, Julien JP, Dupré N. From animal models to human disease: a genetic approach for personalized medicine in ALS. Acta neuropathologica communications. 2016 Dec;4(1):1-29.

Pierre K, Pellerin L. Monocarboxylate transporters in the central nervous system: distribution, regulation and function. Journal of neurochemistry. 2005 Jul;94(1):1-4.

Pin JP, Galvez T, Prézeau L. Evolution, structure, and activation mechanism of family 3/C G-protein-coupled receptors. Pharmacology & therapeutics. 2003 Jun 1;98(3):325-54.

Pinteaux-Jones F, Sevastou IG, Fry VA, Heales S, Baker D, Pocock JM. Myelin-induced microglial neurotoxicity can be controlled by microglial metabotropic glutamate receptors. Journal of neurochemistry. 2008 Jul;106(1):442-54.

Planas-Fontánez TM, Dreyfus CF, Saitta KS. Reactive astrocytes as therapeutic targets for brain degenerative diseases: roles played by metabotropic glutamate receptors. Neurochemical research. 2020 Mar;45(3):541-50.

Pollari E, Goldsteins G, Bart G, Koistinaho J, Giniatullin R. The role of oxidative stress in degeneration of the neuromuscular junction in amyotrophic lateral sclerosis. Frontiers in cellular neuroscience. 2014 May 13;8:131.

Popescu IR, Nicaise C, Liu S, Bisch G, Knippenberg S, Daubie V, Bohl D, Pochet R. Neural progenitors derived from human induced pluripotent stem cells survive and differentiate upon transplantation into a rat model of amyotrophic lateral sclerosis. Stem Cells Transl Med. 2013; 2(3):167–174.

Pramatarova A, Laganière J, Roussel J, Brisebois K, Rouleau GA. Neuron-specific expression of mutant superoxide dismutase 1 in transgenic mice does not lead to motor impairment. Journal of Neuroscience. 2001 May 15;21(10):3369-74.

Prehn JH, Lippert K, Krieglstein J. Are NMDA or AMPA/kainate receptor antagonists more efficacious in the delayed treatment of excitotoxic neuronal injury?. European Journal of Pharmacology: Environmental Toxicology and Pharmacology. 1995 Jan 13;292(2):179-89.

Prézeau L, Gomeza J, Ahern S, Mary S, Galvez T, Bockaert J, Pin JP. Changes in the carboxyl-terminal domain of metabotropic glutamate receptor 1 by alternative splicing generate receptors with differing agonist-independent activity. Molecular pharmacology. 1996 Mar 1;49(3):422-9.

Pringle CE, Hudson AJ, Munoz DG, Kiernan JA, Brown WF, Ebers GC. Primary lateral sclerosis. Clinical features, neuropathology and diagnostic criteria. Brain 1992; 115: 495–520.

Puls I, Jonnakuty C, LaMonte BH, Holzbaur EL, Tokito M, Mann E, Floeter MK, Bidus K, Drayna D, Oh SJ, Brown RH Jr, Ludlow CL, Fischbeck KH: Mutant dynactin in motor neuron disease. Nat Genet 2003, 33:455–456.

Pulst SM, Nechiporuk A, Nechiporuk T, Gispert S, Chen XN, Lopes-Cendes I, Pearlman S, Starkman S, Orozco-Diaz G, Lunkes A, DeJong P. Moderate expansion of a normally biallelic trinucleotide repeat in spinocerebellar ataxia type 2. Nature genetics. 1996 Nov;14(3):269-76.

Pupillo E, Poloni M, Bianchi E, *et al*. Trauma and amyotrophic lateral sclerosis: a European population-based case–control study from the EURALS consortium. Amyotroph Lateral Scler Frontotemporal Degener 2018; 19: 118–125.

Qian K, Huang H, Peterson A, Hu B, Maragakis NJ, Ming GL, Chen H, Zhang SC. Sporadic ALS astrocytes induce neuronal degeneration in vivo. Stem cell reports. 2017 Apr 11;8(4):843-55.

Qiu L, Qiao T, Beers M, Tan W, Wang H, Yang B, Xu Z: Widespread aggregation of mutant VAPB associated with ALS does not cause motor neuron degeneration or modulate mutant SOD1 aggregation and toxicity in mice. Mol Neurodegener 2013, 8:1.

Quiroz JA, Tamburri P, Deptula D, Banken L, Beyer U, Rabbia M, Parkar N, Fontoura P, Santarelli L. Efficacy and safety of basimglurant as adjunctive therapy for major depression: a randomized clinical trial. JAMA psychiatry. 2016 Jul 1;73(7):675-84.

Raab S, Plate KH. Different networks, common growth factors: shared growth factors and receptors of the vascular and the nervous system. Acta neuropathologica. 2007 Jun 1;113(6):607-26.

Rademakers R, Neumann M, Mackenzie IR: Advances in understanding the molecular basis of frontotemporal dementia. Nat Rev Neurol 2012, 8:423–434.

Raiteri M. Presynaptic metabotropic glutamate and GABA B receptors. Pharmacology of Neurotransmitter Release. 2008:373-407.

Ravenscroft TA, Pottier C, Murray ME, Baker M, Christopher E, Levitch D, Brown PH, Barker W, Duara R, Greig-Custo M, Betancourt A. The presenilin 1 p. Gly206Ala mutation is a frequent cause of early-ons*et al*zheimer's disease in Hispanics in Florida. American journal of neurodegenerative disease. 2016;5(1):94.

Ravera S, Bertola N, Pasquale C, Bruno S, Benedicenti S, Ferrando S, Zekiy A, Arany P, Amaroli A. 808-nm Photobiomodulation Affects the Viability of a Head and Neck Squamous Carcinoma Cellular Model, Acting on Energy Metabolism and Oxidative Stress Production. Biomedicines. 2021 Nov;9(11):1717.

Ravera S, Bonifacino T, Bartolucci M, Milanese M, Gallia E, Provenzano F, Cortese K, Panfoli I, Bonanno G. Characterization of the Mitochondrial Aerobic Metabolism in the Pre-and Perisynaptic Districts of the SOD1 G93A Mouse Model of Amyotrophic Lateral Sclerosis. Molecular neurobiology. 2018 Dec;55(12):9220-33.

Ravits JM, La Spada AR. ALS motor phenotype heterogeneity, focality, and spread: deconstructing motor neuron degeneration. Neurology 2009; 73: 805–811.

Re DB, Le Verche V, Yu C, Amoroso MW, Politi KA, Phani S, Ikiz B, Hoffmann L, Koolen M, Nagata T, Papadimitriou D. Necroptosis drives motor neuron death in models of both sporadic and familial ALS. Neuron. 2014 Mar 5;81(5):1001-8.

Redza-Dutordoir M, Averill-Bates DA. Activation of apoptosis signalling pathways by reactive oxygen species. BiochimBiophys Acta. 2016 Dec;1863(12):2977-2992.

Reid ME, Toms NJ, Bedingfield JS, Roberts PJ. Group I mGlu receptors potentiate synaptosomal [3H] glutamate release independently of exogenously applied arachidonic acid. Neuropharmacology. 1999 Apr 1;38(4):477-85.

Reilmann R, Rouzade-Dominguez ML, Saft C, Süssmuth SD, Priller J, Rosser A, Rickards H, Schöls L, Pezous N, Gasparini F, Johns D. A randomized, placebo-controlled trial of AFQ056 for the treatment of chorea in Huntington's disease. Movement Disorders. 2015 Mar;30(3):427-31.

Renton AE, Majounie E, Waite A, Simón-Sánchez J, Rollinson S, Gibbs JR, Schymick JC, Laaksovirta H, Van Swieten JC, Myllykangas L, Kalimo H. A hexanucleotide repeat expansion in C9ORF72 is the cause of chromosome 9p21-linked ALS-FTD. Neuron. 2011 Oct 20;72(2):257-68.

Rezania K, Yan J, Dellefave L, Deng HX, Siddique N, Pascuzzi RT, Siddique T, Roos RP: A rare Cu/Zn superoxide dismutase mutation causing familial amyotrophic lateral sclerosis with variable age of onset, incomplete penetrance and a sensory neuropathy. Amyotroph Lateral Scler Other Motor Neuron Disord 2003, 4:162–166.

Ribeiro FM, Hamilton A, Doria JG, Guimaraes IM, Cregan SP, Ferguson SS. Metabotropic glutamate receptor 5 as a potential therapeutic target in Huntington's disease. Expert opinion on therapeutic targets. 2014 Nov 1;18(11):1293-304.

Riedel WJ, Jolles J. Cognition enhancers in age-related cognitive decline. Drugs Aging. 1996; 8(4):245–274

Riganti C, Gazzano E, Polimeni M, Aldieri E, Ghigo D. The pentose phosphate pathway: an antioxidant defense and a crossroad in tumor cell fate. Free Radical Biology and Medicine. 2012 Aug 1;53(3):421-36.

Rinholm JE, Hamilton NB, Kessaris N, Richardson WD, Bergersen LH, Attwell D. Regulation of oligodendrocyte development and myelination by glucose and lactate. Journal of Neuroscience. 2011 Jan 12;31(2):538-48.

Rizzuto R, De Stefani D, Raffaello A, Mammucari C. Mitochondria as sensors and regulators of calcium signalling. Nature reviews Molecular cell biology. 2012 Sep;13(9):566-78.

Robertson J, Doroudchi MM, Nguyen MD, Durham HD, Strong MJ, Shaw G, Julien J-P, Mushynski WE: A neurotoxic peripherin splice variant in a mouse model of ALS. J Cell Biol 2003, 160:939–949.

Rojas F, Cortes N, Abarzua S, Dyrda A, Van Zundert BA. Astrocytes expressing mutant SOD1 and TDP43 trigger motoneuron death that is mediated via sodium channels and nitroxidative stress. Frontiers in cellular neuroscience. 2014 Feb 7;8:24.

Rosen DR, Siddique T, Patterson D, *et al*. Mutations in Cu/Zn superoxide dismutase gene are associated with familial amyotrophic lateral sclerosis. Nature 1993; 362: 59–62.

Rosen DR, Siddique T, Patterson D, Figlewicz DA, Sapp P, Hentati A, Donaldson D, Goto J, O'Regan JP, Deng HX, Rahmani Z. Mutations in Cu/Zn superoxide dismutase gene are associated with familial amyotrophic lateral sclerosis. Nature. 1993 Mar;362(6415):59-62.

Rosenblum LT, Shamamandri-Markandaiah S, Ghosh B, Foran E, Lepore AC, Pasinelli P, Trotti D. Mutation of the caspase-3 cleavage site in the astroglial glutamate transporter EAAT2 delays disease progression and extends lifespan in the SOD1-G93A mouse model of ALS. Experimental neurology. 2017 Jun 1;292:145-53.

Ross OA, Rutherford NJ, Baker M, Soto-Ortolaza AI, Carrasquillo MM, DeJesus-Hernandez M, Adamson J, Li M, Volkening K, Finger E, Seeley WW. Ataxin-2 repeat-length variation and neurodegeneration. Human molecular genetics. 2011 Aug 15;20(16):3207-12.

Rossi D, Brambilla L, Valori CF, Roncoroni C, Crugnola A, Yokota T, Bredesen DE, Volterra A. Focal degeneration of astrocytes in amyotrophic lateral sclerosis. Cell Death & Differentiation. 2008 Nov;15(11):1691-700.

Rossi D, Volterra A. Astrocytic dysfunction: insights on the role in neurodegeneration. Brain research bulletin. 2009 Oct 28;80(4-5):224-32.

Rothstein JD, Dykes-Hoberg M, Pardo CA, Bristol LA, Jin L, Kuncl RW, Kanai Y, Hediger MA, Wang Y, Schielke JP, Welty DF. Knockout of glutamate transporters reveals a major role for astroglial transport in excitotoxicity and clearance of glutamate. Neuron. 1996 Mar 1;16(3):675-86.

Rothstein JD, Patel S, Regan MR, Haenggeli C, Huang YH, Bergles DE, Jin L, Dykes Hoberg M, Vidensky S, Chung DS, Toan SV, Bruijn LI, Su ZZ, Gupta P, Fisher PB.

Beta-lactam antibiotics offer neuroprotection by increasing glutamate transporter expression. Nature. 2005; 433(7021): 73–77.

Rothstein JD, Patel S, Regan MR, Haenggeli C, Huang YH, Bergles DE, Jin L, Hoberg MD, Vidensky S, Chung DS, Toan SV. β-Lactam antibiotics offer neuroprotection by increasing glutamate transporter expression. Nature. 2005 Jan;433(7021):73-7.

Rothstein JD, Van Kammen M, Levey AI, Martin LJ, Kuncl RW. Selective loss of glial glutamate transporter GLT-1 in amyotrophic lateral sclerosis. Ann Neurol. 1995; 38(1):73–84.

Rothstein JD, Van Kammen M, Levey AI, Martin LJ, Kuncl RW. Selective loss of glial glutamate transporter GLT-1 in amyotrophic lateral sclerosis. Annals of Neurology: Official Journal of the American Neurological Association and the Child Neurology Society. 1995 Jul;38(1):73-84.

Rowland LP, Shneider NA. Amyotrophic lateral sclerosis. N Engl J Med. 2001; 344(22):1688–1700.

Ryan M, Heverin M, McLaughlin RL, Hardiman O. Lifetime risk and heritability of amyotrophic lateral sclerosis. JAMA Neurol 2019; 76: 1367.

Saeed M, Siddique N, Hung WY, Usacheva E, Liu E, Sufit RL, Heller SL, Haines JL, Pericak-Vance M, Siddique T: Paraoxonase cluster polymorphisms are associated with sporadic ALS. Neurology 2006, 67:771–776.

Sakaguchi T, Irie T, Kawabata R, Yoshida A, Maruyama H, Kawakami H: Optineurin with amyotrophic lateral sclerosis-related mutations abrogates inhibition of interferon regulatory factor-3 activation. Neurosci Lett 2011, 505:279–281.

Sanpei K, Takano H, Igarashi S, Sato T, Oyake M, Sasaki H, Wakisaka A, Tashiro K, Ishida Y, Ikeuchi T, Koide R. Identification of the spinocerebellar ataxia type 2 gene using a direct identification of repeat expansion and cloning technique, DIRECT. Nature genetics. 1996 Nov;14(3):277-84.

Sapp PC, Hosler BA, McKenna-Yasek D, Chin W, Gann A, Genise H, Gorenstein J, Huang M, Sailer W, Scheffler M, Valesky M, Haines JL, Pericak-Vance M, Siddique T, Horvitz HR, Brown RH Jr: Identification of two novel loci for dominantly inherited familial amyotrophic lateral sclerosis. Am J Hum Genet 2003, 73:397–403.

Sarlette A, Krampfl K, Grothe C, Neuhoff Nv, Dengler R, Petri S. Nuclear erythroid 2-related factor 2-antioxidative response element signaling pathway in motor cortex and spinal cord in amyotrophic lateral sclerosis. J Neuropathol Exp Neurol. 2008 Nov;67(11):1055-62.

Sasabe J, Miyoshi Y, Suzuki M, Mita M, Konno R, Matsuoka M, Hamase K, Aiso S: D-amino acid oxidase controls motoneuron degeneration through D-serine. Proc Natl Acad Sci USA 2012, 109:627–632.

Sasaki S, Iwata M. Ultrastructural change of synapses of Betz cells in patients with amyotrophic lateral sclerosis. Neuroscience letters. 1999 Jun 11;268(1):29-32.

Sau D, De Biasi S, Vitellaro-Zuccarello L, Riso P, Guarnieri S, Porrini M, Simeoni S, Crippa V, Onesto E, Palazzolo I, Rusmini P. Mutation of SOD1 in ALS: a gain of a loss of function. Human molecular genetics. 2007 Jul 1;16(13):1604-18.

Scekic-Zahirovic J, El Oussini H, Mersmann S, Drenner K, Wagner M, Sun Y, Allmeroth K, Dieterlé S, Sinniger J, Dirrig-Grosch S, René F. Motor neuron intrinsic and extrinsic mechanisms contribute to the pathogenesis of FUS-associated amyotrophic lateral sclerosis. Acta neuropathologica. 2017 Jun 1;133(6):887-906.

Schinkmann KA, Kim TA, Avraham S. Glutamate-stimulated activation of DNA synthesis via mitogen-activated protein kinase in primary astrocytes: involvement of protein kinase C and related adhesion focal tyrosine kinase. Journal of neurochemistry. 2000 May;74(5):1931-40.

Schoepp DD. Unveiling the functions of presynaptic metabotropic glutamate receptors in the central nervous system. Journal of Pharmacology and Experimental Therapeutics. 2001 Oct 1;299(1):12-20.

Schrooten M, Smetcoren C, Robberecht W, Van Damme P. Benefit of the Awaji diagnostic algorithm for amyotrophic lateral sclerosis: a prospective study. Ann Neurol 2011; 70: 79–83.

Schwab C, Yu S, McGeer EG, McGeer PL: Optineurin in Huntington's disease intranuclear inclusions. Neurosci Lett 2012, 506:149–154.

Schwartz G and Fehlings MG. Secondary injury mechanisms of spinal cord trauma: A novel therapeutic approach for the management of secondary pathophysiology with the sodium channel blocker riluzole. Prog Brain Res.2002; 137:177-90.

Schymick JC, Yang Y, Andersen PM, Vonsattel JP, Greenway M, Momeni P, Elder J, Chiò A, Restagno G, Robberecht W, Dahlberg C, Mukherjee O, Goate A, Graff-Radford N, Caselli RJ, Hutton M, Gass J, Cannon A, Rademakers R, Singleton AB, Hardiman O, Rothstein J, Hardy J, Traynor BJ: Progranulin mutations and amyotrophic lateral sclerosis or amyotrophic lateral sclerosis-frontotemporal dementia phenotypes. J Neurol Neurosurg Psychiatry 2007, 78:754–756.

Scussolini M, Bauckneht M, Cossu V, Bruno S, Orengo AM, Piccioli P, Capitanio S, Yosifov N, Ravera S, Morbelli S, Piana M. G6Pase location in the endoplasmic reticulum: Implications on compartmental analysis of FDG uptake in cancer cells. Scientific reports. 2019 Feb 26;9(1):1-4.

Seilhean D, Cazeneuve C, Thuriès V, Russaouen O, Millecamps S, Salachas F, Meininger V, LeGuern E, Duyckaerts C. Accumulation of TDP-43 and α-actin in an amyotrophic lateral sclerosis patient with the K17I ANG mutation. Acta neuropathologica. 2009 Oct 1;118(4):561-73.

Sellier C, Campanari ML, Julie Corbier C, Gaucherot A, Kolb-Cheynel I, Oulad-Abdelghani M, Ruffenach F, Page A, Ciura S, Kabashi E, Charlet-Berguerand N. Loss of C9 ORF 72 impairs autophagy and synergizes with polyQ Ataxin-2 to induce motor neuron dysfunction and cell death. The EMBO journal. 2016 Jun 15;35(12):1276-97.

Sequeiros J, Seneca S, Martindale J. Consensus and controversies in best practices for molecular genetic testing of spinocerebellar ataxias. European Journal of Human Genetics. 2010 Nov;18(11):1188-95.

Serrano A, Donno C, Giannetti S, Perić M, Andjus P, D'Ambrosi N, Michetti F. The astrocytic S100B protein with its receptor RAGE is aberrantly expressed in SOD1G93A models, and its inhibition decreases the expression of proinflammatory genes. Mediators of inflammation. 2017 Oct;2017.

Shah A, Silverstein PS, Singh DP, Kumar A. Involvement of metabotropic glutamate receptor 5, AKT/PI3K signaling and NF-κB pathway in methamphetamine-mediated increase in IL-6 and IL-8 expression in astrocytes. Journal of neuroinflammation. 2012 Dec;9(1):1-0.

Shefner JM, Al-Chalabi A, Baker MR, *et al*. A proposal for new diagnostic criteria for ALS. Clin Neurophysiol 2020; 131: 1975–1978.

Shi P, Gal J, Kwinter DM, Liu X, Zhu H. Mitochondrial dysfunction in amyotrophic lateral sclerosis. Biochimica et Biophysica Acta (BBA)-Molecular Basis of Disease. 2010 Jan 1;1802(1):45-51.

Shodai A, Morimura T, Ido A, Uchida T, Ayaki T, Takahashi R, Kitazawa S, Suzuki S, Shirouzu M, Kigawa T, Muto Y. Aberrant assembly of RNA recognition motif 1 links to pathogenic conversion of TAR DNA-binding protein of 43 kDa (TDP-43). Journal of Biological Chemistry. 2013 May 24;288(21):14886-905.

Siciliano G, D'Avino C, Corona AD, Barsacchi R, Kusmic C, Rocchi A, Pastorini E, Murri L. Impaired oxidative metabolism and lipid peroxidation in exercising muscle from ALS patients. Amyotrophic Lateral Sclerosis and Other Motor Neuron Disorders. 2002 Jan 1;3(2):57-62.

Sies H. Oxidative stress: a concept in redox biology and medicine. Redox biology. 2015 Apr 1;4:180-3.

Simon NG, Lomen-Hoerth C, Kiernan MC. Patterns of clinical and electrodiagnostic abnormalities in early amyotrophic lateral sclerosis. Muscle Nerve 2014; 50: 894–899.

Singh A, Kukreti R, Saso L, Kukreti S. Oxidative stress: a key modulator in neurodegenerative diseases. Molecules. 2019 Jan;24(8):1583.

Skibinski G, Parkinson NJ, Brown JM, Chakrabarti L, Lloyd SL, Hummerich H, Nielsen JE, Hodges JR, Spillantini MG, Thusgaard T, Brandner S, Brun A, Rossor MN, Gade A, Johannsen P, Sørensen SA, Gydesen S, Fisher EM, Collinge J: Mutations in the endosomal ESCRTIII-complex subunit CHMP2B in frontotemporal dementia. Nat Genet 2005, 37:806–808.

Skourti-Stathaki K, Proudfoot NJ, Gromak N: Human senataxin resolves RNA/DNA hybrids formed at transcriptional pause sites to promote Xrn2-dependent termination. Mol Cell 2011, 42:794–805.

Sokoloff L, Reivich M, Kennedy C, Des Rosiers MH. Patlak. CS, Pettigrew, KD, Sakurada, O. and Shinohara, M.(1977) The [~ 4C] deoxyglucose method for the measurement of local cerebral glucose utilization: theory, procedure, and normal values in the conscious and anesthetized albino rat. J. Neurochem.;28:897-916.

Soo KY, Halloran M, Sundaramoorthy V, Parakh S, Toth RP, Southam KA, McLean CA, Lock P, King A, Farg MA, Atkin JD. Rab1-dependent ER–Golgi transport dysfunction

is a common pathogenic mechanism in SOD1, TDP-43 and FUS-associated ALS. Acta neuropathologica. 2015 Nov;130(5):679-97.

Spector R, Johanson CE. Vitamin transport and homeostasis in mammalian brain: focus on Vitamins B and E. Journal of neurochemistry. 2007 Oct;103(2):425-38.

Sreedharan J, Blair IP, Tripathi VB, Hu X, Vance C, Rogelj B, Ackerley S, Durnall JC, Williams KL, Buratti E, Baralle F, de Belleroche J, Mitchell JD, Leigh PN, Al-Chalabi A, Miller CC, Nicholson G, Shaw CE: TDP-43 mutations in familial and sporadic amyotrophic lateral sclerosis. Science 2008, 319:1668–1672.

Stevanin G, Santorelli FM, Azzedine H, Coutinho P, Chomilier J, Denora PS, Martin E, Ouvrard-Hernandez AM, Tessa A, Bouslam N, Lossos A, Charles P, Loureiro JL, Elleuch N, Confavreux C, Cruz VT, Ruberg M, Leguern E, Grid D, Tazir M, Fontaine B, Filla A, Bertini E, Durr A, Brice A: Mutations in SPG11, encoding spatacsin, are a major cause of spastic paraplegia with thin corpus callosum. Nat Genet 2007, 39:366–372.

Stoica R, Paillusson S, Gomez-Suaga P, Mitchell JC, Lau DH, Gray EH, Sancho RM, Vizcay-Barrena G, De Vos KJ, Shaw CE, Hanger DP. ALS/FTD-associated FUS activates GSK-3β to disrupt the VAPB–PTPIP 51 interaction and ER–mitochondria associations. EMBO reports. 2016 Sep;17(9):1326-42.

Storkebaum E: Treatment of motoneuron degeneration by intracerebroventricular delivery of VEGF in a rat model of ALS. Nat Neurosci 2005, 8:85–92.

Strong MJ, Abrahams S, Goldstein LH, *et al*. Amyotrophic lateral sclerosis – frontotemporal spectrum disorder (ALS-FTSD): revised diagnostic criteria. Amyotroph Lateral Scler Frontotemporal Degener. 2017; 18: 153–174.

Suh HS, Zhao ML, Derico L, Choi N, Lee SC. Insulin-like growth factor 1 and 2 (IGF1, IGF2) expression in human microglia: differential regulation by inflammatory mediators. Journal of neuroinflammation. 2013 Dec;10(1):1-2.

Sullivan PG, Rabchevsky AG, Keller JN, Lovell M, Sodhi A, Hart RP, Scheff SW. Intrinsic differences in brain and spinal cord mitochondria: Implication for therapeutic interventions. Journal of Comparative Neurology. 2004 Jul 5;474(4):524-34.

Syková E, Chvátal A. Extracellular ionic and volume changes: The role in glia—Neuron interaction. Journal of chemical neuroanatomy. 1993 Jul 1;6(4):247-60.

Szymański J, Janikiewicz J, Michalska B, Patalas-Krawczyk P, Perrone M, Ziółkowski W, Duszyński J, Pinton P, Dobrzyń A, Więckowski MR. Interaction of mitochondria with the endoplasmic reticulum and plasma membrane in calcium homeostasis, lipid trafficking and mitochondrial structure. International Journal of Molecular Sciences. 2017 Jul;18(7):1576.

Takagi N, Besshoh S, Marunouchi T, Takeo S, Tanonaka K. Metabotropic glutamate receptor 5 activation enhances tyrosine phosphorylation of the N-methyl-D-aspartate (NMDA) receptor and NMDA-induced cell death in hippocampal cultured neurons. Biological and Pharmaceutical Bulletin. 2012 Dec 1;35(12):2224-9.

Takeuchi S, Fujiwara N, Ido A, Oono M, Takeuchi Y, Tateno M, Suzuki K, Takahashi R, Tooyama I, Taniguchi N, Julien JP, Urushitani M. Induction of protective immunity by vaccination with wild-type apo superoxide dismutase 1 in mutant SOD1 transgenic mice. J Neuropathol Exp Neurol. 2010; 69(10):1044–1056

Tardy M, Fages C, Le Prince G, Rolland B, Nunez J. Regulation of the glial fibrillary acidic protein (GFAP) and of its encoding mRNA in the developing brain and in cultured astrocytes. Molecular aspects of development and aging of the nervous system. 1990:41-52.

Taylor JP, Brown RH, Cleveland DW. Decoding ALS: from genes to mechanism. Nature. 2016 Nov;539(7628):197-206.

Taylor, J.P., Brown, R.H., Jr., and Cleveland, D.W. (2016). Decoding ALS: from genes to mechanism. Nature 539, 197–206.

Tefera TW, Borges K. Metabolic dysfunctions in amyotrophic lateral sclerosis pathogenesis and potential metabolic treatments. Frontiers in neuroscience. 2017 Jan 10;10:611.

Teuling E, Ahmed S, Haasdijk E, Demmers J, Steinmetz MO, Akhmanova A, Jaarsma D, Hoogenraad CC: Motor neuron disease-associated mutant vesicle-associated membrane protein-associated protein (VAP) B recruits wild-type VAPs into endoplasmic reticulum-derived tubular aggregates. J Neurosci 2007, 27:9801–9815.

Thandi S, Blank JL, Challiss RJ. Group-I metabotropic glutamate receptors, mGlu1a and mGlu5a, couple to extracellular signal-regulated kinase (ERK) activation via distinct, but overlapping, signalling pathways. Journal of neurochemistry. 2002 Dec;83(5):1139-53.

Thurfjell L, Lilja J, Lundqvist R, Buckley C, Smith A, Vandenberghe R, Sherwin P. Automated quantification of 18F-flutemetamol PET activity for categorizing scans as negative or positive for brain amyloid: concordance with visual image reads. Journal of Nuclear Medicine. 2014 Oct 1;55(10):1623-8.

Ticozzi N, LeClerc AL, Keagle PJ, Glass JD, Wills AM, van Blitterswijk M, Bosco DA, Rodriguez-Leyva I, Gellera C, Ratti A, Taroni F, McKenna-Yasek D, Sapp PC, Silani V, Furlong CE, Brown RH Jr, Landers JE: Paraoxonase gene mutations in amyotrophic lateral sclerosis. Ann Neurol 2010, 68:102–107.

Tollervey JR, Curk T, Rogelj B, Briese M, Cereda M, Kayikci M, König J, Hortobágyi T, Nishimura AL, Župunski V, Patani R. Characterizing the RNA targets and position-dependent splicing regulation by TDP-43. Nature neuroscience. 2011 Apr;14(4):452-8.

Tortarolo M, Grignaschi G, Calvaresi N, Zennaro E, Spaltro G, Colovic M, Fracasso C, Guiso G, Elger B, Schneider H, Seilheimer B, Caccia S, Bendotti C. Glutamate AMPA receptors change in motor neurons of SOD1G93A transgenic mice and their inhibition by a noncompetitive antagonist ameliorates the progression of amytrophic lateral sclerosis-like disease. J Neurosci Res. 2006; 83(1):134–146.

Townley, R. A., Boeve, B. F., & Benarroch, E. E. (2018). Progranulin: Functions and neurologic correlations. Neurology, 90(3), 118–125.

Tradewell ML, Yu Z, Tibshirani M, Boulanger MC, Durham HD, Richard S. Arginine methylation by PRMT1 regulates nuclear-cytoplasmic localization and toxicity of FUS/TLS harbouring ALS-linked mutations. Human molecular genetics. 2012 Jan 1;21(1):136-49.

Trenkwalder C, Stocchi F, Poewe W, Dronamraju N, Kenney C, Shah A, von Raison F, Graf A. Mavoglurant in Parkinson's patients with l-Dopa-induced dyskinesias: Two randomized phase 2 studies. Movement Disorders. 2016 Jul;31(7):1054-8.

Tripathi P, Rodriguez-Muela N, Klim JR, de Boer AS, Agrawal S, Sandoe J, Lopes CS, Ogliari KS, Williams LA, Shear M, Rubin LL. Reactive astrocytes promote ALS-like degeneration and intracellular protein aggregation in human motor neurons by disrupting autophagy through TGF-β1. Stem cell reports. 2017 Aug 8;9(2):667-80.

Tsacopoulos M, Magistretti PJ. Metabolic coupling between glia and neurons. Journal of Neuroscience. 1996 Feb 1;16(3):877-85.

Tsao W, Jeong YH, Lin S, Ling J, Price DL, Chiang PM, Wong PC: Rodent models of TDP-43: recent advances. Brain Res 2012, 1462:26–39.

Tudor EL, Galtrey CM, Perkinton MS, Lau KF, De Vos KJ, Mitchell JC, Ackerley S, Hortobágyi T, Vámos E, Leigh PN, Klasen C, McLoughlin DM, Shaw CE, Miller CC: Amyotrophic lateral sclerosis mutant vesicle-associated membrane protein-associated protein-B transgenic mice develop TAR-DNA -binding protein-43 pathology. Neuroscience 2010, 167:774–785.

Turner MR, Hardiman O, Benatar M, Brooks BR, Chio A, de Carvalho M, Ince PG, Lin C, Miller RG, Mitsumoto H, Nicholson G, Ravits J, Shaw PJ, Swash M, Talbot K, Traynor BJ, Van den Berg LH, Veldink JH, Vucic S, Kiernan MC: Controversies and priorities in amyotrophic lateral sclerosis. Lancet Neurol 2013, 12:310–322.

Turner MR, Wicks P, Brownstein CA, *et al*. Concordance between site of onset and limb dominance inamyotrophic lateral sclerosis. J Neurol Neurosurg Psychiatry 2011; 82: 853–854.

Tyzack GE, Hall CE, Sibley CR, Cymes T, Forostyak S, Carlino G, Meyer IF, Schiavo G, Zhang SC, Gibbons GM, Newcombe J. A neuroprotective astrocyte state is induced by neuronal signal EphB1 but fails in ALS models. Nature communications. 2017 Oct 27;8(1):1-7.

Uccelli A, Milanese M, Principato MC, Morando S, Bonifacino T, Vergani L, Giunti D, Voci A, Carminati E, Giribaldi F, Caponnetto C, Bonanno G. Intravenous mesenchymal stem cells improve survival and motor function in experimental amyotrophic lateral sclerosis. Mol Med. 2012; 18:794–804.

Uday B, Dipak D, Ranajit BK. Reactive oxygen species: Oxidative damage and pathogenesis. Curr. Sci. 1990, 77, 658–666

Ure J, Baudry M, Perassolo M. Metabotropic glutamate receptors and epilepsy. Journal of the neurological sciences. 2006 Aug 15;247(1):1-9.

Valdmanis PN, Kabashi E, Dyck A, Hince P, Lee J, Dion P, D'Amour M, Souchon F, Bouchard JP, Salachas F, Meininger V, Andersen PM, Camu W, Dupré N, Rouleau GA: Association of paraoxonase gene cluster polymorphisms with ALS in France, Quebec, and Sweden. Neurology 2008, 71:514–520.

Valenti O, Conn PJ, Marino MJ. Distinct physiological roles of the Gq-coupled metabotropic glutamate receptors co-expressed in the same neuronal populations. Journal of cellular physiology. 2002 May;191(2):125-37.

van Blitterswijk M, DeJesus-Hernandez M, Rademakers R: How do C9ORF72 repeat expansions cause amyotrophic lateral sclerosis and frontotemporal dementia: can we learn from other noncoding repeat expansion disorders? Curr Opin Neurol 2012, 25:689–700.

van Blitterswijk M, van Es MA, Hennekam EA, *et al*. Evidence for an oligogenic basis of amyotrophic lateral sclerosis. Hum Mol Genet 2012; 21: 3776–3784.

Van Den Bosch L, Van Damme P, Bogaert E, Robberecht W. The role of excitotoxicity in the pathogenesis of amyotrophic lateral sclerosis. Biochimica et Biophysica Acta (BBA)-Molecular Basis of Disease. 2006 Nov 1;1762(11-12):1068-82.

Van Den Bosch L, Vandenberghe W, Klaassen H, Van Houtte E, Robberecht W. Ca2+-permeable AMPA receptors and selective vulnerability of motor neurons. Journal of the neurological sciences. 2000 Nov 1;180(1-2):29-34.

van den Heuvel DM, Harschnitz O, van den Berg LH, Pasterkamp RJ. Taking a risk: a therapeutic focus on ataxin-2 in amyotrophic lateral sclerosis. Trends in molecular medicine. 2014 Jan 1;20(1):25-35.

van Es MA, Hardiman O, Chio A, Al-Chalabi A, Pasterkamp RJ, Veldink JH, Van den Berg LH. Amyotrophic lateral sclerosis. The Lancet. 2017 Nov 4;390(10107):2084-98.

van Es MA, Veldink JH, Saris CG, *et al*. Genome-wide association study identifies 19p13.3 (UNC13A) and 9p21.2 as susceptibility loci for sporadic amyotrophic lateral sclerosis. Nat Genet 2009; 41: 1083–1087.

van Vliet AR, Verfaillie T, Agostinis P. New functions of mitochondria associated membranes in cellular signaling. Biochimica et Biophysica Acta (BBA)-Molecular Cell Research. 2014 Oct 1;1843(10):2253-62.

Vance C, Rogelj B, Hortobágyi T, De Vos KJ, Nishimura AL, Sreedharan J, Hu X, Smith B, Ruddy D, Wright P, Ganesalingam J. Mutations in FUS, an RNA processing protein, cause familial amyotrophic lateral sclerosis type 6. Science. 2009 Feb 27;323(5918):1208-11.

Vance C, Rogelj B, Hortobagyi T, *et al*. Mutations in FUS, an RNA processing protein, cause familial amyotrophic lateral sclerosis type 6. Science 2009; 323: 1208–1211.

Varcianna A, Myszczynska MA, Castelli LM, O'Neill B, Kim Y, Talbot J, Nyberg S, Nyamali I, Heath PR, Stopford MJ, Hautbergue GM. Micro-RNAs secreted through astrocyte-derived extracellular vesicles cause neuronal network degeneration in C9orf72 ALS. EBioMedicine. 2019 Feb 1;40:626-35.

Vargas MR, Pehar M, Cassina P, Beckman JS, Barbeito L. Increased glutathione biosynthesis by Nrf2 activation in astrocytes prevents p75NTR-dependent motor neuron apoptosis. Journal of neurochemistry. 2006 May;97(3):687-96.

Vasko MR, Guo C, Thompson EL, Kelley MR: The repair function of the multifunctional DNA repair/redox protein APE1 is neuroprotective after ionizing radiation. DNA Repair (Amst) 2011, 10:942–952.

Veldink JH, Kalmijn S, Van der Hout AH, Lemmink HH, Groeneveld GJ, Lummen C, Scheffer H, Wokke JH, Van den Berg LH: SMN genotypes producing less SMN protein increase susceptibility to and severity of sporadic ALS. Neurology 2005, 65:820–825.

Veldink JH, Van den Berg LH, Cobben JM, Stulp RP, De Jong JM, Vogels OJ, Baas F, Wokke JH, Scheffer H. Homozygous deletion of the survival motor neuron 2 gene is a prognostic factor in sporadic ALS. Neurology. 2001 Mar 27;56(6):749-52.

Vergouts M, Doyen PJ, Peeters M, Opsomer R, Hermans E. Constitutive downregulation protein kinase C epsilon in hSOD1G93A astrocytes influences mGluR5 signaling and the regulation of glutamate uptake. Glia. 2018 Apr;66(4):749-61.

Verkhratsky A, Kirchhoff F. Glutamate-mediated neuronal–glial transmission. Journal of anatomy. 2007 Jun;210(6):651-60.

Verkhratsky A, Zorec R, Vermeiren C, Najimi M, Vanhoutte N, Tilleux S, De Hemptinne I, Maloteaux JM, Hermans E. Acute up-regulation of glutamate uptake mediated by mGluR5a in reactive astrocytes. Journal of neurochemistry. 2005 Jul;94(2):405-16.

Vickers NJ. Animal communication: when i'm calling you, will you answer too?. Current biology. 2017 Jul 24;27(14):R713-5.

Vijayvergiya C, Beal MF, Buck J, Manfredi G. Mutant superoxide dismutase 1 forms aggregates in the brain mitochondrial matrix of amyotrophic lateral sclerosis mice. Journal of Neuroscience. 2005 Mar 9;25(10):2463-70.

Villa F, Bruno S, Costa A, Li M, Russo M, Cimino J, Altieri P, Ruggeri C, Gorgun C, De Biasio P, Paladini D. The Human Fetal and Adult Stem Cell Secretome Can Exert Cardioprotective Paracrine Effects against Cardiotoxicity and Oxidative Stress from Cancer Treatment. Cancers. 2021 Jan;13(15):3729.

Viwatpinyo K, Chongthammakun S. Activation of group I metabotropic glutamate receptors leads to brain-derived neurotrophic factor expression in rat C6 cells. Neuroscience letters. 2009 Dec 25;467(2):127-30.

Volterra A, Meldolesi J. Astrocytes, from brain glue to communication elements: the revolution continues. Nature Reviews Neuroscience. 2005 Aug;6(8):626-40.

Wang SJ, Wang KY, Wang WC. Mechanisms underlying the riluzole inhibition of glutamate release from rat cerebral cortex nerve terminals (synaptosomes). Neuroscience. 2004;125(1):191-201.

Wang W, Li L, Lin WL, Dickson DW, Petrucelli L, Zhang T, Wang X. The ALS disease-associated mutant TDP-43 impairs mitochondrial dynamics and function in motor neurons. Hum Mol Genet. 2013 Dec 1;22(23):4706-19.

Wang W, Wang L, Lu J, Siedlak SL, Fujioka H, Liang J, Jiang S, Ma X, Jiang Z, Da Rocha EL, Sheng M. The inhibition of TDP-43 mitochondrial localization blocks its neuronal toxicity. Nature medicine. 2016 Aug;22(8):869-78.

Watanabe M, Dykes-Hoberg M, Culotta VC, Price DL, Wong PC, Rothstein JD. Histological evidence of protein aggregation in mutant SOD1 transgenic mice and in amyotrophic lateral sclerosis neural tissues. Neurobiol Dis. 2001; 8(6):933–941.

Webster CP, Smith EF, Bauer CS, *et al*. The C9orf72 protein interacts with Rab1a and the ULK1 complex to regulate initiation of autophagy. EMBO J 2016; 35: 1656–1676.

Webster JM, Darling AL, Uversky VN, Blair LJ. Small heat shock proteins, big impact on protein aggregation in neurodegenerative disease. Frontiers in pharmacology. 2019 Sep 18;10:1047.

Weiduschat N, Mao X, Hupf J, Armstrong N, Kang G, Lange DJ, Mitsumoto H, Shungu DC. Motor cortex glutathione deficit in ALS measured in vivo with the J-editing technique. Neuroscience letters. 2014 Jun 6;570:102-7.

Weydt P, Yuen EC, Ransom BR, Möller T. Increased cytotoxic potential of microglia from ALS-transgenic mice. Glia. 2004 Nov 1;48(2):179-82.

Wichterle H, Lieberam I, Porter JA, Jessell TM. Directed differentiation of embryonic stem cells into motor neurons. Cell. 2002; 110(3):385–397.

Wijesekera LC, Mathers S, Talman P, *et al*. Natural history and clinical features of the flail arm and flail leg ALS variants. Neurology 2009; 72: 1087–1094.

Wild P, Farhan H, McEwan DG, Wagner S, Rogov VV, Brady NR, Richter B, Korac J, Waidmann O, Choudhary C, Dötsch V, Bumann D, Dikic I: Phosphorylation of the autophagy receptor optineurin restricts Salmonella growth. Science 2011, 333:228–233.

Wollmuth LP. Ion permeation in ionotropic glutamate receptors: Still dynamic after all these years. Current opinion in physiology. 2018 Apr 1;2:36-41.

Woodruff TM, Lee JD, Noakes PG. Role for terminal complement activation in amyotrophic lateral sclerosis disease progression. Proceedings of the National Academy of Sciences. 2014 Jan 7;111(1):E3-4.

Wright GS, Antonyuk SV, Hasnain SS. The biophysics of superoxide dismutase-1 and amyotrophic lateral sclerosis. Quarterly reviews of biophysics. 2019;52.

Xia M, Zhang Y, Jin K, Lu Z, Zeng Z, Xiong W. Communication between mitochondria and other organelles: a brand-new perspective on mitochondria in cancer. Cell & bioscience. 2019 Dec;9(1):1-9.

Xiao Q, Zhao W, Beers DR, Yen AA, Xie W, Henkel JS, Appel SH. Mutant SOD1G93A microglia are more neurotoxic relative to wild-type microglia. Journal of neurochemistry. 2007 Sep;102(6):2008-19.

Xiao S, Tjostheim S, Sanelli T, McLean JR, Horne P, Fan Y, Ravits J, Strong MJ, Robertson J: An aggregate-inducing peripherin isoform generated through intron retention is upregulated in amyotrophic lateral sclerosis and associated with disease pathology. J Neurosci 2008, 28:1833–1840.

Xu L, Yan J, Chen D, Welsh AM, Hazel T, Johe K, Hatfield G, Koliatsos VE. Human neural stem cell grafts ameliorate motor neuron disease in SOD-1 transgenic rats. Transplantation. 2006 Oct 15;82(7):865-75.

Xu ZS: Does a loss of TDP-43 function cause neurodegeneration? Mol Neurodegener 2012, 7:27.

Yamanaka K, Chun SJ, Boillee S, Fujimori-Tonou N, Yamashita H, Gutmann DH, Takahashi R, Misawa H, Cleveland DW. Astrocytes as determinants of disease

progression in inherited amyotrophic lateral sclerosis. Nature neuroscience. 2008 Mar;11(3):251-3.

Yamanaka K, Komine O. The multi-dimensional roles of astrocytes in ALS. Neuroscience research. 2018 Jan 1;126:31-8.

Yang HC, Stern A, Chiu DT. G6PD: A hub for metabolic reprogramming and redox signaling in cancer. biomedical journal. 2021 Jun 1;44(3):285-92.

Yin S, Niswender CM. Progress toward advanced understanding of metabotropic glutamate receptors: structure, signaling and therapeutic indications. Cellular signalling. 2014 Oct 1;26(10):2284-97.

Youssef EA, Berry-Kravis E, Czech C, Hagerman RJ, Hessl D, Wong CY, Rabbia M, Deptula D, John A, Kinch R, Drewitt P. Effect of the mGluR5-NAM basimglurant on behavior in adolescents and adults with fragile X syndrome in a randomized, double-blind, placebo-controlled trial: FragXis phase 2 results. Neuropsychopharmacology. 2018 Feb;43(3):503-12.

Yu YC, Kuo CL, Cheng WL, Liu CS, Hsieh M. Decreased antioxidant enzyme activity and increate mitochondrial DNA damage in cellular models of Machado Joseph disease. J Neurosci Res. 2009 Jun;87(8):1884-91.

Zamanian JL, Xu L, Foo LC, Nouri N, Zhou L, Giffard RG, Barres BA. Genomic analysis of reactive astrogliosis. Journal of neuroscience. 2012 May 2;32(18):6391-410.

Zhang Y, Zolov SN, Chow CY, Slutsky SG, Richardson SC, Piper RC, Yang B, Nau JJ, Westrick RJ, Morrison SJ, Meisler MH, Weisman LS: Loss of Vac14, a regulator of the signaling lipid phosphatidylinositol 3,5-biphosphate, results in neurodegeneration in mice. Proc Natl Acad Sci USA 2007, 104:17518–17523.

Zhao W, Beers DR, Bell S, Wang J, Wen S, Baloh RH, Appel SH. TDP-43 activates microglia through NF-κB and NLRP3 inflammasome. Experimental neurology. 2015 Nov 1;273:24-35.

Zhao W, Beers DR, Henkel JS, Zhang W, Urushitani M, Julien JP, Appel SH. Extracellular mutant SOD1 induces microglial-mediated motoneuron injury. Glia. 2010 Jan 15;58(2):231-43.

Zhao W, Xie W, Xiao Q, Beers DR, Appel SH. Protective effects of an anti-inflammatory cytokine, interleukin-4, on motoneuron toxicity induced by activated microglia. Journal of neurochemistry. 2006 Nov;99(4):1176-87.

Zu T, Gibbens B, Doty NS, Gomes-Pereira M, Huguet A, Stone MD, Margolis J, Peterson M, Markowski TW, Ingram MA, Nan Z. Non-ATG–initiated translation directed by microsatellite expansions. Proceedings of the National Academy of Sciences. 2011 Jan 4;108(1):260-5.

Zu T, Liu Y, Bañez-Coronel M, Reid T, Pletnikova O, Lewis J, Miller TM, Harms MB, Falchook AE, Subramony SH, Ostrow LW. RAN proteins and RNA foci from antisense transcripts in C9ORF72 ALS and frontotemporal dementia. Proceedings of the National Academy of Sciences. 2013 Dec 17;110(51):E4968-77.

CONFERENCES/SEMINARS

During my PhD period, I attended or presented our data as poster in number of conferences as follows:

1. BraYn: 2nd Brainstorming Research Assembly for Young Neuroscientists, Milano, 14th -16th November 2019.

2. Glial cells- Neurons crosstalk in CNS health and disease, University of Turin, 27th-28th February 2020.

3. 40th National Congress of the SIF, 10th-13th March, 2021.

4. FENS 2020 virtual form, 11th-15th July 2020.

5. BraYn: 3rd Brainstorming Research Assembly for Young Neuroscientists, 25th-27th November 2020.

6. 31st International Symposium on ALS/MND, 9th-11th December 2020.

7. BraYn: 4th Brainstorming Research Assembly for Young Neuroscientists, 20th-22nd October 2021.

8. Motor Neuron Diseases: Understanding the pathogenetic mechanisms to develop therapies, 6th-7th November 2020.

PUBLICATIONS

The data described in this thesis represent the work done for my PhD project and are the matter of a manuscript in preparation. During my doctorate course I collaborated to other research of the group on ALS producing the following papers:

Marini C, Cossu V, **Kumar M**, Milanese M, Cortese K, Bruno S, Bellese G, Carta S, Zerbo RA, Torazza C, Bauckneht M. The Role of Endoplasmic Reticulum in the Differential Endurance against Redox Stress in Cortical and Spinal Astrocytes from the Newborn SOD1^{G93A} Mouse Model of Amyotrophic Lateral Sclerosis. Antioxidants. 2021 Sep;10(9):1392.

Milanese M, Bonifacino T, Torazza C, Provenzano F, **Kumar M**, Ravera S, Zerbo AR, Frumento G, Balbi M, Nguyen TN, Bertola N. Blocking metabotrobic glutamate receptor 5 by the negative allosteric modulator CTEP improves disease course of ALS in SOD1^{G93A} mice. British Journal of Pharmacology. 2021 Apr 30.

Kumar M, Nguyen TN, Milanese M, Bonanno GB. Insights over Human-Induced Pluripotent Stem Cells-Derived Astrocytes in Neurodegenerative Disorders. Biomolecules. 2022 Feb 23.